

**IDENTIFICATION AND FUNCTIONAL  
CHARACTERIZATION OF m6A RNA  
MODIFICATIONS IN CISPLATIN-TREATED  
HELA CELLS**

**A Thesis Submitted to  
the Graduate School of  
İzmir Institute of Technology  
in Partial Fulfillment of the Requirements for the Degree of**

**DOCTOR OF PHILOSOPHY**

**in Molecular Biology and Genetics**

**by  
Ayşe Bengisu GELMEZ**

**June 2024  
İZMİR**

We approve the thesis of **Ayşe Bengisu GELMEZ**

Examining Committee Members:

---

**Prof. Dr. Bünyamin AKGÜL**

Molecular Biology and Genetics, Izmir Institute of Technology

---

**Prof. Dr. Volkan SEYRANTEPE**

Molecular Biology and Genetics, Izmir Institute of Technology

---

**Prof Dr. Ayşe Semra KOÇTÜRK**

Medical Biochemistry, Dokuz Eylül University

---

**Prof Dr. Hatice Güneş ÖZHAN**

Molecular Biology and Genetics, Izmir Institute of Technology

---

**Prof Dr. Kemal Sami KORKMAZ**

Bioengineering, Ege University

**27 June 2024**

---

**Prof. Dr. Bünyamin AKGÜL**

Supervisor, Molecular Biology and Genetics,  
Izmir Institute of Technology

---

**Prof. Dr. Özden YALÇIN ÖZUYSAL**

Head of Department of  
Molecular Biology and Genetics  
Izmir Institute of Technology

---

**Prof. Dr. Mehtap EANES**

Dean of Graduate School of  
Izmir Institute of Technology

## ACKNOWLEDGEMENTS

First and foremost, I am extremely grateful to my supervisor, Prof. Bünyamin AKGÜL, for his advice, support, and patience during my PhD study. His immense knowledge and plentiful experience have directed and encouraged me to be a better scientist throughout my academic career. My gratitude extends to the TUBİTAK (COST, #217Z234) and YÖK 100/2000 Ph.D. Scholarship for funding to undertake my studies at the Department of Molecular Biology and Genetics, Izmir Institute of Technology. Additionally, I would like to thank Prof. Volkan SEYRANTEPE and Prof. Ayşe Semra KOÇTÜRK for their treasured support and advice, which was really influential in shaping my thesis, and the rest of my thesis jury members, Prof. Hatice Güneş ÖZHAN and Prof. Kemal Sami KORKMAZ for their valuable time and comments on my study.

I would like to express gratitude to Dr. İpek ERDOĞAN VATANSEVER for her treasured support, which was really influential in shaping the experimental methods and discussing results, and most importantly, calming me down at the most stressed moments of my PhD. I would also like to thank non-coding RNA Lab members, prioritizing Dilek Cansu GÜRER, Şirin Elife CEREN, Yusuf Cem ÇİFTÇİ, and Dr. Seda BAYKAL not only for scientific discussion, experimental support and sharing the challenging of graduate life but also for being my dearest friends, which the pages is not enough to express my feelings for them.

Finally, I would like to express my gratitude and deepest love for my mother, my father, my grandmother, and my grandfather. Each one of them has given me the strength to face and solve every challenge in my life. They have trusted me and supported me with their wisdom while I chose my path.

# ABSTRACT

## IDENTIFICATION AND FUNCTIONAL CHARACTERIZATION OF m<sup>6</sup>A RNA MODIFICATIONS IN CISPLATIN-TREATED HELA CELLS

N<sup>6</sup>-methyladenosine (m<sup>6</sup>A) modification is the most abundant and dynamic RNA modification that critically influences transcript fate post-transcriptionally. This study investigated the role of m<sup>6</sup>A RNA modification in regulating the response to cisplatin (CP) treatment in HeLa cells. The status of core m<sup>6</sup>A modulators following CP exposure was examined, followed by a transcriptome-wide analysis of m<sup>6</sup>A methylation. The findings revealed significant alterations in the m<sup>6</sup>A RNA methylation landscape by possible effects of changes in the expression of key m<sup>6</sup>A writer proteins, particularly METTL14.

METTL14 depletion increased CP sensitivity, significantly elevating RNA levels of cell-death-related genes at the 72<sup>nd</sup> and 96<sup>th</sup> hrs after siRNA transfection. Genes such as ATF3, ATF5, DUSP6, and PEA15 displayed consistent expression patterns, while TP73, BMF, DAPK1, and DAB2IP exhibited opposite mRNA levels compared to those identified in CP RNA-seq data. These findings suggest that METTL14-directed methylation plays a crucial role in the mRNA regulation of these genes.

Furthermore, YTHDF2 was found to regulate mRNA abundance of candidates through mRNA decay, with enriched binding to pro-apoptotic genes (TP73, DAPK1, ATF3, BMF, GADD34, ATF3, DUSP6) in control cells rather than CP-treated cells. This indicates that these genes might be subject to YTHDF2-mediated post-transcriptional regulation.

This study highlights the dynamic nature of m<sup>6</sup>A modification in response to CP treatment. It underscores the significant role of METTL14 in modulating transcript fate, providing a foundation for future research into therapeutic strategies targeting m<sup>6</sup>A regulatory pathways in cancer treatment.

# ÖZET

## SİSPLATİN UYGULANMIŞ HELA HÜCRELERİNDE m<sup>6</sup>A RNA MODİFİKASYONLARININ BELİRLENMESİ VE FONKSİYONEL KARAKTERİZASYONU

N6-metiladenozin (m<sup>6</sup>A), RNA üzerinde en fazla bulunan ve dinamik bir modifikasyondur. Bu çalışmada m<sup>6</sup>A modifikasyonunun HeLa hücrelerinin sisplatin (CP) uygulamasına verdiği yatının düzenlenmesindeki fonksiyonu araştırılmıştır. İlk olarak, CP uygulanmış HeLa hücrelerinde temel m<sup>6</sup>A düzenleyicilerinin seviyeleri ve ardından m<sup>6</sup>A metilasyon dağılımı tüm transkriptom çapında incelendi. Analiz sonucunda, m<sup>6</sup>A yazıcılarının, özellikle METTL4'ün ekspresyonunun değişikliğinin olası etkisi olarak, m<sup>6</sup>A metilasyon profilinde anlamlı farklar belirlendi. Özellikle, CP uygulamasını takriben global metilasyon seviyesindeki düşüş aynı uygulama sonucunda gözlemlenen METTL4'ün protein seviyesindeki önemli azalma ile ilişkilendirilebilir.

METTL4 susturması sonucunda hücrelerin, özellikle transfeksiyonun 72. ve 96. saatlerinde CP'ye daha hassasiyet gösterdiği tespit edildi. Bu hassasiyet hücre ölümü ile ilgili genlerin RNA seviyelerinde METTL4 susturulması sonucunda gözlemlenen artıştan kaynaklanıyor olabilir. Bununla birlikte, aday genler arasından, ATF3, ATF5, DUSP6 ve PEA15 gibi genler tutarlı ifade modelleri sergilerken, TP73, BMF, DAPK1 ve DAB2IP, CP RNA-seq verilerinde tanımlanan yönlere zıt mRNA seviyeleri sergiledi. Bu bulgular, METTL4'e bağlı gerçekleşen metilasyonun, bu genlerin mRNA düzenlenmesinde, dolayısıyla CP etkisini artırmasında çok önemli bir rol oynadığını göstermektedir.

Ayrıca, YTHDF2'nin pro-apoptotik adaylara koşula özgün olarak kontrol hücrelerinde daha fazla bağlanma yatkınlığı gösterdiği belirlenmiştir. Bu durum bu genlerin normal koşullarda YTHDF2 tarafından indüklenen RNA bozulması ile seviyelerinin kontrol edildiğini ancak CP uygulaması ile bağlanma etkinliğinin azalması nedeni ile aynı genlerin sabitliğinin arttığını işaret etmektedir.

Bu çalışma, CP yanıtı ile dinamik m<sup>6</sup>A modifikasyonu arasındaki karşılıklı etkileşimi göstermektedir. Özellikle METTL4'ün sisplatin etkinliğini m<sup>6</sup>A metilasyonu ekseninde artırdığının altını çizerek, kanser tedavisinde m<sup>6</sup>A dağılımını düzenleyen yolları hedef alan terapötik stratejilere yönelik araştırmalar için temel sağlayabilir.

***To my grandmother,***

*whose unconditional love and acceptance have gifted me the ability to embrace every facet of life and the strength to follow my dreams.*

# TABLE OF CONTENTS

LIST OF FIGURES .....	ix
LIST OF TABLES .....	XI
CHAPTER 1. INTRODUCTION .....	1
1.1. Epitranscriptomics: A Matter of RNA Fate.....	1
1.1.1. <i>N</i> <sup>6</sup> -methyladenosine (m <sup>6</sup> A) RNA Modification .....	3
1.1.1.1. An Emerging Players on RNA Fate: Regulators of m <sup>6</sup> A RNA Modification .....	4
1.1.1.1.1. The Control of m <sup>6</sup> A Presence through “Writers” and “Erasers” .....	5
1.1.1.1.2. “Readers” and the Molecular Functions of m <sup>6</sup> A Modification.....	9
1.1.1.2. The Effects of m <sup>6</sup> A Modification on Cell Survival and Death .....	13
1.2. Cisplatin as an Anti-cancer Drug and Its Action in Mechanism .....	17
1.2.1. Cisplatin-Induced Apoptosis .....	19
1.2.3. Downstream Events in HeLa Cells after Cisplatin Exposure .....	21
CHAPTER 2. MATERIAL AND METHODS .....	27
2.1. Cell Culture and CP Treatment .....	27
2.2. Detection of Apoptosis by Flow Cytometry .....	27
2.3. WST-8 Assay for Cell Proliferation and Viability .....	28
2.4. Total RNA Isolation .....	28
2.5. Quantitative Polymerase Chain Reaction (qPCR) .....	29
2.6. Western Blotting.....	29
2.7. m <sup>6</sup> A-eCLIP-seq and Bioinformatic Analysis .....	31

2.8. Candidate Selection and Primer Designing for m <sup>6</sup> A Points.....	33
2.9. METTL14 Knockdown by siRNA.....	35
2.10. Overexpression of METTL14 and Halo-tagged YTHDF Proteins ....	35
2.11. Formaldehyde Cross-linking and Immunoprecipitation and qPCR (fCLIP-qPCR).....	37
2.12. Statistical Analysis .....	39
CHAPTER 3. RESULTS .....	41
3.1. CP Alters the Abundance of mRNAs and Proteins of m <sup>6</sup> A Modulators in HeLa Cells .....	41
3.2. m <sup>6</sup> A-eCLIP-seq Reveals Changes in the m <sup>6</sup> A Profile of CP-Treated HeLa Cells .....	45
3.3. Pathway Analysis Demonstrates m <sup>6</sup> A RNA Modification as a Part of CP Response.....	53
3.4. Integrative RNA-seq and m <sup>6</sup> A-eCLIP-seq Analysis Reveal Positive Correlation between RNA Abundance and m <sup>6</sup> A Levels in CP-Responsive Genes.....	56
3.6. m <sup>6</sup> A RNA Modification Involves the Regulation of Key Transcripts Fate Linked to CP Response .....	69
3.7. Differential m <sup>6</sup> A Modification of Candidate Genes May Influence Transcript Fate via YTHDF2 under CP Exposure .....	76
CHAPTER 4. DISCUSSION.....	80
CHAPTER 5. CONCLUSION .....	89
REFERENCES .....	91
VITAE.....	130

# LIST OF FIGURES

## **Figure**

Figure 1.1. Epigenetics And Epitranscriptomics in The Concept Of DNA/RNA Modifications .....	2
Figure 1.2. Visual Representation of Different Modifications on mRNA .....	3
Figure 1.3. The Distribution of m <sup>6</sup> A on a Transcript and Consensus Sequence (DRACH) of Methylation Site .....	4
Figure 1.4. The m <sup>6</sup> A Regulators Deposit Methylation on the Sixth Nitrogen Residue of Adenosines in Various Transcripts .....	6
Figure 1.5. The Suggested Model of m <sup>6</sup> A Methylation Mechanism by the METTL3:METTL14 Heterodimer .....	7
Figure 1.6. Three Classes of m <sup>6</sup> A Reader Proteins .....	10
Figure 1.7. Diverse Molecular Mechanisms Regulating mRNA Fate Mediated by m <sup>6</sup> A Readers .....	12
Figure 1.8. The Schematic Representation of the Molecular Action of CP after Its Uptake .....	18
Figure 1.9. The Schematic Representation of the HeLa Cell Response against CP Cytotoxicity .....	24
Figure 2.1. Schematic Representation of the m <sup>6</sup> A-eCLIP Streamline .....	32
Figure 2.2. Schematic Representation of m <sup>6</sup> A-eCLIP Data Analysis Pipeline .....	34
Figure 3.1. The Effect of CP on HeLa Cell Viability and Apoptosis .....	41
Figure 3.2. The effect of CP on the expression of MTC complex .....	43
Figure 3.3. The Preparation of Total RNA Replicates for m <sup>6</sup> A-eCLIP-seq .....	46
Figure 3.4. The Validation of m <sup>6</sup> A Peaks and Crosslink Sites in CP and DMSO Samples .....	48
Figure 3.5. Schematic Representation of Each Feature Location in a Gene .....	50
Figure 3.6. The m <sup>6</sup> A RNA Modification Profile of HeLa Cells upon CP Treatment ....	51
Figure 3.7. The Pathway Analysis of Genes Exhibiting Differential m <sup>6</sup> A Modification .....	54
Figure 3.8. The Analysis of RNA-seq Was Used as “Input” for m <sup>6</sup> A Enrichment .....	57
Figure 3.9. The Correlation Analysis between “DMGs” and “DEGs” .....	59

## **Figure**

Figure 3.10. The GSEA Plots Showing the Top Five Gene Sets Enriched in “Hyper-Induced” and “Hyper-Reduced” Gene Groups in HeLa Cells .....	61
Figure 3.11. The Selection Criteria of Candidate Genes Exhibiting Differential Methylation Sites and mRNA Levels .....	63
Figure 3.12. The Functional Analysis in Only METTL14 Depleted and CP-Treated METTL14 Knockdown HeLa Cells .....	67
Figure 3.13. The Effect of METTL14 Overexpression on Cell Proliferation and CP Response in HeLa Cells .....	70
Figure 3.14. The mRNA Levels of Pro-Apoptotic Genes and JUN in METTL14 Silenced HeLa Cells through Time .....	72
Figure 3.15. The mRNA Levels of ATF5 and Anti-apoptotic Genes in METTL14 Silenced HeLa Cells Through Time .....	74
Figure 3.16. The Overexpression of HaLo-tagged YTHDF2 Protein and Impact on CP Response .....	77
Figure 3.17. The qPCR Amplification of YTHDF2-bound mRNA of Candidate Genes Obtained from fCLIP Protocol .....	78

## LIST OF TABLES

### **Table**

Table 1.1. Human m <sup>6</sup> A Methyltransferases and Their Target RNAs .....	5
Table 2.1. qPCR Components .....	29
Table 2.2. Cycling Conditions for GoTaq qPCR Master Mix .....	30
Table 2.3. The Primer Sequences for Each Gene Utilized in the qPCR .....	30
Table 2.4. The List of Antibodies Utilized in Western Blotting .....	31
Table 2.5. The Primer Sequences of Each Gene for Amplifying Their Coding Sequences .....	36
Table 2.6. HeLa Cell Density and pcDNA/PEI Concentrations .....	37
Table 2.7. Buffers and Their Contents Used in CLIP-qPCR Protocol .....	39
Table 3.1. m <sup>6</sup> A Sites Detected in All Biological Replicates .....	47
Table 3.2. The Feature Types Where m <sup>6</sup> A Sites Were Annotated .....	50
Table 3.3. The List of 16 Genes Exhibiting a Significant Change in m <sup>6</sup> A Status and mRNA Levels Related to CP Response in HeLa Cells .....	65
Table 3.4. The List of Candidate Genes With the Value of log <sub>2</sub> Fold Change .....	74
Table 3.5. The List of Candidate Genes With the Value of Input Percentages and Fold Enrichments .....	79

# CHAPTER 1

## INTRODUCTION

### 1.1. Epitranscriptomics: A Matter of RNA Fate

Transfer of the information stored in DNA through nucleotide sequences to mRNA and its consecutive conversion into protein are two pillars of gene expression, known as transcription and translation. The principles of this info flux were first declined by Francis Crick in 1958, termed “the Central Dogma of Molecular Biology” (CRICK 1958), direct and rigid change of information from DNA to mRNA and then to protein. The first challenge against the unidirectional transfer of nucleotide sequence-based data was suggested by Temin and Baltimore, independently from one another, in the early 70s. They reported a DNA polymerase in viruses using RNA as a template to produce DNA, named reverse transcriptase (Perevozchikov, Kuznetsov, and Zerov 1970; Baltimore 1970). Furthermore, investigating biochemical processes on DNA and RNA molecules, started by the Central Dogma idea, gained significant importance by observing nucleotide modification. The development of DNA/RNA sequencing methods by Sanger and colleagues led to the incredible rise of modern genomics (Bkownlee, Sanger, and Barrell 1968; Sanger, Nicklen, and Coulson 1977). These revolutionary findings led scientists to consider the exception of Central dogma and whether there is a link between environment and heritable content in gene regulation.

What began as broad research focused on combining genetics and environment by well-respected scientists, including Waddington and Hadorn, during the mid-twentieth century has evolved into the field we currently refer to as epigenetics. Epigenetics, which was coined by Waddington in 1942 (Waddington 2012), is the study of heritable or reversible alterations in gene expression (active versus inactive genes) that do not involve changes to the underlying DNA sequence - an alter in phenotype without a change in genotype - which in turn affects how cells read the genes. Beginning in the 1990s, epigenetics has become of renewed interest. Completing the human genome project and sequencing other organisms' whole genomes gave incredible acceleration to studies and,

thus, its importance in gene regulation (Holliday 2006). DNA methylation is one of the most broadly studied and well-characterized epigenetic modifications dating back to studies done by Griffith and Mahler in 1969. Other significant modifications include chromatin remodeling, histone modifications, and non-coding RNA mechanisms. The renewed interest in epigenetics has led to new findings about the relationship between epigenetic changes and various disorders, including cancers, mental retardation-associated diseases, immune disorders, neuropsychiatric disorders, and pediatric disorders (Zoghbi and Beaudet 2016).

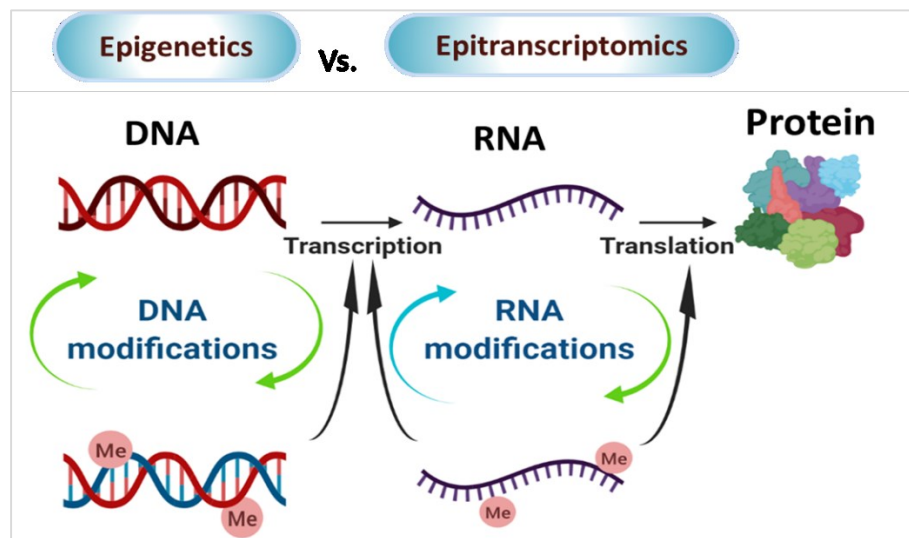


**Figure 1.1. Epigenetics and Epitranscriptomics in the concept of DNA/RNA modifications.** This image was created with BioRender (<https://biorender.com/>).

The increased knowledge about the other regulatory processes reposing DNA to protein enlightens another layer of perspective about the biochemical recipes of RNA processing. In analogy to epigenetics, a rising branch of RNA biology focuses on the potential modifications of different types of RNA and their functional role in the regulation of RNA processing, termed “Epitranscriptomics” (Figure 1.1) (Kan, Chen, and Sallam 2022). These dynamic and reversible RNA epi-modifications are pervasive, conserved, and critical for many aspects of biology, including germline development, cellular signaling, and circadian rhythm control (Wilkinson, Cui, and He 2022). Interestingly, these modifications may impact as many as ~16,000 human genes, and thus far, they have been observed in almost all species, but their genome-wide prevalence has been discerned only in the past few years (Saletore et al. 2012). Indeed, it is believed that there are more than 170 RNA modifications, including m<sup>7</sup>G (5' Cap), m<sup>1</sup>A, m<sup>6</sup>Am, m<sup>5</sup>C,

I, and  $\Psi$ , across the three domains of life, but the roles and activities of many of them remain unclarified (S. Li and Mason 2014) (Figure 1.2).

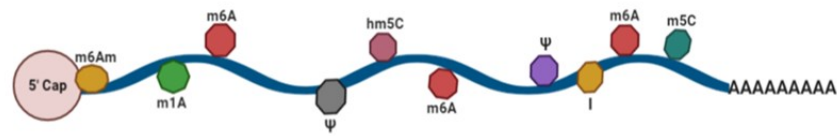


**Figure 1.2. Visual representation of different modifications on mRNA.** This image was created with BioRender (<https://biorender.com/>).

### 1.1.1. $N^6$ -methyladenosine ( $m^6A$ ) RNA Modification

Among all internal mRNA modifications,  $N^6$ -methyladenosine ( $m^6A$ ) is the most prevailing type characterized in eukaryotes, preferentially occurring in three to six sites per transcript (Dominissini et al. 2012). Beginning with the first detection of  $m^6A$ -containing mRNA isolated from rats (Desrosiers, Friderici, and Rottman 1974) and mice (Perry and Kelley 1974) in 1974, it was reported in a variety of organisms dispersing the tree of life, such as yeasts (Agarwala et al. 2012; Schwartz et al. 2013), viruses (Courtney et al. 2017; Martínez-Pérez et al. 2017), plants (Zhong et al. 2008; Duan et al. 2017), fruit flies (Lence et al. 2016; Haussmann et al. 2016), and mammals (Dominissini et al. 2012; Zheng et al. 2013). Moreover, the observation of  $m^6A$  abundancy not only in mRNAs from various organisms but also in different types of ncRNAs such as lncRNAs, miRNAs, snRNAs, and circRNAs (H. Ma et al. 2019) has given scientists an influential clue about its critical role in the regulation of gene expression affecting the widespread cellular processes.

Despite its first identification of  $m^6Am$  RNA modification in mammals in 1974, the exact distribution of  $m^6A$  in the concept of gene regions (coding or non-coding), frequency, location on a transcript (5' UTR, CDS, 3'UTR, etc.) and its regulatory proteins were started to emerge just a decade ago (Dominissini et al. 2013). The insight into the prevalence of  $m^6A$  RNA modification was sparked by the first identification of enzymes removing  $m^6A$  (G. Jia et al. 2011; Zheng et al. 2013) and through the development of detection methods with improved sensitivity and high-throughput sequencing approaches to map modified sites (Meyer et al. 2012; Dominissini et al. 2013).

Since a complete understanding of the fundamental roles of  $m^6A$  in RNA biology

requires determining the positions of m<sup>6</sup>A in the gene transcripts, the transcriptome-wide analysis of m<sup>6</sup>A modification in various conditions and cell types provided much valuable information and pointed to the conservativeness of this modification. m<sup>6</sup>A modification occurs in highly conserved regions with a consensus sequence identified as DRACH. In this motif, "A" represents the methylated adenosine, "D" can be A, U, or G, "R" can be A or G, and "H" can be A, C, or U (Figure 1.3) (Grozhik et al. 2017). However, the frequency of this consensus sequence in the genome is much higher than that of m<sup>6</sup>A occurrence; therefore, additional sequences or RNA structures may also play a role in determining the methylation sites (Linder et al. 2015). Next-generation sequencing (NGS) studies have additionally demonstrated that the m<sup>6</sup>A modification is not randomly distributed but is enriched near stop codons and 3'-UTRs and translated near 5'-UTR or in CDS, especially in long exons (Figure 1.3) (Linder et al. 2015; Meyer et al. 2012). In addition to mRNAs, m<sup>6</sup>A modification was detected on rRNAs, tRNAs, and ncRNAs, including snRNAs, miRNAs, lncRNAs, and circRNAs, but not within the same consensus motifs as it does in mRNA (Huang, Weng, and Chen 2020; L. Luo et al. 2022). An in vitro analysis using U6 snRNA demonstrated that a 30-stem loop structure was necessary for m<sup>6</sup>A formation, suggesting that m<sup>6</sup>A in other RNA species may have structural functions, unlike the m<sup>6</sup>A on mRNA (Shimba et al. 1995).

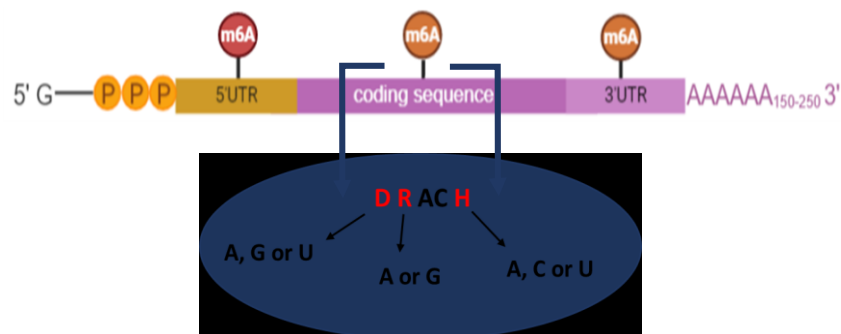


**Figure 1.3. The distribution of m<sup>6</sup>A on a transcript and consensus sequence (DRACH) of methylation site.** This image was created with BioRender (<https://biorender.com/>).

### 1.1.1.1. An Emerging Players on RNA Fate: Regulators of m<sup>6</sup>A RNA Modification

Three major protein groups modulate the control of RNA fate through m<sup>6</sup>A

modification; i. m<sup>6</sup>A RNA mTase complex, “writers” introduce methyl to sixth nitrogen on adenine and controls localization on target RNA, ii. enzymes that dislodge methyl group so-called “erasers,” and iii. RNA binding proteins, “readers,” determine RNA fate upon specifically interacting with RNA in a m<sup>6</sup>A-dependent manner (Guo et al. 2021).

### 1.1.1.1.1. The Control of m<sup>6</sup>A Presence through “Writers” and “Erasers”

Two crucial categories of enzymes play a dynamic and reversible role in regulating the m<sup>6</sup>A modification of RNA. These enzymes are commonly referred to as methyltransferases and demethylases. The first group, known as writers, comprises a complex that includes core enzymes such as methyltransferase like 3, 14, and 16 (METTL3, METTL14, and METTL16), along with associated co-factors such as Wilms tumor 1-associated protein (WTAP), RNA-binding motif protein 15 (RBM15/15B), Cbl-proto-oncogene-like 1 (CBLL1 or HAKAI), zinc finger CCCH-type containing 13 (ZC3H13), and Vir-like m<sup>6</sup>A methyltransferase-associated protein (VIRMA or KIAA1429). Functioning collaboratively, these proteins facilitate the addition of m<sup>6</sup>A modifications to specific segments of RNA molecules (H. Shi, Wei, and He 2019).

Before the recent increase in interest in m<sup>6</sup>A, the discovery of the initial writer can be traced back to 1994 when Bokar and his colleagues successfully cloned METTL3 (Bokar et al., 1994; 1997). Subsequently, three more methyltransferases encoded in the mammalian genome have been identified and are recognized for modifying specific RNAs with m<sup>6</sup>A (Table 1.1) (Figure 1.4) (Pendleton et al. 2017; Van Tran et al. 2019; H. Ma et al. 2019; Satterwhite and Mansfield 2022).

**Table 1.1. Human m<sup>6</sup>A methyltransferases and their target RNAs**

METTL3:METTL14	mRNAs, ncRNAs (lncRNAs, miRNAs, circRNAs)
METTL5	18S rRNA

Although these four mTases function in critical processes in RNA regulation, most attention has focused on m<sup>6</sup>A marks in mRNAs mediated by the methyl transferase

complex (MTC). MTC comprises seven major proteins (Figure 1.4), predominantly targeting mRNAs and RNA polymerase II-generated ncRNAs. The central component of the MTC is the METTL3:METTL14 core, which initiates the installation of methyl groups specifically on adenosine residues located within the DRACH consensus motif. (Dominissini et al., 2012; Jia et al., 2011; Linder et al., 2015). The catalytic subunit is present only in METTL3 among the seven subunits of the MTC (Śledź & Jinek, 2016). However, METTL14 is crucial for stabilizing the MTC core and recognizing the substrate, even though it has little to no methyltransferase activity (G. Jia et al. 2011; Dominissini et al. 2012; Linder et al. 2015).

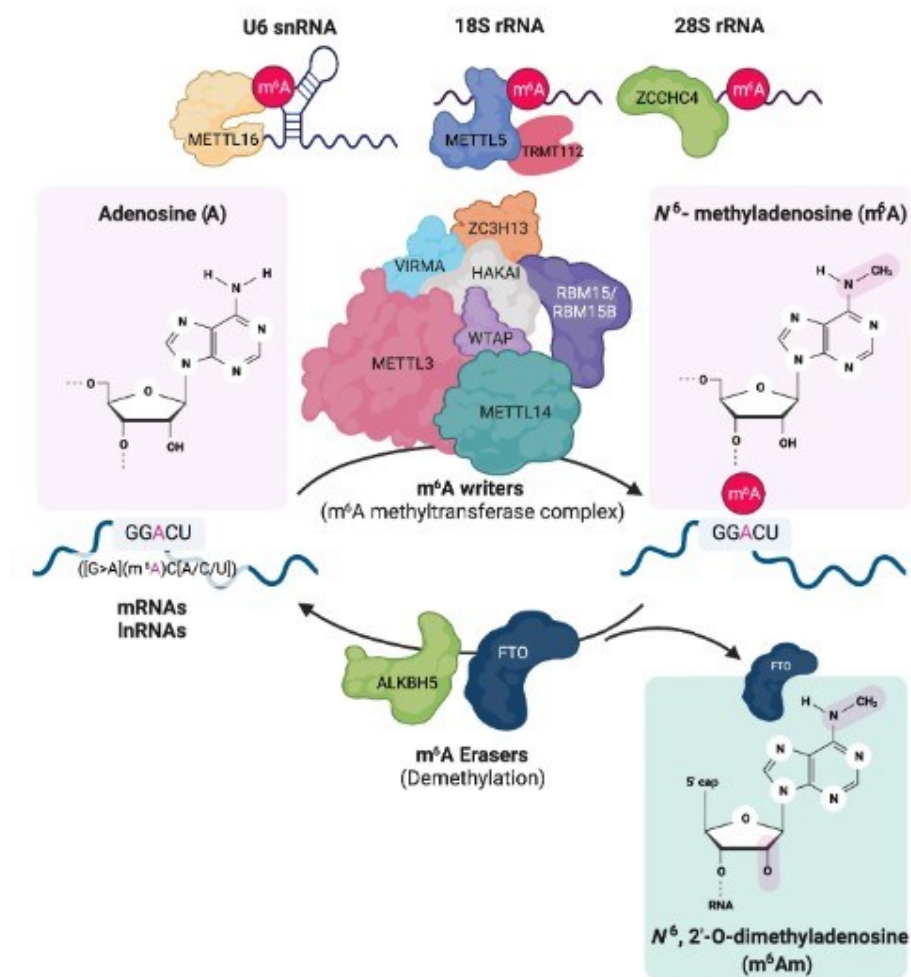


**Figure 1.4. The m<sup>6</sup>A regulators deposit methylation on the sixth nitrogen residue of adenosines in various transcripts.** The m<sup>6</sup>A methyltransferase complex consists of seven core components, adding methyl to mainly mRNAs and lncRNAs. Another group of methyltransferases, comprising METTL16, METTL5, and ZCCHC4, specifically methylates snRNA, rRNA, and a few noncoding RNAs. The single subunit erasers, FTO and ALKBH5, play a role in removing methyl groups (J. Hong, Xu, and Lee, 2022).

As a heterodimer, the human METTL3:METTL4 complex is formed in the cytoplasm with a 1 to 1 ratio. Then, it translocates to the nucleus through a nuclear localization signal (NLS) located in the N-terminal extension of METTL3 (Schöller et al. 2018). The N-terminal extension of METTL3 consists of a zinc finger domain (ZFD) containing two consecutive CCCH zinc finger motifs (ZF1 and ZF2), a partially ordered linker, and a C-terminal MTase domain (MTD3) (P. Wang, Doxtader, and Nam 2016). The MTD3 domain (ASL1 – ASL2 loops) houses the SAM cofactor, which binds to the catalytic pocket in the center. The cofactor pocket includes one side of a  $\beta$ -sheet and an enclosed catalytic helical loop in the center. The catalytic activity of the loop is governed by the DPPW motif (D395-W398), which is conserved among metazoan m<sup>6</sup>A MTases as D/N-PP-F/W/Y (Figure 1.5) (Śledź and Jinek 2016).

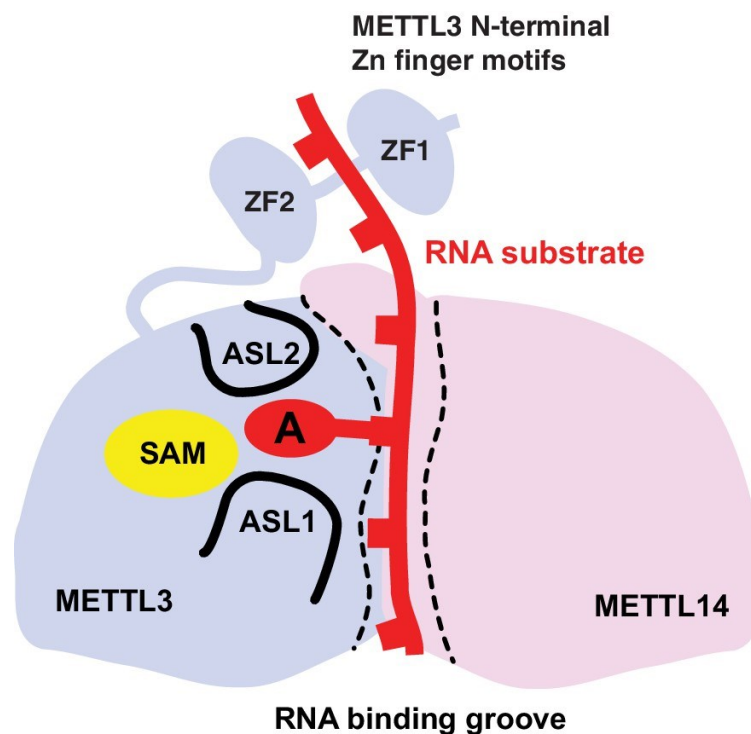


**Figure 1.5. The proposed model of m<sup>6</sup>A methylation mechanism by the METTL3:METTL14 heterodimer (Śledź and Jinek 2016).**

Structural analysis of the METTL3 ZFD has revealed its direct interaction with MTD3. It functions as a domain that recognizes the DRACH motif, which is essential for stabilizing MTD3 on the target adenosine. However, the binding between the ZFD and the DRACH motif occurs with low affinity. Despite METTL14 possessing enzymatic activity, detailed investigations employing biochemical and structural approaches have

demonstrated that the METTL3-METTL14 complex exhibits markedly more significant activity than METTL3 or METTL14 alone (Śledź and Jinek 2016; Xiang Wang et al. 2016).

Recently, more proteins affecting writers' function, localization, and stability have been identified as co-factors. The recruitment of METTL3 and METTL14 into nuclear speckles is facilitated by WTAP, which enhances the RNA-binding capability of the m<sup>6</sup>A methyltransferase. WTAP and METTL3 collectively regulate various genes associated with transcription and RNA processing (Ping et al. 2014). RBM15/15B assists the binding of METTL3 and WTAP, directing the two proteins to their target sites (Knuckles et al. 2018). VIRMA recruits the MTC and interact with polyadenylation cleavage factors CPSF5 and CPSF6. Thus, VIRMA preferentially locates mRNA methylation sites near the 3'-UTR and stop codon regions (Jianzhao Liu et al. 2018). Other proteins, such as ZC3H13 and CBLL1 (HAKAI), control nuclear m<sup>6</sup>A methylation. They both maintain the localization of the MTC through its binding with WTAP (Wen et al. 2018; Bawankar et al. 2021) (Figure 1.4). On the other hand, the recently identified writer protein METTL16 acts as an independent m<sup>6</sup>A methyltransferase that regulates RNA stability and splicing without overlapping its binding regions with those of the METTL3/14 complex (Warda et al. 2017).

m<sup>6</sup>A modification of transcripts shows elevated levels in various cellular processes, and the emergence of new m<sup>6</sup>A sites is responsive to stimuli and stress conditions (Engel et al. 2018; Z. Lu et al. 2021; Mao et al. 2022). The specificity of m<sup>6</sup>A methylation in terms of the transcript and its position largely relies on recruiting the writer complex to specific transcription sites, likely facilitated by transcription factors (TFs) and epigenetic marks (H. Shi, Wei, and He 2019). For instance, when heat shock is induced, METTL3 is observed to localize at the genes related to heat shock, and m<sup>6</sup>A-dependent regulation of these genes through time-dependent decay is observed (Knuckles et al. 2017). In response to the formation of DNA double-strand breaks (DSBs), METTL3, phosphorylated by ATM, localizes to the site of the DSB and methylates the N<sup>6</sup> position of adenosine (m<sup>6</sup>A) in RNAs associated with DNA damage, thereby regulating homologous recombination (C. Zhang et al. 2020). An example of stimulus-dependent regulation involves the interaction of SMAD2/3, members of the SMAD family activated by the TGF-β pathway, with METTL3/14 and WTAP. This interaction facilitates the co-transcriptional installation of m<sup>6</sup>A on specific transcripts (Bertero et al. 2018).

While m<sup>6</sup>A addition is processed via the large multi-unit m<sup>6</sup>A writer complex, so

far, only two enzymes, fat mass and obesity-associated protein (FTO) and AlkB homolog 5 (ALKBH5), have been identified as enzymes removing the methyl group from N<sup>6</sup>-adenosine residues. These two proteins are mainly localized in the nucleus, where demethylation occurs (Figure 1.4). However, recent studies demonstrated that FTO might localize both in the nucleus and cytoplasm (Aas et al. 2017). FTO was the first identified eraser protein, which has pointed the reversibility of m<sup>6</sup>A RNA modification. Even though ALKBH5 has a more-conserved catalytic domain, FTO has garnered significant interest due to its impact on human obesity. It has led to a better understanding of m<sup>6</sup>A removal (G. Jia et al. 2011). ALKBH5 was the second RNA demethylase to be identified that could oxidatively reverse m<sup>6</sup>A modifications (Zheng et al. 2013). ALKBH5 is expressed in most tissues, particularly in the testes, in which overexpression of ALKBH5 promotes prostate cancer development (Q. Wu et al. 2021). Recently, several groups have resolved the unique crystal structure of ALKBH5 (Aik et al. 2014). Remarkably, FTO could mediate m<sup>6</sup>Am (N<sup>6</sup>,20-O-dimethyl adenosine) demethylation (X. Zhang et al. 2019). Unlike FTO, ALKBH5 seems to be a m<sup>6</sup>A-specific demethylase in mRNA (Zou et al. 2016) (Figure 1.4).

These two groups of enzymes are considered the effector proteins of m<sup>6</sup>A stimuli-dependent regulation and biogenesis. When it comes to the impact of m<sup>6</sup>A marks on RNA fate, there is a third group of proteins that recognize the m<sup>6</sup>A marks and dictate the fate of transcript, called “readers.”

#### **1.1.1.1.2. “Readers” and the Molecular Functions of m<sup>6</sup>A Modification**

Advancements in the field of m<sup>6</sup>A methylation have been facilitated by the emergence of immunoprecipitation (IP)-dependent enrichment of RNA-binding proteins followed by sequencing technologies. These studies have unveiled the involvement of m<sup>6</sup>A marks in various physiological and pathological processes, encompassing differentiation (Edens et al. 2019; Furlan et al. 2019), cancer progression (T. Wang et al. 2020), circadian rhythm (Hastings 2013), neuronal function and sex determination in *Drosophila* (Lence et al. 2016), and X chromosome inactivation (Coker et al. 2020). All physiologic effects of m<sup>6</sup>A are mediated by its regulatory role in the fate of mRNA in cells. To mediate its functions, m<sup>6</sup>A relies on a class of RNA-binding proteins (RBPs) called m<sup>6</sup>A reader proteins, which selectively bind to m<sup>6</sup>A-modified RNAs (Patil,

Pickering, and Jaffrey 2018). Thus, the identification and characterization of reader proteins have offered valuable insights into the molecular mechanisms underlying m<sup>6</sup>A-dependent co/post-transcriptional regulation (Han et al. 2021). Through methylated probe pull-down and quantitative protein mass spectrometry assays, several RBPs have been identified that exhibit preferences for m<sup>6</sup>A probes (Dominissini et al. 2012; Edupuganti et al. 2017), thereby highlighting diverse binding modes (Figure 1.6). Consequently, many regulatory or functional machinery can be recruited to m<sup>6</sup>A-modified mRNA through m<sup>6</sup>A readers, impacting the target mRNA's fate.

The known m<sup>6</sup>A reader proteins employ different mechanisms to recognize m<sup>6</sup>A-modified RNAs. One mechanism involves the utilization of a YT521-B homology (YTH) domain, which directly binds to the m<sup>6</sup>A base (Patil, Pickering, and Jaffrey 2018). Another mechanism involves binding to single-stranded RNA motifs exposed due to structural changes induced by m<sup>6</sup>A modifications (Nian Liu et al. 2015; N. Liu and Pan 2017). Additionally, a distinct class of m<sup>6</sup>A reader proteins has been discovered, which employ K homology (KH) domains to recognize m<sup>6</sup>A-modified RNAs. These reader proteins selectively enhance the translation and stability of m<sup>6</sup>A-containing RNAs (Figure 1.6) (Huang et al. 2018).

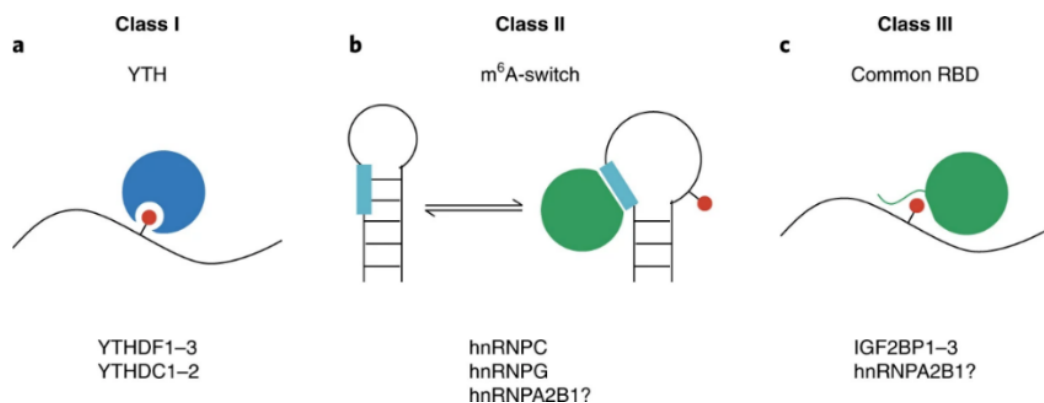


**Figure 1.6. Three classes of m<sup>6</sup>A reader proteins:** **a.** Class I, m<sup>6</sup>A reader proteins possess a YTH domain that directly interacts with the m<sup>6</sup>A base. **b.** Class II, m<sup>6</sup>A reader proteins employ an m<sup>6</sup>A-switch mechanism to recognize and bind to transcripts containing m<sup>6</sup>A modifications. **c.** Class III m<sup>6</sup>A reader proteins utilize a common RNA-binding domain (RBD), specifically the KH domain, and its adjacent regions to identify and bind to transcripts containing m<sup>6</sup>A modifications (Zhou K.I. and Pan 2018).

The YTH domain-containing proteins, specifically the YTH domain family 1-3 (YTHDF1-3) and YTH domain-containing 1-2 (YTHDC1-2) in humans, constitute the

first class of m<sup>6</sup>A readers that strongly and directly bind to the m<sup>6</sup>A base. Among these, cytoplasmic YTHDF2 has been extensively shown to promote the degradation of its target transcripts by recruiting the CCR4-NOT deadenylase complex (Xiao Wang et al. 2014; H. Du et al. 2016). Controversially, the other two cytoplasmic m<sup>6</sup>A readers, YTHDF1 and YTHDF3, are suggested to enhance the translation of target transcripts in HeLa cells by recruiting translation initiation factors (Xiao Wang et al. 2014; H. Shi et al. 2017). Furthermore, the coordinated action of these three proteins mediates the m<sup>6</sup>A-dependent degradation of methylated mRNA according to the location of the m<sup>6</sup>A region in HeLa cells (Zaccara and Jaffrey 2020). A nuclear reader, YTHDC1, has been demonstrated to play multiple roles, including regulating mRNA splicing by preferably recruiting a particular splicing factor (Xiao et al. 2016), expediting mRNA export (Roundtree et al. 2017), and accelerating the decay of specific transcripts (Shima et al. 2017). Cytoplasmic YTHDC2, on the other hand, mediates mRNA stability and translation and regulates spermatogenesis (Hsu et al. 2017) (Figure 1.7).

The second group of m<sup>6</sup>A reader proteins binds to mRNA through a structural switch induced by m<sup>6</sup>A modifications. This remodeling facilitates RNA-protein interactions by altering the accessibility of RNA binding motifs (Nian Liu et al. 2015). Several heterogeneous nuclear ribonucleoproteins (HNRNPs), including HNRNPC, HNRNPG, and HNRNPA2B1, fall into this category. They regulate alternative splicing or processing of target transcripts (Alarcón et al. 2015; Nian Liu et al. 2015; N. Liu and Pan 2017; B. Wu et al. 2018). Additionally, HNRNPs and the third group of m<sup>6</sup>A binding proteins also utilize RNA binding domains (RBDs) such as K homology (KH) domains, RNA recognition motif (RRM) domains, and arginine/glycine-rich (RGG) domains to bind m<sup>6</sup>A-modified RNAs preferentially. Fragile X mental retardation 1 (FMR1), for example, contains three KH domains and one RGG domain and has been shown to exhibit a preference for m<sup>6</sup>A-modified RNA. It influences RNA decay and translation by cooperating with YTHDF2 and YTHDF1 (Edupuganti et al. 2017; F. Zhang et al. 2018).

Another class of readers, insulin-like growth factor 2 binding proteins 1–3 (IGF2BP1-3), has been implicated in maintaining the stability of target transcripts in a m<sup>6</sup>A-dependent manner. Huang et al. reported that mRNA stabilization mediated by IGF2BPs is further enhanced through the recruitment of various co-factors, including ELAV-like RNA binding protein 1 (ELAVL1 or HuR), matrin 3 (MATR3), and poly(A) binding protein cytoplasmic 1 (PABPC1). These co-factors contribute to increased translation efficiency of oncogenes (Huang et al. 2018). Recently, a newly identified m<sup>6</sup>A

binding protein, proline-rich coiled-coil 2A (Prcc2a), has been found to selectively bind to methylated RNA probes. Prcc2a stabilizes a crucial m<sup>6</sup>A-modified transcript required for myelination (R. Wu et al. 2019) (Figure 1.7).

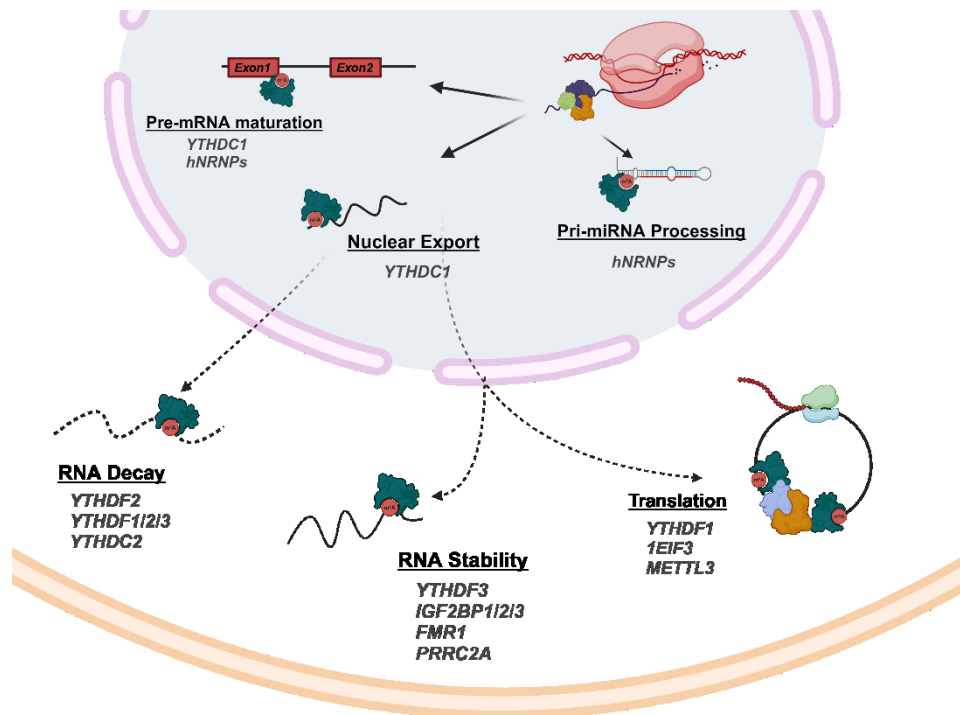


**Figure 1.7. Diverse molecular mechanisms regulating mRNA fate mediated by m<sup>6</sup>A readers.** This image was created with BioRender (<https://biorender.com/>).

Selective binding to specific m<sup>6</sup>A sites or m<sup>6</sup>A-deposited transcript(s) of a reader protein remains unknown. Thus far, scientists have proposed different scenarios based on their findings. The first notion is that readers may be localized to different regions of mRNA by interacting with other RBPs that recognize distinct features of the RNA. For example, YTHDF2 and IGF2BPs functioning in opposite directions were demonstrated to have different binding sites on mRNA: As YTHDF2 predominantly favors 3' UTR as a binding region, IGF2BPs showed increased binding efficiency to CDS (Panneerdoss et al. 2018). Because RBPs' recognition of RNA is mediated through multiple variables, including binding site sequences, flanking sequences, and RNA secondary structures, readers may transmit specificity toward specific m<sup>6</sup>A-modified transcripts (H. Shi, Wei, and He 2019). Secondly, the density and sequence contexts of m<sup>6</sup>A sites predominantly affect reader recognition. A combination of CLIP-seq and m<sup>6</sup>A-seq analysis widely demonstrated that m<sup>6</sup>A readers more frequently occupy increased density in m<sup>6</sup>A regions. Additionally, the compartmentalization of reader proteins mediates the preferential

interaction with local RNA species (W. Zhao et al. 2022). It was also demonstrated that the distribution and expression of m<sup>6</sup>A reader proteins are strongly regulated by a variety of stimuli initiated internally and externally. Because of this regulation, m<sup>6</sup>A modification plays a vital role in many cellular processes.

### **1.1.1.2. The Effects of m<sup>6</sup>A Modification on Cell Survival and Death**

Due to its ability to regulate RNA structure and interactions with RNA-binding proteins, the m<sup>6</sup>A modification plays a crucial role in modulating various aspects of mRNA, including splicing (Xiao et al. 2016; Fish et al. 2019), export (Z. H. Chen et al. 2020), translation (Slobodin et al. 2017), and stability (Zaccara and Jaffrey 2020). As a result, this modulation is involved in numerous physiological processes such as development, somatic cell cycle regulation, and cellular differentiation. Any dysregulation in m<sup>6</sup>A modifications that disrupts gene expression and cellular function can contribute to developing diseases, including cancer, psychiatric disorders, and metabolic disorders. Extensive research has focused on understanding the structural properties and enzymatic processes of m<sup>6</sup>A writers, erasers, and readers and their roles in normal physiological and pathological states.

Various studies have suggested a positive correlation between m<sup>6</sup>A abundance and cell cycle regulation. Cancer research especially enables us to reveal the importance of this modification on cell proliferation, cancer stemness, epithelial to mesenchymal transition (EMT), and finally, resistance to drugs (Deng et al. 2018; Z. Ma et al. 2020; Chuhan Wang et al. 2023). On the other hand, m<sup>6</sup>A regulatory mechanisms play critical roles in mRNA fate and are also responsible for programmed cell death (Hong Wang, Xu, and Shi 2020; Hou et al. 2020). It has been shown that m<sup>6</sup>A governs the cell fate through four main mechanisms: (i) via enhancing cell death or survival-related gene translation, (ii) decreasing the number of transcripts by YTHDF2 binding, via preventing the expression of (iii) methylating or (iv) demethylating enzymes (Jiaxin Chen et al. 2019). Therefore, the dual effect of m<sup>6</sup>A control mechanisms became one of the main subjects of various physiological conditions and diseases.

METTL3 is the most studied protein in tumorigenesis due to its central regulatory function in controlling cellular fate through m<sup>6</sup>A modification. Elevated METTL3 levels have been observed in various cancer types, promoting cell survival by amplifying the

expression of the oncogenes (Visvanathan et al. 2018; Q. Y. Du et al. 2022). The most remarkable results were that METTL3 knocking down prompts a significant increase in apoptosis by targeting B-cell lymphoma-2 (Bcl-2) in various cancers such as breast (BC), lung (LC), gastric (GC), and acute myeloid leukemia (AML) (Vu et al. 2017; W. et al. 2019; T. Wang et al. 2020; Q. Wang et al. 2020). Additional studies have exposed more mechanistic details about how the m<sup>6</sup>A regulatory system works in breast cancer. Cai et al. have demonstrated that elevated METTL3 expression is promoted by hepatitis B X-interacting protein (HBXIP) in aggressive breast carcinomas, driving the inhibition of tumor suppressor genes such as let-7g (Cai et al. 2018). Moreover, elevated m<sup>6</sup>A sites by METTL3 enhance the frequency of mRNA recognition by reader proteins. For example, in breast carcinogenesis, an increased level of m<sup>6</sup>A methylation on 3'UTR of large tumor suppressor kinase 1 (LATS1), which is recognized by the YTHDF2 reader protein, resulted in a dramatic reduction in mRNA level in this gene (Y. Xu et al. 2023). Another supporting data by Wan et al. has revealed that PD-L1 is one of the downstream targets of METTL3, and upregulated m<sup>6</sup>A levels are recognized by IGF2BP3, leading to increased PD-L1 mRNA translation and, thus, immune surveillance of breast cancer (Wan et al. 2022). Additionally, METTL3 is responsible for aberrant expression of survival genes in various cancer types, such as c-MYC and PTEN in AML (Vu et al. 2017), and EGFR-TAZ and PARP in LC (Lin et al. 2016; W. Wei, Huo, and Shi 2019). Besides the anti-apoptotic effect of METTL3, it also regulates (EMT) through TGF- $\beta$  signaling. Enhanced methylation through the METTL3-METTL14-WTAP axis regulated TGF- $\beta$  levels, both stabilizing TGF- $\beta$  itself and increasing the expression of transcription factors, SMAD, and Snail in HeLa cells and JUNB in lung cancer cells (J. Li et al. 2020; Wannanodom et al. 2020). Controversially, METTL3 functions as an apoptosis inducer in cardiomyocytes subjected to hypoxia followed by reoxygenation conditions. Song et al. explored that METTL3 activates apoptosis and reduces autophagy flux by methylating the transcription factor EB (TFEB), the primary gene for lysosome biogenesis (Song et al. 2019). In triple-negative breast cancer, METTL3 also suppresses tumor metastasis via increasing methylation levels on COL3A1 mRNAs, leading to its degradation (Y. Shi et al. 2020).

In addition to METTL3, METTL14, and WTAP participate in cell survival and proliferation in AML through NF- $\kappa$ B and PI3K/AKT/mTOR pathways by increasing MYB, MYC, and mTOR oncogenes. When METTL14 is silenced in AML cells, it enhances apoptotic activity, and this effect appears to be associated with the regulation of

MYB and MYC target mRNA through m<sup>6</sup>A-mediated mechanisms (Weng et al. 2018). Recent studies reveal that METLL14 can also affect cancer progression in both ways. In pancreatic carcinoma (PC), the poor prognosis might be correlated with a high level of METTL14. PC metastasis was dramatically reduced after METL14 knockout lines, downregulating metastasis-promoting lncRNA, LINC00941 (J. Lu et al. 2023). Conversely, METTL14 facilitates autophagy in the METTL14/RB1CC1/IGF2BP2 axis (Liang et al. 2023). Basal et al. reported that suppressing WTAP can heighten apoptosis in leukemia cells by acting through the mTOR pathway, particularly in response to etoposide treatment (Bansal et al. 2014).

Contrary to the writers, FTO and ALKBH5 are primary regulatory factors that target downstream genes of both autophagy and apoptosis. Several groups have demonstrated that FTO regulates apoptosis-related genes such as BNIP3, MZF1, and MYC/CEBPA (Jiqin Liu et al. 2018; Su et al. 2018; Niu et al. 2019). For example, FTO depletion significantly elevates m<sup>6</sup>A modification on pro-apoptotic BNIP3, thus its stability and expression in BC (Niu et al. 2019). FTO is also involved in autophagy. Wang et al. showed that demethylation of autophagy-related 5 (ATG5) and autophagy-related 7 (ATG7) by FTO triggers autophagy. Mechanistically, YTHDF2 interacts with the methyl group on 3'UTR of ATG5 and ATG7 mRNA, accelerating their degradation. Removal of the methyl group in these regions reduces the degradation of their mRNAs, promoting autophagy in adipocytes (Xinxia Wang et al. 2020). It was also shown that FTO reverses YTHDF2-mediated degradation of unc-51-like kinase 1 (ULK1) transcripts (S. Jin et al. 2018). Additionally, ALKBH5 was demonstrated to inhibit apoptosis by targeting anti-oncogenes such as histidine triad nucleotide-binding protein 2 (HINT2). The upregulation of ALKBH5 removes m<sup>6</sup>A on HINT2, which is necessary for its transcript expression, leading to the uncontrolled proliferation of ocular carcinoma (R. Jia et al. 2019). Another target of ALKBH5 is TIMP metalloproteinase inhibitor 3 (TIMP3), of which stability is suppressed by demethylation in LC cells, inhibiting apoptosis (Z. Zhu et al. 2020). Conversely, ALKBH5 inhibits autophagy by promoting Bcl-2 mRNA stability in ovarian cancer (H. Zhu et al. 2019).

The m<sup>6</sup>A reader proteins, as the third group of m<sup>6</sup>A regulators, also actively participate in cell survival and death. Accumulating evidence from different research groups has pointed out that readers can support cell survival or promote cell death in different cell types and conditions. Taking consideration of direct recognition of N<sup>6</sup>-methyladenosine residues, YTH domain reader proteins play an active role in cell fate,

specifically in cancer tissues (Han et al. 2021).

YTHDF1 promotes cell survival either by increasing translation efficiency or stabilizing target transcripts. YTHDF1 is able to affect overall translation by amplifying eukaryotic initiation factor 3C (eIF3C) translation in ovarian cancer (OC) (T. Liu et al. 2020). The aberrant expression of YTHDF1 governs the stabilization and translation of Wnt receptor frizzled7 (FZD7) and ubiquitin-specific peptidase 14 (USP14) in a m<sup>6</sup>A-dependent mechanism, resulting in the poor prognosis in GC (Pi et al. 2021; X. Y. Chen et al. 2021). Two recent studies have also revealed that YTHDF1 supports cell survival in hypoxia conditions through intensifying glycolysis via augmenting pyruvate kinase M2 (PKM2) and inducing autophagy via upregulating both ATG2A and ATG14 (Yao et al. 2022). The other target of this reader is YAP, the co-activator of transcription factor TEAD, which controls the expression of genes related to cell proliferation, migration, and invasion (M. Fu et al. 2022). YAP translation is regulated via direct targeting of YTHDF1 or indirectly by YTHDF2 in a m<sup>6</sup>A-dependent manner in osteosarcoma and lung cancer (D. Jin et al. 2020; Y. Yuan et al. 2021). Similarly, upregulated expression of YTHDF1 is found to be correlated with worse prognosis in patients with breast cancer. Investigation among tissue samples from patients and breast cancer cell lines demonstrated that cells underwent G0/G1 cell cycle arrest after silencing of YTHDF1, which facilitates FOXM1 translation (H. Chen et al. 2022).

In addition to YTHDF1, other reader proteins have been associated with poor prognosis in most cancer types. For instance, YTHDF3 modulates translation and mRNA stability by cooperating with YTHDF1 (H. Shi et al. 2017). In BC, YTHDF3 promotes the translation of proliferation and metastasis-associated genes such as CDK1, MKI67, and VEGFA via stabilizing their transcripts (Anita et al. 2020). Another group of readers, IGF2BPs, also play critical roles in cell proliferation and survival. They mainly bind to 5'UTR, CDS, and upstream of 3'UTR regions of methylated mRNAs, increasing their half-life (T. Y. Zhu, Hong, and Ling 2023). MYC, NOTCH1, HIF1A, PDK4, VEGF, and CDK4 are some examples of their target genes that prove their roles in cell survival and metastasis (Huang et al. 2018; Z. Li et al. 2020; Jiang et al. 2021; Gu et al. 2021; X. Liu et al. 2022; Feng et al. 2022).

On the other hand, YTHDF2 can act as both an oncogene and tumor suppressor, depending on its targets. Unlike the rest of the readers, YTHDF2 causes mRNA degradation via two main mechanisms: (i) CCR4/NOT deadenylase complex (H. Du et al. 2016) or (ii) mRNA cleavage via HRSP12–RNase P/MRP complex (Park et al. 2019).

Depending on its expression profile and target gene(s), YTHDF2 can play a dual role in the same cancer type. In 2019, Yan and colleagues concluded that the upregulation of YTHDF2 in GC cells both from patients and lines (MKN45, AGS) facilitates proliferation and migration via fastening the degradation of PTEN transcripts, thus mediating uncontrolled PI3K/Akt cascade activation (Yan et al. 2020). However, subsequent reports showed that YTHDF2 expression differs depending on the stage of GC. The lower expression of YTHDF2 accelerates the cancer progression due to the increased translation of forkhead box protein C2 (FOXC2). The overexpression of YTHDF2 caused the inhibition of proliferation and prolonged OS (X. Shen et al. 2021). YTHDF2 is one of the global regulators for pro-apoptotic proteins such as BMF, TP53, and PER1. Thus, the enhanced activity of this reader tends to dysregulate apoptosis-cell cycle balance (F. Xu et al. 2021; J. Yu et al. 2021; Weiwei Liu et al. 2022).

Since the m<sup>6</sup>A regulators act as mediators or inhibitors for cell proliferation in distinct cancer types, they become novel targets as therapeutic agents. Indeed, recent studies mostly focus on the effects of these proteins on drug resistance and response. Moreover, altering the m<sup>6</sup>A methylation profile on target genes or m<sup>6</sup>A regulators using gene editing methods such as CRISPR/Cas systems becomes relevant in treatment options.

## **1.2. Cisplatin as an Anti-cancer Drug and Its Action in Mechanism**

Cisplatin [(cis-diamminedichloridoplatinum(II), CDDP or CP] is a platinum-containing small molecule coincidentally detected by Barnett Rosenberg during his studies on bacterial growth (Rosenberg, Van Camp, and Krigas 1965). Later in his studies, he also recognized the pernicious effect of CP on tumor cells (Rosenberg 1973). This discovery then became a milestone in the innovation of anti-cancer therapeutic agents. Until now, CP has been utilized effectively for diverse types of malignant tumor treatment combined with other chemicals (Brown, Kumar, and Tchounwou 2019). Wide-range usage of CP appears with resistance to the tumor itself and several side effects for tissues, such as muscle atrophy, kidney toxicity, or neuropathy or the body itself, dramatically reducing its effectiveness (Sakai et al. 2014; S. H. Chen and Chang 2019; Volarevic et al. 2019; Calls et al. 2021). To overcome these problems, researchers are continuously attempting to uncover its action mechanism at the molecular level. Accumulating DNA

adducts after CP treatment stimulates apoptosis, resulting in cell death (Nagane et al. 1998; Moon, De Leon, and Devarajan 2002; Y. Liu et al. 2008). Additionally, high dosage and long-term usage of this chemical trigger metabolic, genetic, and epigenetic changes resulting in resistance, consequently, cell survival (D. W. Shen et al. 2012; L. Wang et al. 2021).

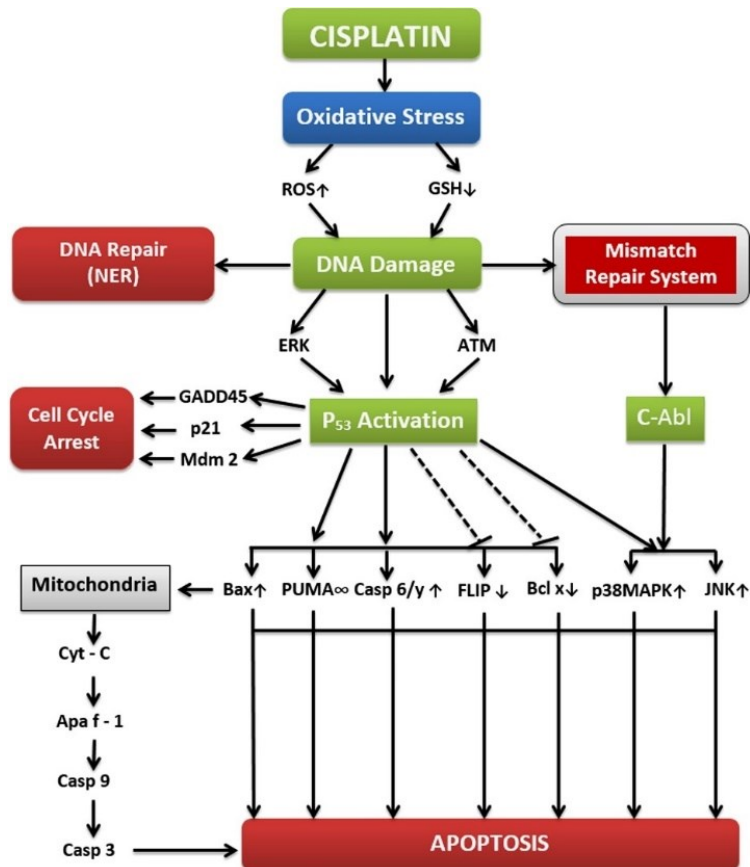


Figure 1.8. The schematic representation of the molecular action of cisplatin after its uptake (Dasari and Bernard Tchounwon 2014).

CP is marketed as a metal (platinum) coordinated white or dark yellow powder and is partially soluble in water or completely soluble in dimethyl sulfoxide (DMSO). The action of CP influence begins with its uptake through mostly passive membrane diffusion and copper transport protein (CTR1) (Eljack et al. 2014). Once it penetrates the cell, CP undergoes activation. Within the cytoplasm, water molecules displace the chloride atoms attached to CP. Hence, the activation of CP is influenced by its milieu. CP exhibits low activity in blood or extracellular tissue fluid, where the chloride concentration is between 96 and 106 mM. However, the chloride ion concentration drops significantly to just a few mM upon entering cells, forming explosive mono- and bi-

aquated CP species (Waissbluth and Daniel 2013). This hydrolyzed form of CP possesses strong electrophilic properties, enabling it to interact with various nucleophiles, such as sulfhydryl groups found on proteins and nitrogen donor atoms in nucleic acids (Ishida et al. 2002). CP's damaging effect is mainly forming DNA-platinum di-adducts by intra-strand crosslinking with purine bases [Pt-d(GpG), Pt-d(ApG), Pt-d(GpXpG)], inducing the DNA damage in both nucleus and mitochondria (Z. Yang et al. 2006; Hu et al. 2016). It further prevents replication and transcription by partially blocking the DNA damage response (DDR) and increases mitochondrial reactive oxygen species (ROS) production, leading to cell death (Figure 1.8) (Fuertes et al. 2003; Kleih et al. 2019).

### **1.2.1. Cisplatin-Induced Apoptosis**

When CP is aquated inside cells, it induces apoptosis via attacking nuclear DNA (nDNA) or mitochondria (Siddik 2003; Z. Yang et al. 2006). Besides binding and forming DNA adducts in the nucleus, the significant apoptotic effect of CP comes about through reactive oxygen species (ROS) production, followed by the induction of oxidative stress (Kleih et al. 2019). In normal cellular conditions, a low ROS concentration triggers fundamental physiological processes such as proliferation and cell cycle, migration, development, and cell death (Hebbar and Knust 2021; Kirova et al. 2022). ROS is an activator for diverse signaling pathways and transcription factors, including ERK/MAPK, PI3K/Akt, p53, and NF- $\kappa$ B, to maintain the balance between cell survival and death (Kaminsky and Zhivotovsky 2014; J. Zhang et al. 2016). To keep equilibrium and avoid excessive ROS production, cells utilize antioxidant enzymes and chemical agents like catalase or glutathione (GSH) (Chaudhary et al. 2023). Active CP inside the cell binds and inhibits GSH and disturbs the respiratory system, engendering a dramatic increase in ROS (Choi et al. 2015). ROS, such as superoxide or hydroxyl radicals, diminish sulfhydryl groups, peroxidize lipids, proteins, and nucleotides, and thus change signaling cascades and DNA, frequently causing apoptosis (Juan et al. 2021). ROS display their apoptotic effect mainly through the mitochondrion. Together with pro-apoptotic Bax and  $Ca^{+2}$ , ROS attacks the mitochondrial outer membrane (MOM) and perturbs membrane permeabilization, resulting in mitochondrial DNA (mtDNA) damage and Cyt-c release (Chunxin Wang and Youle 2009; Orrenius, Gogvadze, and Zhivotovsky 2015). In the direct activation, Cyt c in cytoplasm forms a platform together with APAF1 for initiator

pro-caspase-9 (apoptosome) to dimerize and then activate the executor caspases (-3, -7). Conversely, caspase activation is supported by inhibiting IAPs via Smac/DIABLO and Omi molecules with different mechanisms (Cheng et al. 2001; Y. Li et al. 2017). Studies showed that Smac/DIABLO contains an XIAP binding domain with higher affinity than caspases. As a result of their existence in the cytoplasm, they capture XIAP and prevent the inhibitory function of caspase proteins (Chai et al. 2000).

CP also alters the plasma membrane, causing the upregulation of FAS and FASL proteins (Maurmann et al. 2015). FAS, as a transmembrane receptor, is the chief molecule in the death-inducing signaling complex (DISC), which is composed of the Fas-associated death domain (FADD) and inactive caspase-8 (Siegel et al. 2000). CP activates FADD in two ways: (i) via enhancing FasL expression that binds to the Fas receptor, and (ii) by upregulating Fas itself and changing FADD conformation independent of FasL presence (Micheau et al. 1999; Siegel et al. 2000). Switch in conformation activates caspase-8, which targets both tBid-Bax (intrinsic pathway) and directly executive caspases (caspase-3 and -7), finalizing with apoptosis (Scaffidi et al. 1998; Kantari and Walczak 2011).

CP can induce cell death by producing DNA breaks that initiate the DNA damage response (DDR). Even if one of the main targets of CP is gDNA, merely 1% of it can bind gDNA (Jung and Lippard 2007). However, several non-histone proteins called high-mobility group (HMG) proteins display high affinity for the DNA-CP complex (Pil and Lippard 1992), embodying a shield that protects the DNA adducts from repair mechanisms (Zamble et al. 2002). Three types of pathways participate in the repair process, either to save the cell or to kill it for the good of the organism (Rocha et al. 2018). The Nucleotide excision repair (NER) is the first pathway that recognizes the lesions forming at active transcription sites. Due to the NER system's rapid response and repair capacity, cytotoxicity can be reversed, and the cell survives (Kiss, Xia, and Acklin 2021). The second way is that cells react to the DNA-damaging effect of CP with the Mismatch repair (MMR) system. In contrast to NER, MMR exacerbates CP cytotoxicity by inducing both c-Abl/JNK and p73/p53 cascades (Nehmé et al. 1999; Shimodaira et al. 2003). The final but most potent effect of CP occurs through the formation of double-strand breaks (DSBs) in DNA originating from excessive ROS accumulation (Salehi et al. 2018). In response to DSBs, ERK and ATM/ATR signaling pathways are activated, and phosphorylates p53 become active (Hammond et al. 2002). Consequently, p53 induces cell senescence through MDM2/p53/p21 in the G0/G1 phases and by dimerizing GADD45 family proteins in the S/M phase (Jiandong Chen 2016; Jia Liu et al. 2018).

The stabilized p53 accumulation upon DNA damage mediates apoptosis through the intrinsic pathway. p53 targets a wide range of pro-apoptotic and anti-apoptotic genes; it accelerates apoptosis specifically through PUMA and NOXA. Enhancing the expression of Bid, Bax, and Apaf-1, as well as some death receptors or Bcl-2 and Bcl-xL suppression, can be considered an indirect effect of p53 (Aubrey et al. 2018). Secondly, the aberrant expression of oncogenes, such as c-Myc and E2F, induces apoptosis too. c-Myc and E2F regulate and arrest the cell cycle in normal physiological conditions. Each protein's half-life is relatively short, so they are degraded quickly if the cell cycle processes correctly. Activated DNA damage response machinery leads PTMs to stabilize both proteins, contributing to the expression of pro-apoptotic genes such as PUMA/NOXA, Bax, and TNFR/TRAILR. On the other hand, cytokines/growth factors activated transcription factors such as NF- $\kappa$ B, STAT, IRF-1, and FOXO may feature as both anti-apoptotic (e.g., via targeting pro-survival Bcl-2s and IAPs) and pro-apoptotic (e.g., through Bax/Bak, death receptors or caspases) (Dudgeon et al. 2009; Shirjang et al. 2019).

### **1.2.3. Downstream Events in HeLa Cells after Cisplatin Exposure**

The HeLa cell line is one of the human papillomaviruses (HPV) infected CC types widely used in cancer research. In contrast to many cancer types from different tissues, p53 mutations are not observed in HeLa. Instead, dysregulation of p53 relies on the ubiquitination-dependent proteolysis and inhibited phosphorylation through the action of the HPV-E6 protein complex (Ajay, Meena, and Bhat 2012; C. H. Yuan, Filippova, and Duerksen-Hughes 2012). Moreover, the proteins synthesized through HPV infections contribute to apoptosis regulation as suppressors. It is demonstrated that the HPV-E5 and E6 proteins suppress extrinsic induction of apoptosis, leading to the degradation of death receptors TNFR, Fas, and TRAILR. Bak, caspase-8, and cMyc are also other targets of E6-derived degradation. Besides HPV, E5 and E6 protect the cell from DNA damage via enhancing PI3K/Akt and MAPK pathways (Ciarimboli 2012). Taken into consideration, the anti-apoptotic effects of HPV result in uncontrolled cell growth and proliferation in HeLa cells; thus, HPV-infected other cancer cells.

As a therapeutic agent, CP impedes HPV-E6 expression, halting the degradation of p53. This disruption results in a substantial increase in DNA adducts, ultimately leading to p53-driven apoptosis. Detailed investigations involving both time and dose

dependencies have revealed that the peak levels of p53 accumulation in the nucleus and cytoplasm occur after a 16-hour interval (Y. Liu et al. 2008).

Nevertheless, despite CP's inhibition of HPV expression, cells initiate various alternative mechanisms to mitigate its cytotoxic effects. These mechanisms encompass the reduction of CP accumulation within the cellular milieu, augmentation of DNA repair capacity, attenuation of apoptotic pathways, induction of epithelial-mesenchymal transition (EMT), and the recruitment of non-coding RNAs (ncRNAs) and chaperone molecules (Figure 1.9) (Bhattacharjee et al. 2022).

HeLa-CP-resistant cells (HeLa-CRC) can reduce CP levels inside the cell by almost 50%, inhibiting its uptake and accelerating efflux (Correia and Bissell 2012). The CP uptake is controlled by passive diffusion and CTR1 membrane transporter (Eljack et al. 2014). Even though CP-DNA dimers elevate and disturb the transcription machinery, studies with mouse models expressing HPV-E6 showed that CTR1 proteins were considerably expressed in cervix cancers (Ishida et al. 2002). On the other hand, the efflux of CP was supported by ATP-binding cassette transporters (ABCs) such as MRPs and ABC1 (Gupta et al. 2020). Another transmembrane protein, lysosome-associated protein transmembrane 4B-35 (LAPTM4B-35), promotes CP tolerance and was shown that the upregulated LAPTM4B-35 is correlated with the poor prognosis in patients with CC (F. Meng et al. 2010; Y. Meng et al. 2016). Nucleolin (NCL) is a multifunctional protein primarily located in the nucleoplasm, which instigates resistance to CP in CC through the Y-box protein1/Multidrug Resistant Protein 1 (YB1-MDR1) pathway. Elevated levels of NCL in HeLa-CRCs are associated with heightened expression of MDR1, resulting in intensified CP efflux. Furthermore, the upregulation of NCL prompts increased transcription of the YB1 transcription factor (J. Ke et al. 2021).

The final control mechanism for inhibiting reactive CP inside the cells is the activation of nucleophilic proteins such as GSH. It has been implicated that GSH recognizes intracellular CP and chelates it to keep balance in ROS production (Galluzzi et al. 2012). Doherty et al. reported that GSH-encoding genes like GSTK1, GSTP1, and GSTA4 were upregulated in CP-resistant CC cells (Doherty et al. 2014).

In response to CP, HeLa cells exhibit an augmentation in their DNA repair capabilities. Preliminary investigations into the cellular response to CP-induced DNA damage unveiled that HeLa-CRC cells demonstrated a more significant presence of intact repair-associated DNA regions and an elevated functionality of both NER and MMR mechanisms. Consequently, this heightened repair activity enhances the cells' resilience

to DNA damage caused by CP (Chao 1994). Excision repair cross-complementation group 1 (ERCC1) represents a pivotal component within the NER system, interacting with single-stranded DNA and facilitating its excision. Depleting ERCC1 significantly diminishes the cellular tolerance to CP in various cancer types and exhibits an inverse relationship with the resistance of CC to this chemotherapy (Usanova et al. 2010; Ryu et al. 2017). The MMR system, serving as the secondary pivotal system, operates in a contrasting manner to NER. It predominantly identifies DNA adducts through the action of MSH2 and MLH1 proteins. This recognition event sets upstream apoptotic signals in motion in collaboration with c-Abl and post-meiotic segregation (PMS2), thereby inducing heightened sensitivity to CP. (G. M. Li 2007; R. Li et al. 2020). An additional compensatory mechanism involves enhancing the catalytic function of DNA polymerase by upregulating the expression of REV3L, which serves as the catalytic subunit of DNA polymerase  $\zeta$ . It seems that REV3L facilitates cell proliferation by stimulating the cells to enter the S phase of the cell cycle. Knockout experiments have proved that silencing REV3L leads to notable alterations in the anti-apoptotic genes Bcl-2, Mcl-1, and Bcl-xl, but in an opposing direction. (Gan et al. 2007; L. Yang et al. 2015).

Aside from inhibiting apoptosis, cells orchestrate autophagy and EMT as mechanisms for survival. Much like its capacity to either initiate cell death or support cell viability, an expanding number of research highlight the dual function of autophagy in chemotherapeutic treatment, where its activation can either enhance or undermine their anticancer efficacy. On one side of this spectrum, autophagy is triggered as a protective mechanism and mediates the development of acquired resistance in specific cancer cells (J. Xu and Gewirtz 2022). The ATM-CHK2 pathway plays a pivotal role in the DDR, instigating subsequent signaling cascades such as the activation of p53-p21, p38 MAPK, and PTEN following exposure to CP (Reinhardt et al. 2007). In addition to its role in promoting cell survival pathways, Chen et al. have elucidated that ATM-CHK2 phosphorylates FOXK, a suppressor of autophagy, thereby instigating the process of autophagy (Y. Chen et al. 2020). In addition to the ATM-CHK2-FOXK axis, autophagy is orchestrated through various survival mechanisms such as ATG5-Beclin 1, BCAT1-mTOR, Ras-p38MAPK-ERK, and NF- $\kappa$ B in distinct cancer types, including cervical cancer (Tanaka et al. 2002; D. Lu, Wolfgang, and Hai 2006; Giri et al. 2020; Jianhua Chen et al. 2018).

In conclusion, CP is one of the earliest and most widely employed chemotherapeutic agents. However, over time, its extensive usage in cancer treatment has

given rise to resistance. One approach to addressing this resistance involves elevating its dosage and combining it with other drugs, although this strategy can potentially harm healthy systems (Basak et al. 2022; Tsvetkova and Ivanova 2022). In response to this challenge, ongoing research is directed toward unraveling the mechanisms underlying CP resistance in various carcinomas. This endeavor is further motivated by the emergence of innovative technologies like gene therapy and immunotherapy (Rangel-Sosa, Aguilar-Córdova, and Rojas-Martínez 2017; Stefanoudakis et al. 2023). Thus far, these therapeutic approaches have primarily targeted essential proteins to hinder cancer cell survival or trigger programmed cell death mechanisms at the transcriptional level. Even if gene/immunotherapies exhibit greater specificity toward tumor tissues, the manipulation of essential genes can yield side effects, including neurological, renal, and cardiovascular complications (Roth et al. 2021; Shaikh 2022; Brumberger et al. 2022; T. Li et al. 2023).

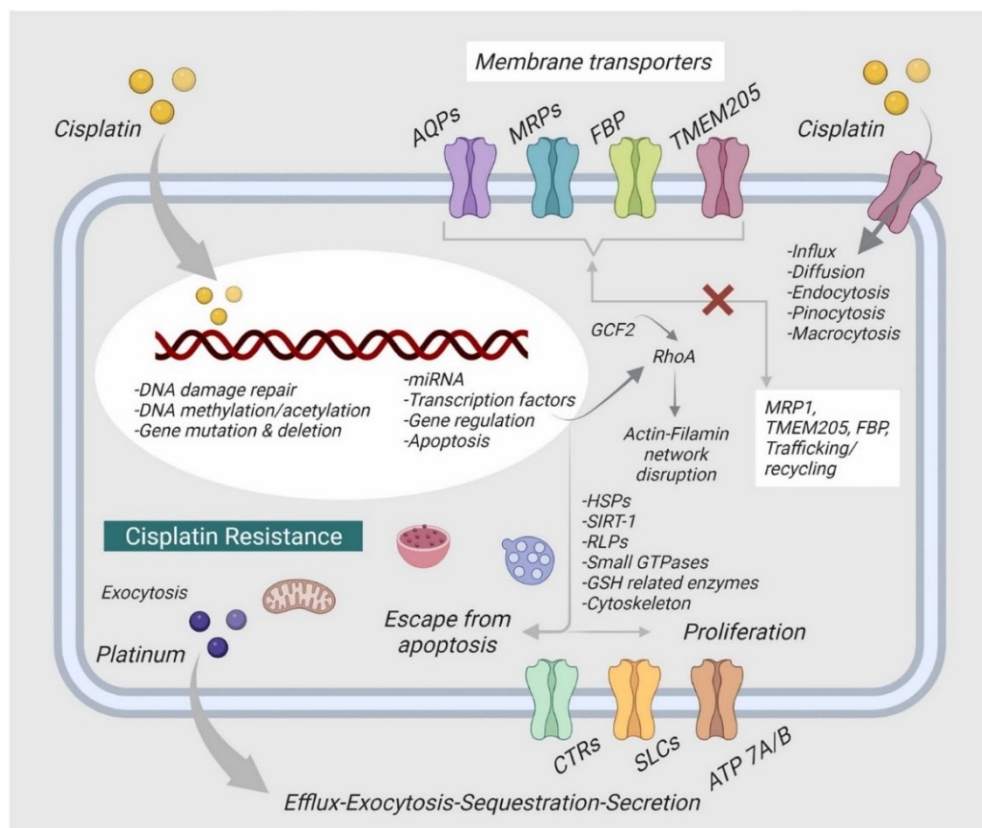


**Figure 1.9. The schematic representation of the HeLa cell response against cisplatin cytotoxicity (Bhattacharjee et al. 2022)**

Post-transcriptional regulation represents a crucial facet of gene expression, facilitating precise adjustments in the protein profile of cells to align with the prevailing

cellular requirements. This mechanism initially evolved as an adaptive response to enhance survival under adverse conditions but has, in turn, been co-opted by cancer cells. Change in this organizing mechanism allows cancer cells to reshape the proteome, thereby signaling pathways in response to chemotherapy (DeOcesano-Pereira et al. 2018).

The N<sup>6</sup>-methyladenosine (m<sup>6</sup>A) modification of mRNA represents one of the most widespread post-transcriptional mechanisms. It substantially influences mRNA fate owing to the abundance of thousands of adenosine residues scattered throughout the transcriptome (Yin et al. 2024). Recent research in the field of cancer has directed its attention toward investigating m<sup>6</sup>A RNA modification and its impact on the efficacy of chemotherapy (Chuhan Wang et al. 2023; W. W. Liu et al. 2023). It has been widely demonstrated that the protein levels of core “writers” are positively correlated with CP resistance by affecting the fate of various genes in an m<sup>6</sup>A -dependent manner. RIPK4 (serine-threonine kinase) acts as an oncogene by inducing NF-κB activators IKKs, thereby inhibiting apoptosis. Increased level of METTL3 in CP-resistant epithelial ovarian cancer (EOC) enhances the stability of RIPK4 in a METTL3-m<sup>6</sup>A RIPK4-YTHDF1 manner (Yin et al. 2024). Co-culture studies have demonstrated that tumor-associated macrophages influenced the expression of m<sup>6</sup>A modulators via cytokines in ovarian cancer. The enhanced levels of WTAP and YTHDF1 and the decrease in ALKBH5 drive the cells to develop CP resistance, indicating the reverse effects of writers and erasers on CP response (L. Hong et al. 2023).

METTL14, an indispensable part of a methyltransferase core, is involved CP resistance by targeting the key axis in ER stress, proliferation, and tumorigenesis in different cancer types. Pancreatic cancer cells express higher METTL14 compared to healthy tissue. The downregulation of METTL14 effectively sensitized the tumor cell to CP by targeting AMPKα, ERK1/2, and mTOR signaling cascades in the m<sup>6</sup>A -dependent axis. (Kong et al. 2020). The oncogenic nature of METTL14 in non-small cell lung cancer (NSCL) was also demonstrated. Moreover, the oncogenic role of METTL14 impacts CP resistance by advancing the maturation of miRNA by directing the microprocessor complex in an m<sup>6</sup>A -driven recognition, leading to the rapid degradation of RBM24. RBM24, a multifunctional protein, is involved in different processes, such as proliferation and apoptosis, and depletion of its protein level elevates the resistance to CP in NSCLS (Gong, Wang, and Shao 2022). METTL14 additionally targets circRNAs and regulates their function. circUGGT2 markedly upregulated in CP-resistant gastric cancer cells. Depletion of METTL14 results in a dramatic decrease in circUGGT2 levels, affecting the

MAP3K9 axis and causing the CP sensitization (X. Y. Chen et al. 2024).

Besides the impact of m<sup>6</sup>A regulators on CP resistance, CP influences their expression pattern. Our group revealed that CP exposure influences the RNA abundance of m<sup>6</sup>A effectors, particularly METTL14 in MCF7 and A549 cell lines and FTO in HeLa, MCF7, and A549 cells, with a reduction (Alasar et al. 2022; Akçaöz Alasar et al. 2023). However, the mechanism behind the CP response in HeLa cells through m<sup>6</sup>A -methylation patterns is required for more detailed investigation. This study hypothesizes that the m<sup>6</sup>A RNA modification is an essential regulatory mechanism participating in the CP response.

The aim of this thesis is to identify the CP-derived alteration in m<sup>6</sup>A marks in the transcriptome manner, mainly focusing on the relation in CP response and to investigate the functional role of METTL14 on CP response and the possible mechanisms behind it. In brief, the main objective is subdivided into five parts: (i) detecting the protein levels of m<sup>6</sup>A core modulators in response to CP exposure due to their effects on the m<sup>6</sup>A landscape, (ii) analyzing the transcriptome-wide extent of m<sup>6</sup>A methylation in CP-treated HeLa cells comparison to control, (iii) selecting differentially methylated and expressed genes playing roles in the CP-induced phenotype oh HeLa cells, (iv) evaluating the relation between METTL14-derived m<sup>6</sup>A modification and CP effect on HeLa cells, and (v) investigating the differential binding affinity of YTHDFs to those candidates highlighting the possible mechanism behind the m<sup>6</sup>A modification involving the CP response.

The results obtained from this thesis are valuable in enhancing our understanding of the interplay between m<sup>6</sup>A RNA modification and its role in CP response with two main outcomes. First, the impact of CP on transcriptome-wide m<sup>6</sup>A patterns may elucidate the regulation of this modification in response to an external stimulus. Second, understanding the temporal dynamics of m<sup>6</sup>A methylation and the status of m<sup>6</sup>A regulators affecting the overall cellular response can provide insights into optimizing chemotherapy regimens via targeting the m<sup>6</sup>A modulators.

## CHAPTER 2

### MATERIAL AND METHODS

#### 2.1. Cell Culture and CP Treatment

HeLa cell line was procured from DSMZ GmbH (Germany), frozen stock cells were thawed in a 37°C water bath and suspended in RPMI 1640 (Gibco, Thermo Fischer, USA) medium with 2 mM L-glutamine and 10% fetal bovine serum (FBS) (Gibco, Thermo Fischer, USA). The suspension was transferred into a T-25 flask and kept in a sterile, humidified incubator at 37°C, with 5% CO<sub>2</sub>. The medium was refreshed every 2 days until cells reached 95% confluency. Cells were passaged every two days by trypsinization and divided (2 x 10<sup>6</sup> cells for each flask) into T-75 flasks until needed.

CP was applied to HeLa cells seeded into 10 cm<sup>2</sup> dishes (0.5 x 10<sup>6</sup> cells/dish) as triplicates the day before treatment. Because of its chemical instability, CP (Santa Cruz) was freshly dissolved in DMSO to prepare 80 mM stock before each treatment. Thus, DMSO, as the solvent of CP, was utilized as a negative control in 0.1 % (v/v) concentration. Based on previously established time- and dose-kinetic studies (Yaylak, Erdogan, and Akgul 2019) in our lab, cells were incubated with full RPMI containing 80 µM CP (Santa Cruz) for 16 hrs to obtain approximately 40 to 50% apoptosis. Lower doses of CP were applied to siRNA-transfected HeLa cells due to fragility infringed by transfection, where a similar concentration of DMSO was maintained.

#### 2.2. Detection of Apoptosis by Flow Cytometry

Flow Cytometry technique was performed to analyze the apoptosis rate after CP treatment. The membrane of apoptotic cells exhibits the externalization of cytosolic phosphatidylserine (PS) and an increased presence of DNA adducts within the cytoplasm. To this extent, the disturbed membrane and DNA of the cells were targeted by Annexin V-7AAD antibodies (Steensma, Timm, and Witzig 2003; Dong et al. 2009). At the end of CP treatments, cells were harvested using 1x Trypsin-EDTA (Gibco, Thermo-Fisher, USA). Cell pellets from both DMSO and CP samples were washed with 1x Phosphate-

buffered saline (PBS) (Gibco, Thermofisher, USA), then 1X Annexin binding buffer (BD Biosciences, USA), 1:10 diluted AnnexinV-FITC (BD Biosciences, USA), and 1:10 7AAD (BD Biosciences, USA), respectively. After a 15-minute incubation at room temperature (RT) in the dark, the population percentages were quantified using the FACSCanto flow cytometer (BD Biosciences, USA). The gating strategy classified the cells into four categories: Annexin V<sup>-</sup>/7AAD<sup>-</sup> (alive), Annexin V<sup>+</sup>/7AAD<sup>-</sup> (early apoptotic), Annexin V<sup>+</sup>/7AAD<sup>+</sup> (programmed cell death/late apoptotic), and Annexin V<sup>-</sup>/7AAD<sup>+</sup> (necrotic).

### **2.3. WST-8 Assay for Cell Proliferation and Viability**

The proliferation/viability rates were quantified by Cell Counting Kit – 8 (CKK-8, Sigma-Aldrich, USA) according to the manufacturer's protocol. The kit is based on WST-8, an anionic tetrazolium salt, which penetrates a living cell in the presence of dehydrogenase enzyme activity and is reduced to form a purple precipitate, formazan. This color change is rated by absorbance measurement (Tsukatani et al. 2014).

Upon the completion of treatments in 96-well plates, 10 µL WST-8 reagent was added directly to the 100 µl culture media, and all were incubated for 2 hrs in a humidified incubator. The absorbance was quantified by spectrophotometer (Thermo-Fisher, USA) at 450 nm wavelength. Culture media without cells was used as blank control.

### **2.4. Total RNA Isolation**

Total RNA from HeLa cells was isolated with RiboEx total RNA isolation solution (GeneAll, ROK). Cell pellets were homogenized in RiboEx solution (500 µL/ 2 – 5 x10<sup>6</sup> cells) through pipetting. After 5 min of incubation in RT to disassociate RNA from other macromolecules, chloroform, a 1 to 5 ratio of RiboEx, was added, followed by shaking vigorously for 15 sec and 2 min of incubation at RT, respectively. Following the centrifugation at 12,000 x g for 15 min at 4°C, phase separation, the aqueous phase containing total RNA was carefully transferred into a new tube, avoiding the contamination of lower phases. Then, the total RNA was precipitated by mixing with 10 µM glycogen (Sigma-Aldrich, USA) and 100% isopropyl alcohol [1 to 2 (v/v) of RiboEx]. To increase precipitation efficiency, the mixture was incubated for 2 hrs at -20°C, then

centrifuged for 10 min at 12,000 x g at 4°C. The pellet was washed with 75% ethanol [1 to 1 (v/v) of RiboEx] prior to centrifugation for 5 min at 7500 x g at 4°C. The RNA pellet was air-dried for 10 - 20 min at RT to remove traces of ethanol contamination. Dried RNA was suspended in nuclease-free ddH<sub>2</sub>O and heated at 60°C for 10 min to remove secondary structures. RNA integrity was then determined in a 1% TBE-agarose gel. RNAs were kept at -80°C until use. The reagent amounts in this protocol were adjusted according to the cell number collected from various experimental set-ups, such as CP treatment or transfection with different well-plates and dishes.

## 2.5. Quantitative Polymerase Chain Reaction (qPCR)

cDNA was prepared from total RNA utilizing iScript™ cDNA Synthesis Kit (Bio-Rad, USA) according to the manufacturer's instructions. cDNA was then diluted 20-fold with nuclease-free water before use.

**Table 2.1. qPCR components**

<b>Component</b>	<b>Volume</b>	<b>Final Concentration</b>
GoTaq® qPCR Master Mix (2X)	10 µl	1X
Forward Primer (10 µM)	0.6 µl	300 nM
Reverse Primer (10 µM)	0.6 µl	300 nM
cDNA (~200 ng/µl)	1 µl	~10 ng/µl
Nuclease-free water	Up to 20 µl	-

The qPCR reactions were performed in triplicates using the GoTaq qPCR master mix (Promega, USA) and primers (Table 2.1) in Rotor-Gene Q thermal cycler (Qiagen, Germany) (Table 2.2). The primer sequences are listed in Table 2.3. RNA abundance for each gene was calculated using the  $2^{-\Delta\Delta Ct}$  method after normalizing against the reference gene (GAPDH).

## 2.6. Western Blotting

The total protein was extracted with lysis buffer composed of 1X radio-immunoprecipitation assay (RIPA) solution (CST, USA) and 1X protease inhibitor cocktail (Abcam, USA). The protein concentrations were determined by the Bradford

assay, in which BSA was the protein standard.

**Table 2.2. Cycling conditions for GoTaq qPCR Master**

Step	Cycles	Temperature	Time
Polymerase activation	1	95°C	2 min
Denaturation		95°C	15 sec
Annealing	40	60°C	30 sec
Extension		72°C	30 sec

**Table 2.3. The primer sequences for each gene utilized in**

CDCA5	CCCTGAAATCTGGCCGAAGA	GATTGGACAGCTGGGACCTC
ATF3	GCAAGTGCATCTTTGCCTCA	GCTGCCTGAATCCTAACGGT
JUN (AP-1, cJUN)	GCAGTATAGTCCGAACTGCAAAT	CTCTCTGGACACTCCCCGAAAC
ATF5	GCTACAGCCATGTCACTCCT	CAAGGACCTCATAGGGAGCC
BMF	CAAGGCCATCAGCTTCAGAGA	GAGACAGTGCAGTCAGACCA
BCL2	TTCCTGATGCGGAAGTCACC	CCAACTCCCAATACTGGCTCT
MAD1L1	AGCATGACTGACAGACACGC	CACAAGGTGAGGAACCCAGG
DAPK1	GCCGCAGACTTTTTGCTGAA	CCCTCACCGGGATAACAACAG

25 µg of total protein was fractionated on a 10% SDS-polyacrylamide gel in 1 x Tris-glycine (25 mM Tris, 192 mM Glycine, and 0.1% SDS) buffer utilizing SDS-PAGE system (Bio-Rad, USA). Then, resolved proteins were transferred onto the PVDF membranes (Millipore, USA). The membrane was blocked with 5% non-fat dry milk (CST, USA) in 1X TBS-T buffer. Primary and secondary antibody concentration and incubation conditions were applied, as listed in Table 2.4. The blotting signals were visualized with an ECL substrate (Bio-Rad, USA and ThermoFischer, USA) and quantified using the ChemiDoc XRS+ imaging system (Bio-Rad).

**Table 2.4. The list of antibodies utilized in western**

<b>Antibody</b>	<b>Dilution Factor</b>	<b>Company</b>
Anti-Caspase 3	1:1000 in 5% BSA	CST, USA
Anti-Caspase 9	1:1000 in 5% BSA	CST, USA
Anti-METTLL3	1:1000 in 5% BSA	CST, USA
Anti-METTLL14	1:1000 in 5% BSA	CST, USA
Anti-FTO	1:1000 in 5% BSA	CST, USA
Anti-WTAP	1:1000 in 5% BSA	CST, USA
Anti-PARP	1:1000 in 5% BSA	CST, USA
Anti-HaLo Tag	1:1000 in 1X TBST	Promega, USA
Anti- $\beta$ -actin (Mouse)	1:2000 in 0.5% Milk	CST, USA
Anti- $\beta$ -actin (Rabbit)	1:2000 in 0.5% Milk	CST, USA
Anti-Mouse	1:10000 in 0.5% Milk	CST, USA
Anti-Rabbit	1:10000 in 0.5% Milk	CST, USA

## 2.7. m<sup>6</sup>A-eCLIP-seq and Bioinformatic Analysis

Three biological replicates of total RNAs isolated from both DMSO- and CP-treated HeLa cells were subjected to the m<sup>6</sup>A-enhanced crosslinking and immunoprecipitation followed by RNA sequencing (m<sup>6</sup>A-eCLIP-seq) by Eclipse Bioinnovations (USA) as shown in Figure 2.1 (Roberts, Porman, and Johnson 2021). The m<sup>6</sup>A-eCLIP-seq method, a revolutionary approach in RNA analysis, simplifies the processes of mRNA isolation, eCLIP sample preparation, and library preparation. This method, known for its precision, employs a reliable and consistent approach to accurately identify and locate binding sites on target RNA molecules. The immunoprecipitation step utilizes a particular antibody, ensuring the selective enrichment of RBP-bound target RNAs. To generate high-quality libraries, the RNA is chemically fragmented into 100 nucleotides or smaller fragments (Van Nostrand et al. 2016) (Figure 2. 1).

Eclipse Bioinnovations performed the raw data analysis based on their standard workflow for m<sup>6</sup>A-eCLIP-seq. The m<sup>6</sup>A-eCLIP data processing pipeline initiates by trimming unique molecular identifiers (UMIs) by UMI tools (Smith, Heger, and Sudbery 2017) and adapter sequences from the raw sequencing reads by Cutadapt (Martin 2011). The filtered reads undergo the removal of repetitive genomic elements, such as rRNA, and are aligned to the reference genome, human GRCh38/hg38, by STAR aligner. After alignment, PCR duplicates are eliminated (UMI-tools), and the identification of m<sup>6</sup>A

modification peaks, represented by clusters of reads, was initially performed using the CLIPper tool (<https://github.com/YeoLab/clipper>). The reproducibility of these clusters among biological triplicates of each sample was assessed through IDR analysis (Q. Li et al. 2011)

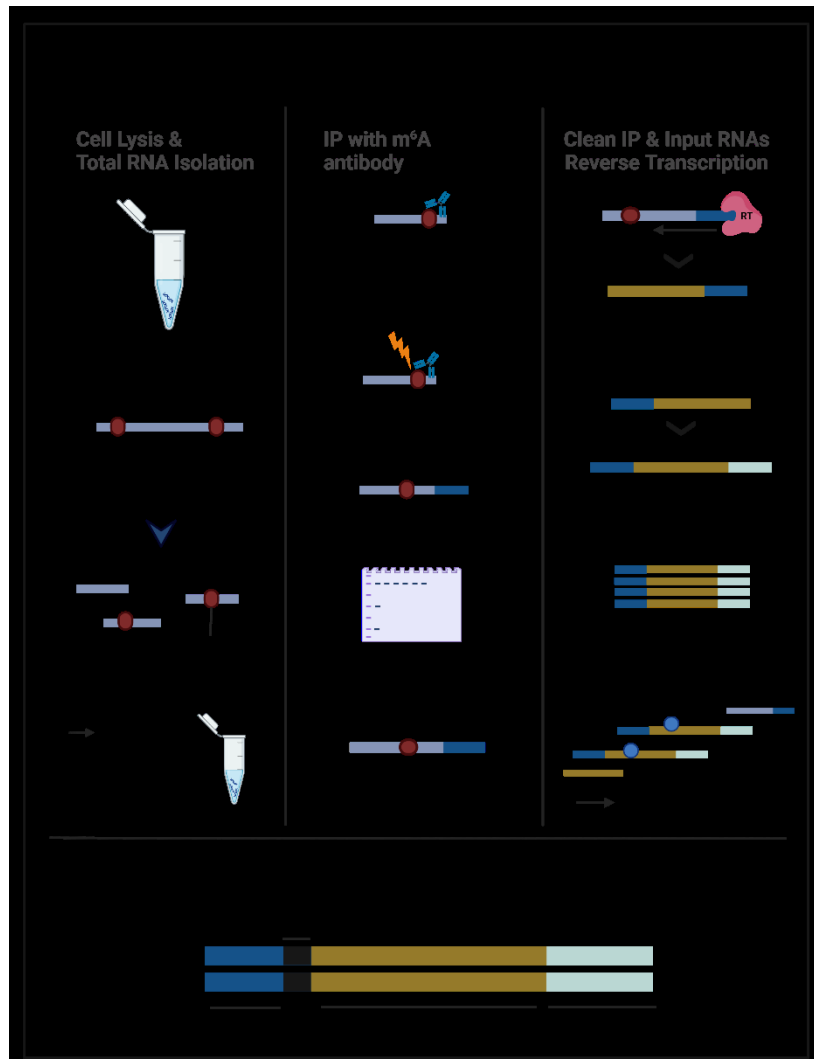


**Figure 2.1. Schematic representation of the m<sup>6</sup>A-eCLIP streamline.** (Eclipsebio, m<sup>6</sup>A-eCLIP Technology, Data Sheet).

To determine the fold change, a logarithmic transformation ( $\log_2$ ) was calculated in two steps: (i) comparing the  $\log_2$  fold change of the IP samples relative to their corresponding inputs and (ii) comparing the  $\log_2$  fold change of the CP-treated samples relative to their corresponding DMSO controls, and vice versa. Further analysis aimed at determining crosslink sites at a single nucleotide resolution in IP-enriched samples was conducted using PureCLIP (Krakau, Richard, and Marsico 2017). The validation of crosslink sites involved evaluating the reproducibility of m<sup>6</sup>A sites among the three

replicates and identifying the presence of the DRACH motif, which is commonly associated with m<sup>6</sup>A sites. Each crosslink site was annotated to the corresponding gene and feature type based on the GENCODE Release 32 (GRCh38.p13). The data were further sorted according to their relative peak frequency, which maps each feature represented by a metagene plot with MetaPlotR package (Olarerin-George and Jaffrey 2017). The motif analysis was carried out utilizing HOMER motif analysis (Heinz et al. 2010).

m<sup>6</sup>A-eCLIP- and RNA-sequencing were performed simultaneously to identify m<sup>6</sup>A marks whose abundance is independent of transcript changes. The peaks from RNA-seq data were accepted as “input” to normalize IP sequencing data. To gain comprehensive insights, differential expression analysis was performed by processing expression data from BAM files. The data underwent trimming, deduplication, alignment, and sorting before being used for gene counting. A count matrix was generated by featureCounts from the Subread package in the Conda environment. (Liao, Smyth, and Shi 2014). Both normalization and differential expression analysis were executed using the DESeq2 package upon the count matrix loaded into R (Love, Huber, and Anders 2014). Heatmap analysis was also carried out using the heatmap package to confirm differential expression patterns of the top thousand genes in each DMSO and CP sample.

Finally, target enrichment analyses, including KEGG, GO, and Reactome pathway analyses were conducted to interrogate the m<sup>6</sup>A extent in more detail, as explained in section 2.8 (Figure 2.2). In addition to pathway analysis, the distribution of features that map to m<sup>6</sup>A methylated points and the frequency of m<sup>6</sup>A sites on a transcript were visualized by the ggplot2 graphic package (Heinz et al. 2010).

## **2.8. Candidate Selection and Primer Designing for m<sup>6</sup>A Points**

Several parameters were taken into account to identify candidate genes with de-regulated m<sup>6</sup>A marks for further analysis. First of all, considering the impact of CP on cell survival and death, priority was given to the genes with de-regulated m<sup>6</sup>A marks that are known to be associated with cell cycle, DNA damage response, cellular response to stress, NF-κB signaling cascade, autophagy, and programmed cell death (apoptosis). This screening was performed using standard pathway analysis tools, such as KEGG, GO, and Reactome (Kanehisa and Goto 2000; Kanehisa 2019; Thomas et al. 2022; Kanehisa et al.

2023; Milacic et al. 2024).

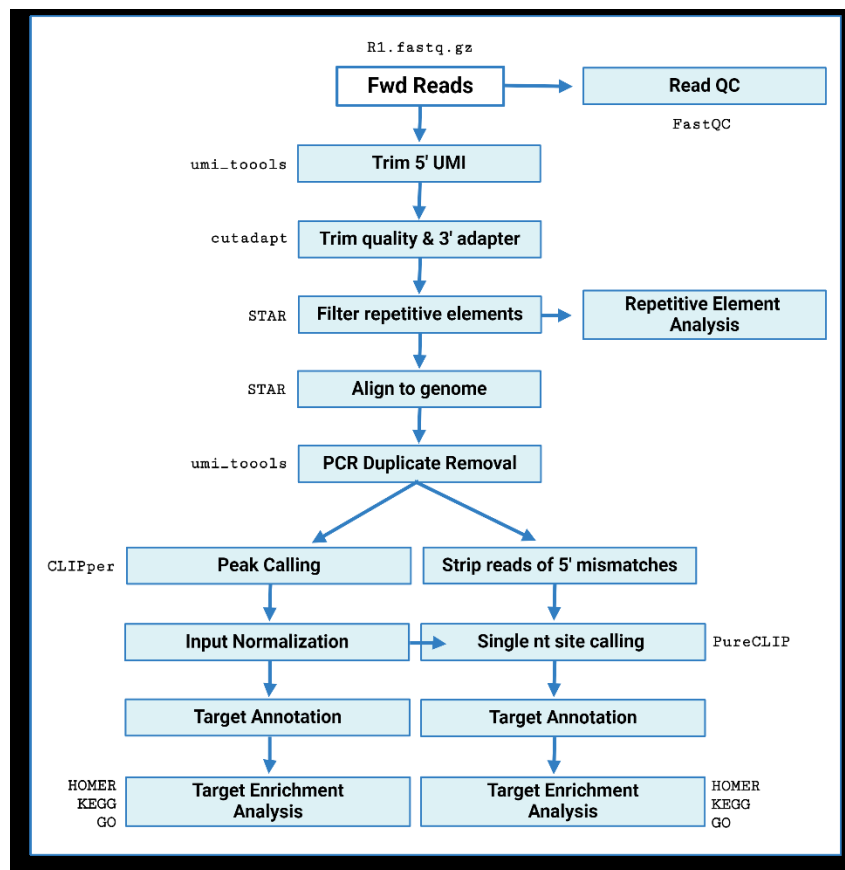


Figure 2.2. Schematic representation of m<sup>6</sup>A-eCLIP data analysis pipeline.

(Eclipsebio, m<sup>6</sup>A-eCLIP, Data Review Guide).

At the second stage, the genes were categorized based on their expression and methylation levels, as observed in our RNA-seq and m<sup>6</sup>A-eCLIP-seq data, respectively. To ensure the generation of more pertinent findings in line with the hypothesis, a log<sub>2</sub> fold-change threshold of  $\pm 1$  was set for differential expression, and a threshold of  $\pm 3$  was considered for differential methylation. The genes in the intersection set between RNA-seq and m<sup>6</sup>A-eCLIP were further subjected to GSEA (Subramanian et al. 2005). Then, the 30 potential genes that function in apoptosis, the p53 pathway, TNFA-NF $\kappa$ B pathway, stress response, and cell cycle regulation were selected for the subsequent sorting step.

Finally, the last sorting was performed based on the number and location of methylation sites on candidate transcripts. The rationale was that the genes with more differential methylated points on 5'UTR, CDS, and 3'UTR might be regulated post-transcriptionally or translationally by m<sup>6</sup>A methylation. In addition to these steps, the binding potential of three selected reader proteins (YTHDFs) to the target methylated points was confirmed by the CLIP database in the POSTAR3 platform (W. Zhao et al.

2022).

## **2.9. METTL14 Knockdown by siRNA**

The effect of m<sup>6</sup>A modification on cellular response to CP concerning apoptosis and proliferation was further interrogated by METTL14 knockdown in HeLa cells. To target METTL14 mRNA, an On-target METTL14 siRNA (siMETTL14) cocktail and non-targeting control siRNA (siNC) (Dharmacon, USA) were separately transfected into HeLa cells utilizing DharmaFECT-1 transfection reagent (Dharmacon, USA).

3000 HeLa cells were seeded per well in a 96-well plate one day before transfection. In individual tubes, 0.5 µl of 5 µM siRNA (25 nM final concentration) and 0.2 µl of DharmaFECT-1 transfection reagent were diluted with serum-free media (SFM) to achieve a total reaction volume of 10 µl per tube. At the end of a 5-min incubation period, the contents of the tubes were gently combined and incubated for 20 min. Subsequently, the transfection mixture was mixed with an appropriate volume of RPMI supplemented with 10% FBS to achieve a final volume of 100 µl per well. Cells were treated with appropriate CP concentration (in section 2.1) at 16 hrs before the 24<sup>th</sup>, 48<sup>th</sup>, 72<sup>nd</sup>, and 96<sup>th</sup>-hour time points and analyzed for cell viability with WST-8.

For the transfection of 100 mm dishes, 6 x 10<sup>5</sup> cells were used per dish. 16 µl of DharmaFECT-1 reagent and 2 µl of siRNA were diluted in 800 µl SFM. The rest of the protocol was applied as explained for a 96 well-plate, while the final volume was 8 ml/dish at this set-up. Finally, the cells were treated with 40 µM CP for 16 hrs before the 24<sup>th</sup>, 48<sup>th</sup>, 72<sup>nd</sup>, and 96<sup>th</sup>-hour time points. Following this treatment, the cell proliferation and apoptosis rate were determined, as explained previously. Additionally, total RNA and protein were isolated for further analyses.

## **2.10. Overexpression of METTL14 and Halo-tagged YTHDF Proteins**

The overexpression plasmids were constructed according to the traditional molecular cloning method (Sambrook, Fritsch, and Maniatis 1989). The coding region of METTL14 was cloned in the pcDNA 3.1(+) expression vector. METTL14 (ENST00000388822.10) coding sequence obtained from the Ensembl genome browser was amplified with Q5 High Fidelity DNA polymerase (NEB, USA) using the primer

sequences listed in Table 2.5. To generate sticky ends, the insert was double-digested with the same enzyme combination used in the vector linearization (explained below). The amplicon was purified through a 1% agarose gel followed by a clean-up step utilizing a PCR clean-up kit (Macherey-Nagel, Germany) per the manufacturer's protocol. The purity and concentration of the eluate were determined by NanoDrop ND-1000 spectrometer (Thermo Fisher, USA).

**Table 2.5. The primer sequences of each gene for amplifying their coding**

METTL14	CATGCTAGCATGGATAGCCGCTTG	GTAGCGGCCGCTTATCGAGGTGGAAAG
---------	--------------------------	-----------------------------

pcDNA 3.1 (+) backbone was simultaneously digested by NheI-HF (NEB, USA) and NotI-HF (NEB, USA) and dephosphorylated by calf intestinal-alkaline phosphatase (CIP) (NEB, USA). The digested vector was isolated from an agarose gel and cleaned with a PCR clean-up kit (Macherey-Nagel, Germany). The insert and the backbone were ligated in a 6:1 ratio (w/w) by incubation with T4 DNA Ligase at 16°C overnight. The next day, both the ligation mixtures and the linearized backbone as negative control were transformed into appropriate competent cells (DH5 $\alpha$  or Top10) and incubated at 37°C for 12 hrs right after being spread onto LB agar with ampicillin (50mg/ml). Transformants were confirmed first by colony PCR and then via Sanger sequencing after plasmid isolation by plasmid mini-prep kit (Macherey-Nagel, Germany).

Similar to the METTL14 overexpression vector construction approach, the same protocol was applied to construct Halo-tagged YTHDF2 (ENST00000373812.8) (Table 2.5). However, in this cloning set-up, pHTN-HaLoTag CMV Neo (Promega, USA) instead of pcDNA3.1 (+) was used to tag these three readers with the HaLo epitope at the N-terminus.

The resulting plasmids were amplified on a large scale and prepared as endotoxin-free via a midi-prep EF plasmid isolation kit (Macherey-Nagel, Germany) according to the manufacturer's instructions before transfection.

HeLa cells were transiently transfected with plasmids (overexpression or empty vectors) using Fugene HD transfection reagent (Promega, USA) according to the manufacturer's recommendations for METTL14. For HaLo-YTHDF2, cells were transfected using a polyethyleneimine (PEI)/chloroquine diphosphate protocol as

described by Longo P.A. et al. (2013). Prior to transfection, stock solutions of PEI (linear, MW 25,000) (Polysciences Inc., USA) and chloroquine diphosphate (Sigma, USA) were prepared at concentrations of 1 mg/ml and 25 mg/ml, respectively.

**Table 2.6. HeLa cell density and pcDNA/PEI**

150 mm	$1.2 - 1.3 \times 10^6$	20 ml	20 $\mu$ g in 1 ml SFM	70 $\mu$ g in 1 ml SFM
6-well	$0.8 - 1 \times 10^5$	2 ml	2 $\mu$ g in 100 $\mu$ l SFM	7 $\mu$ g in 100 $\mu$ l SFM

HeLa cells were detached using trypsin and seeded in appropriate amounts as specified in Table 2.6. The following day, the cells were treated with chloroquine diphosphate at a final concentration of 25  $\mu$ g/ml for 5 hrs before transfection. The pHTN-HaLoTag plasmid and PEI were prepared separately with serum-free media (SFM) in two tubes, as shown in Table 2.6. After a 5-min incubation, the two tubes were gently mixed and further incubated for 25 min at room temperature. The resulting transfection mix was then added to the complete media containing chloroquine. After 8 hrs, the media was refreshed with RPMI complete (with 10% FBS) to minimize any potential toxic effects caused by the transfection reagent. Cells transfected with each plasmid were monitored under the microscope for potential phenotypic changes or collected at specific time points for downstream functional analysis (Flow cytometry, WST-8 assay, CLIP-qPCR, western blotting, etc.).

## **2.11. Formaldehyde Cross-linking and Immunoprecipitation and qPCR (fCLIP-qPCR)**

The functionality of m<sup>6</sup>A marks primarily depends on an interaction with general reader proteins (Yang Y. et al. 2018). To investigate and validate the target RNAs of reader proteins under CP-induced apoptotic conditions in HeLa cells, cross-linking and immunoprecipitation sequencing (CLIP-seq) was performed to determine the exact binding points of RBP on transcripts through UV-induced covalent bonds between RNA and RBP (Ule, Hwang, and Darnell 2018). CLIP, followed by reverse transcription and

qPCR, were developed from this technique to quantify target RNA-RPB interactions (Yoon and Gorospe 2016). To address the challenges of UV crosslinking for fixing detached apoptotic cells post-CP treatment, we refined the CLIP-qPCR protocol by incorporating formaldehyde crosslinking in place of UV (B. Kim and Kim 2019).

HeLa cells expressing Halo-YTHDF2, or EV (negative control for overexpression), were treated with CP for 16 hrs before the end of optimal expression time for YTHDF2 (48<sup>th</sup> hrs) as explained in section 2.1.  $2 \times 10^7$  cells/reaction were determined to be the optimal number of cells to obtain enough amount of protein and RNA product after immunoprecipitation. After harvesting and washing with 1 x PBS (Gibco, ThermoFisher, USA), HeLa cells were crosslinked with 1% formaldehyde (ThermoFisher, USA) for 30 min at RT. The reaction was quenched with 0.125M Glycine (Sigma Aldrich, USA) for 5 min. Then, samples were washed twice with 1x PBS to remove the fixation mix. Residual PBS was aspirated, followed by lysis of cells with pre-chilled 1 x Cell Lysis buffer (Table 2.7) and the sonication with the 30 sec on, 30 sec off, 75% amplitude setting for a total of 2 hrs at 4°C. The lysates were centrifuged at 15000 x g at 4°C for 10 min to remove residual cellular materials. Cell lysates were kept in ice during bead pre-clearing. The precipitation of protein-bound RNAs was performed using Magne HaLoTag (Promega, USA) magnetic beads. Before hybridizing beads and halo-tagged proteins, magnetic beads were pre-cleared by washing three times with 1 x Equilibrium buffer and three times with 1x Cell Lysis Buffer (Table 2.7). Before the hybridization with the beads, 1% of lysate for each protein and RNA “input” was saved in two separate 1.5 ml Eppendorf tubes. Then, beads and cell lysates were merged and incubated on a rotator overnight at 4°C. The next day, the hybridized mix was placed on the magnetic rack (Millipore, USA), and the supernatant of each sample was collected into a new tube as an unbound protein control. Bead-protein-RNA pellets were washed four times for 5 min on a rotator at 4°C with 1 x DWB (Table 2.7), followed by three times with 1 x IsoWB (Table 2.7). Afterward, the pooled duplicates were divided into twelve independent tubes (six for protein detection and six for RNA isolation).

For precipitated RNA isolation, the bead complex was washed with 2 x pK-U/rea (three times) to remove residual components such as lipids and unwanted chemicals except the bead-protein-RNA complex and to equilibrate for protease reaction. The mixture was subjected to the protein digestion protocol. The 2x pK-Urea buffer was diluted with nuclease-free water in a 1:1 ratio. After the addition of 15 µl (12 units) Proteinase K (NEB, USA) enzyme, the tubes were incubated at 65°C with 800 rpm

shaking overnight. The following day, the beads were separated from RNAs by the degradation of proteins using the magnetic rack. The supernatant was divided into new tubes, 100  $\mu$ l of each. 500  $\mu$ l TRIzol was added to each tube, vortexed, and incubated for 5 min at RT, followed by 100  $\mu$ l chloroform addition. The mixture was centrifuged at 12000 x g for 15 min at 4°C to separate the RNA containing aqueous phases from the rest. The RNA was eluted using miRNeasy Kit (Qiagen, USA) according to the manufacturer's protocol for qPCR analysis.

**Table 2.7. Buffers and their contents used in CLIP-qPCR**

Cell Lysis Buffer	50 mM Tris-HCl (pH 7.4), 15 mM NaCl, 10 mM EDTA, 0.1% SDS, 0.1% Na-Deoxycholate, 0.5% NP-40, 0.1% Triton X-100, 1xPMSF, 1xProtease Inhibitor Cocktail, 0.1 U/ $\mu$ l RNase Inhibitor.
Isotonic Wash Buffer (IsoWB)	50 mM Tris-HCl (pH 7.4), 150 mM NaCl, 10 mM EDTA, 0.5% NP-40, 1x PMSF, 1xProtease Inhibitor Cocktail, 0.1 U/ $\mu$ l RNase Inhibitor.
2x pK-Urea Buffer	200 mM Tris-HCl (pH 7.4), 100 mM NaCl, 20 mM EDTA, 2% SDS, 7 M Urea

The western blotting of proteins isolated from input and IP samples was performed to assess the IP efficiency. TEV protease digestion was performed to release target protein from covalently bound beads. Beads were resolved in 50  $\mu$ L of 1x TEV Buffer (Table 2.7) supplemented with 1  $\mu$ l TEV Protease (NEB, USA). The tubes were then incubated in a thermomixer for one hour at 30°C, shaking at 500 rpm. The beads were separated from the lysate by magnetic racks. The protein was further denatured with 1 X Laemmli buffer and prepared for western blotting protocol.

## 2.12. Statistical Analysis

All results obtained from flow cytometry, WST-8 assay, qPCR, and western blotting were analyzed using GraphPad Prism 8 software (La Jolla, CA, USA). The student's t-test was employed to assess the statistical differences between the two groups. Two-way ANOVA analysis was preferred to simultaneously calculate the significance among multiple parameters (silencing, drug treatment, hrs) for the WST-8 assay. Each

experiment was replicated three times, and the data were presented as mean $\pm$ SD (standard deviation).

The statistical analysis of gene ontology (GO) enrichment and Reactome pathway was performed using a Bonferroni correction for multiple tests. This correction multiplies the single-test P-value by the number of independent tests to obtain an expected error rate. The Bonferroni correction was chosen because it simultaneously proceeds many statistical tests (one for each pathway or ontology term), representing more accurate results (Goeman and Solari 2014).

## CHAPTER 3

### RESULTS

#### 3.1. CP Alters the Abundance of mRNAs and Proteins of m<sup>6</sup>A Modulators in HeLa Cells

CP, a time-tested chemotherapeutic drug, has been a stalwart in the fight against cancer for nearly three decades. Its efficacy in inducing apoptosis across various cancer types is well-documented (Kelland 2007; Dilruba and Kalayda 2016). In our study, we meticulously applied different dosages of CP, ranging from 10 $\mu$ M to 160 $\mu$ M (Figure 3.1A), to determine the IC<sub>50</sub>, a measure of the drug's potency, for HeLa cells, as previously reported by our group (Gurer et al. 2021). The WST-8 results indicated that the cell viability was reduced to 97%, 82%, 84%, 53%, and 20%, respectively, in a dose-dependent manner where the viability of DMSO control was 94% (Figure 3.1A).

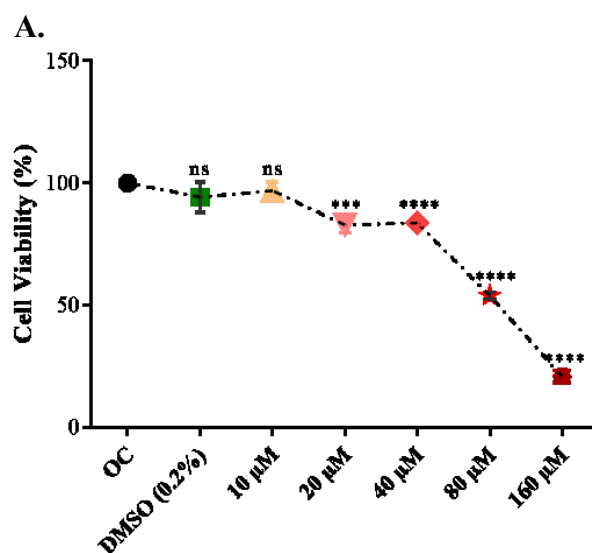


**Figure 3.1. The effect of cisplatin on HeLa cell viability and apoptosis.** 10 to 160  $\mu$ M CP and 0.1% (v/v) DMSO were applied to 5000 cells/well (96-well plate) for 16 hrs. **A.** WST-8 assay was performed to measure the viability. **B.** The rate and stage of apoptosis among the population after 80  $\mu$ M CP treatment for 16 hrs compared to the 0.1% DMSO control were measured by Annexin V//AAD staining in flow cytometry. Dot-blot analysis shows the distribution of alive and apoptotic cells, with the percentage of live, early, and late apoptosis. **C.** Western blot analysis of total protein collected from the same cell population demonstrating caspase 9 and 3 cleavage in HeLa cells. Experiments executed as triplicates. (\*:  $p \leq 0.05$ , \*\*\*:  $p \leq 0.001$ , \*\*\*\*:  $p \leq 0.0001$ ). (Continues on next page)

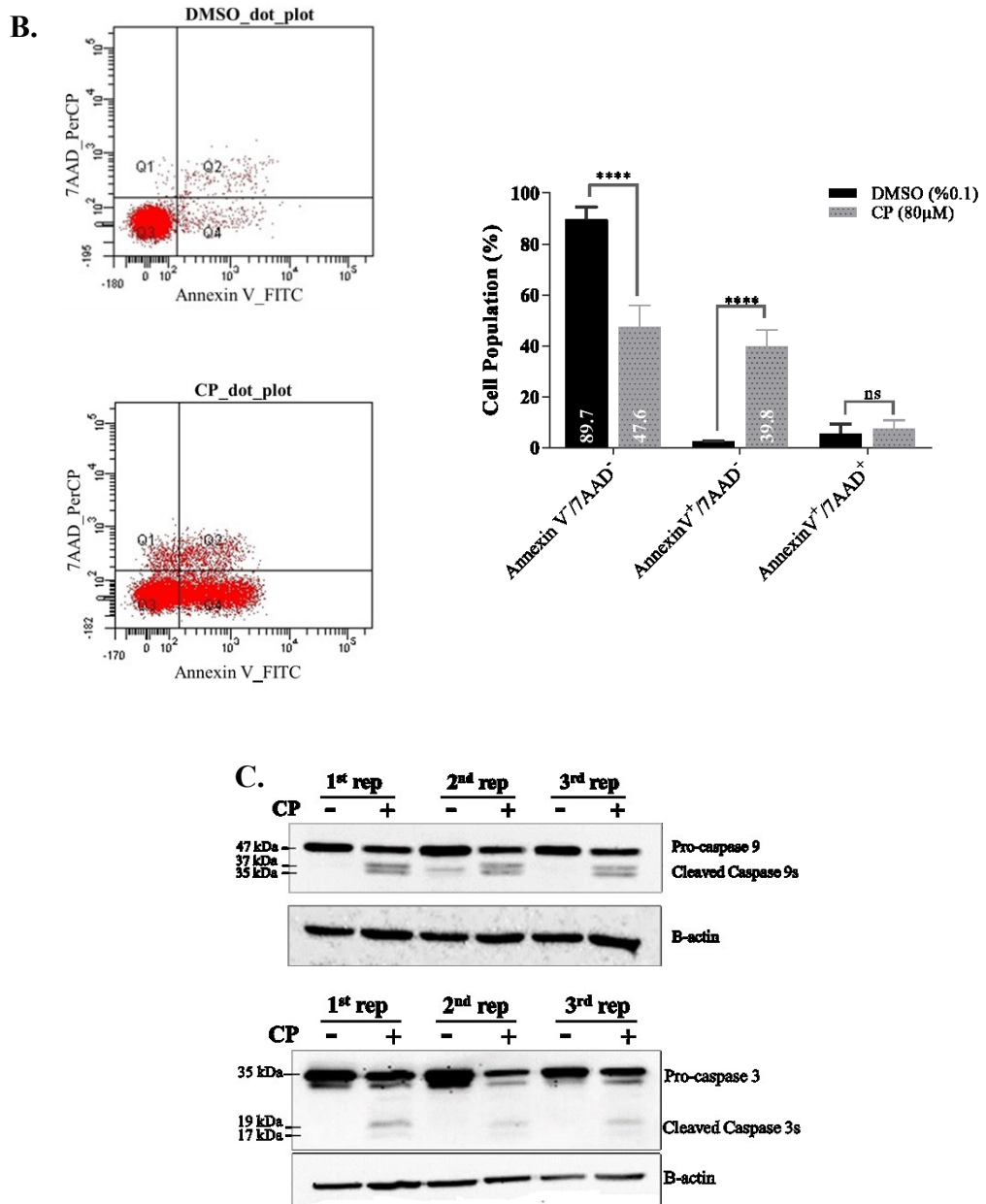
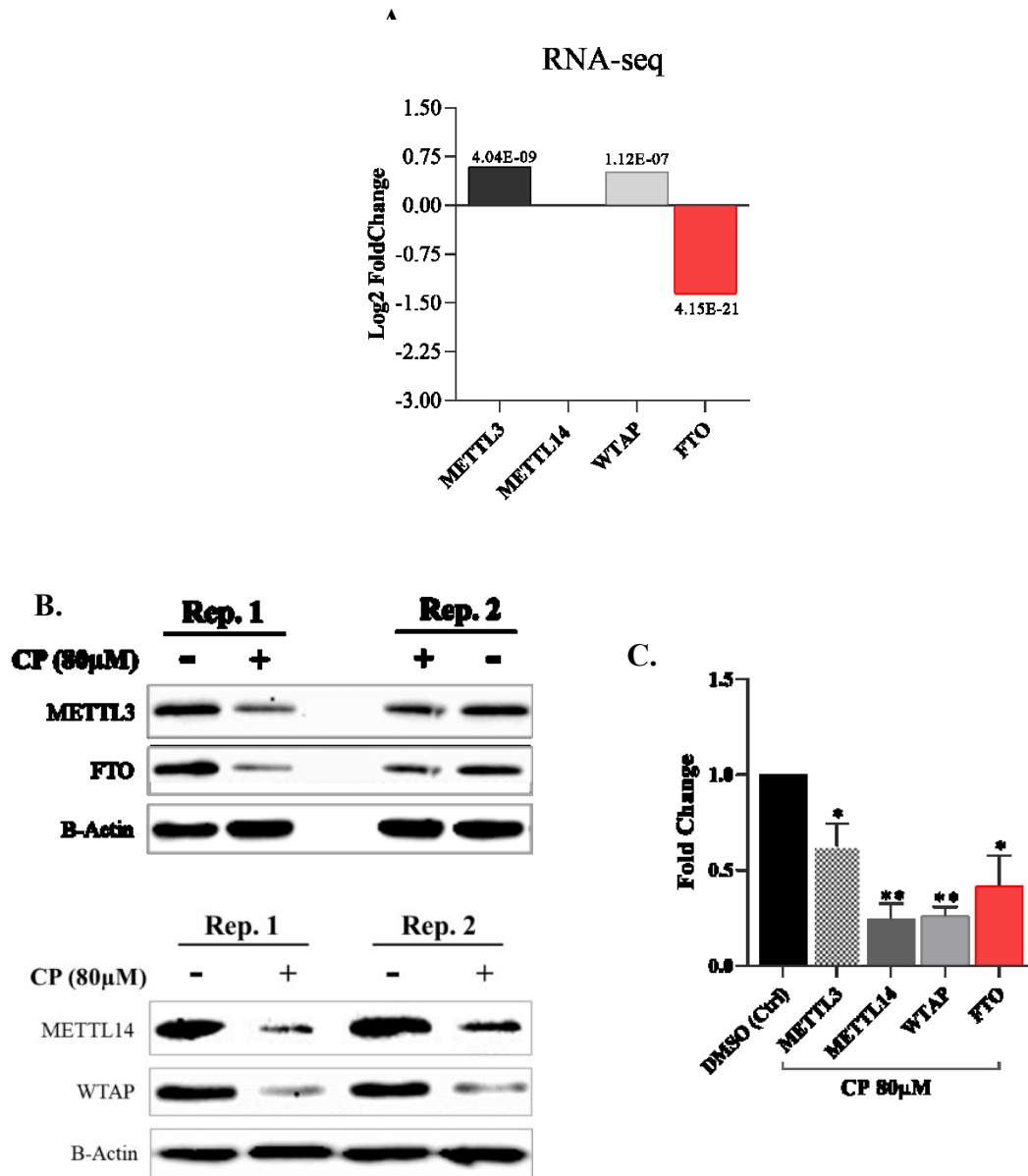


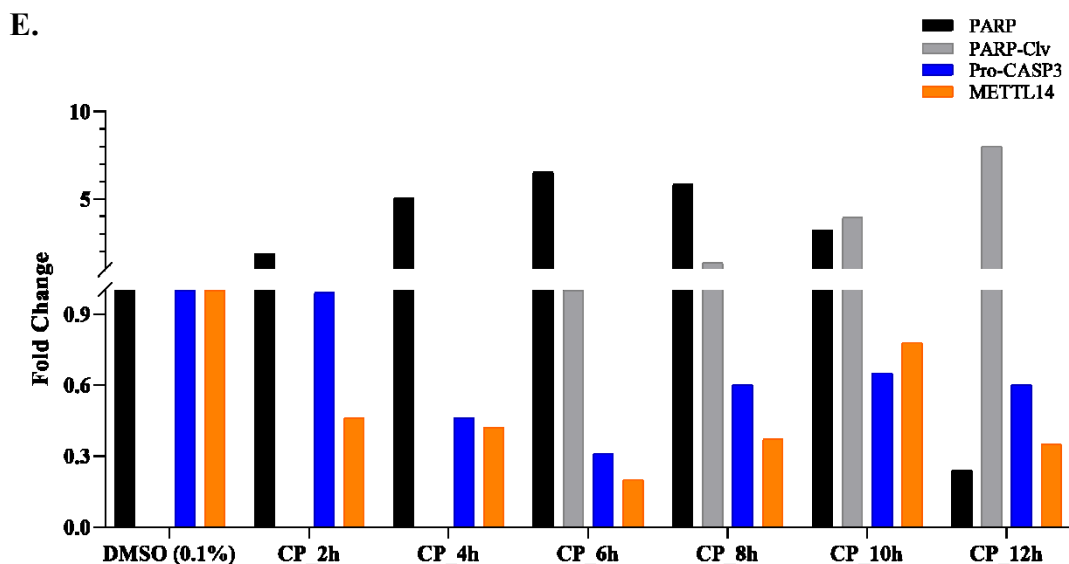
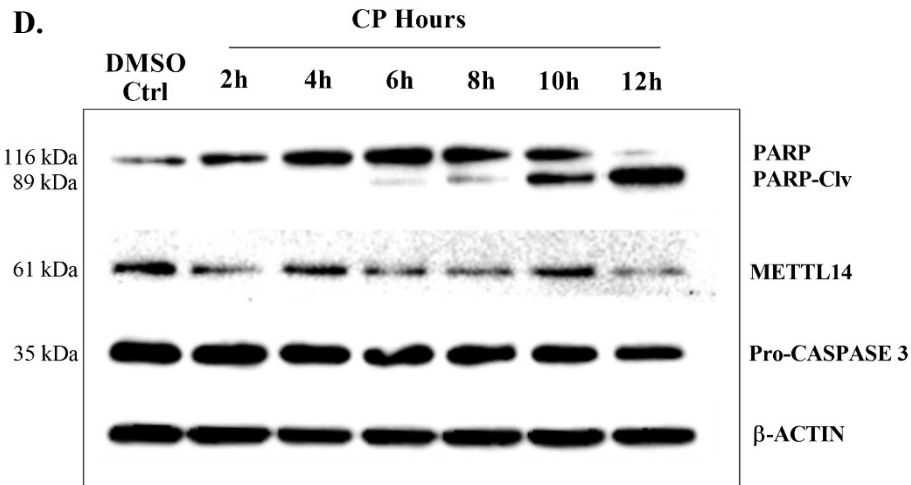
Figure 3.1. (Cont.)

The rate of apoptotic population in HeLa cells treated with 80  $\mu$ M CP was also defined by flow cytometry with the gating strategy of Annexin V and 7AAD. The results indicated that approximately 40% of cells underwent PCD. 38% of cells appeared to be Annexin V<sup>+</sup>/7AAD<sup>-</sup> (early apoptosis), and only 2% were Annexin V<sup>+</sup>/7AAD<sup>+</sup> (other PCD types) (Figure 3.1B). Based on WST-8 and flow cytometry analysis, 80  $\mu$ M CP was selected as the optimal drug concentration, leading to the best rate of early apoptosis. It is already known that CP intrinsically triggers apoptosis through three different mechanisms: death receptors, mitochondrial pathway, and endoplasmic reticulum (ER)-stress activation (J. Y. Hong et al. 2012; Kleih et al. 2019). Thus, the cleavage of two

major caspases (caspase 9 and 3) further confirmed the induction of intrinsic apoptosis after CP treatment (Figure 3.1C).



**Figure 3.2. The effect of cisplatin on the expression of MTC complex (writers) and FTO (eraser).**  $0.5 \times 10^6$  HeLa cells were stimulated with 80  $\mu$ M CP for 16 hrs to perform further experiments, where the DMSO (0.1%) was the control group. **A.** RNA-seq results of METTL3, METTL14, WTAP, and FTO transcripts. **B.** Western blot images show the protein status of these four genes. **C.** The graphic abstract demonstrates the differentiated protein levels of each modulator. The time-dependent cleavage of caspase 3 and its effect on METTL14 levels.  $0.5 \times 10^6$  HeLa cells were stimulated with 80  $\mu$ M CP for 2, 4, 8, 10, and 12 hrs to perform western blotting **D.** Western blot images show the protein status of PARP, PARP-C1v, METTL14 and pro-caspase 3. **E.** The graphic abstract demonstrates the protein abundance of each protein in Figure 3.2D. The intensities were calculated after  $\beta$ -actin normalization. Experiments were executed as triplicates (RNA-seq), duplicates (C and D), and one replica for D and E. (\*:  $p \leq 0.05$ , \*\*\*:  $p \leq 0.001$ , \*\*\*\*:  $p \leq 0.0001$ ). (Continues on next page)



To delve into the profound implications of CP on the m<sup>6</sup>A RNA methylation state, we initially examined the expression pattern of core m<sup>6</sup>A modulators, METTL3-METTL14-WTAP [core methyltransferase complex (MTC)] and FTO (core demethylase) in HeLa cells post-treatment with CP. The influence of CP treatment on the MTC and FTO transcript levels was discerned from RNA-seq data obtained in the previous project (TUBĪTAK, #113Z371) (Figure 3.2A). The canonical mRNA expression slightly increased by 1.5 and 1.4-fold in METTL3 and WTAP, respectively, while there was no change in METTL14 mRNA level. On the contrary, FTO was downregulated by 2.57-fold in CP-treated HeLa cells. The protein levels of these three writers, METTL3, METTL14, WTAP, and erasers FTO, were observed to be 0.6, 0.3, 0.3, and 0.4-fold, respectively, in CP-treated HeLa cells (Figure 3.2B-C).

METTL14 downregulation at protein levels was further investigated to uncover

whether this decrease resulted from caspase 3 activation. 80  $\mu$ M CP was applied to HeLa cells, and then the cells were collected every 2 hrs (after 2, 4, 6, 8, 10, and 12 hrs) to measure the time-dependent activation of caspase 3 and its effect on the protein levels of METTL14. PARP, a target of caspase 3, was utilized as a positive control. The results demonstrated that the reduction in METTL14 protein levels began at 2<sup>nd</sup> hr with a 0.5-fold decrease and continued with 0.5-, 0.8-, 0.6-, 0.2, and 0.7-fold reduction at the 4<sup>th</sup>, 6<sup>th</sup>, 8<sup>th</sup>, 10<sup>th</sup>, and 12<sup>th</sup> hrs, respectively. However, the reduction in pro-caspase 3 was detected first at the 4<sup>th</sup> hr with 0.5-fold and 0.7-, 0.4-, 0.3-, and 0.4-fold at the 4<sup>th</sup>, 6<sup>th</sup>, 8<sup>th</sup>, 10<sup>th</sup>, and 12<sup>th</sup> hrs, respectively. Consistent with the pro-caspase 3 abundance, the initial PARP cleavage was observed at the 6<sup>th</sup> hr. Then, the cleaved PARP levels increased at the 8<sup>th</sup>, 10<sup>th</sup>, and 12<sup>th</sup> hrs with a 1.3-, 4-, and 8-fold elevation (Figure 3.2D-E).

This alteration in protein levels of the central m<sup>6</sup>A modulators indicates that the transcriptome-wide m<sup>6</sup>A profile might differ upon the CP treatment. Furthermore, these changes in METTL14 might involve the response to CP, potentially influencing the drug's effectiveness in inducing apoptosis.

### **3.2. m<sup>6</sup>A-eCLIP-seq Reveals Changes in the m<sup>6</sup>A Profile of CP-Treated HeLa Cells**

m<sup>6</sup>A-eCLIP sequencing, a widely preferred approach in the field, is used to analyze the distribution of m<sup>6</sup>A RNA modification throughout transcripts, allowing the identification of m<sup>6</sup>A sites at a single-nucleotide resolution (Roberts, Porman, and Johnson 2021). This technique was crucial in our study as it allowed us to detect and compare the m<sup>6</sup>A extent upon CP treatment. To this extent, HeLa cells were first incubated separately with the DMSO (0.02%) as control and 80  $\mu$ M CP for 16 hrs. The rate of alive and dead populations in HeLa cells was identified by flow cytometry. Forty-seven percent of the cells were Annexin V<sup>-</sup>/7AAD<sup>-</sup> (alive), and 48% were Annexin V<sup>+</sup>/7AAD<sup>-</sup> (early apoptotic) in the CP-treated samples, while 93% of the population was alive (Annexin V<sup>-</sup>/7AAD<sup>-</sup>) in the DMSO control group (Figure 3.3A). The integrity of total RNA isolated from triplicates from each group was examined by agarose gel electrophoresis before sending them to ECLIPSEBIO for m<sup>6</sup>A sequencing (Figure 3.3B).

The m<sup>6</sup>A sites were identified through the m<sup>6</sup>A-eCLIP technique based on the C-T conversion in the DRACH motif from UV exposure to anti-m<sup>6</sup>A antibody-bound

residues (Linder et al. 2015; Roberts, Porman, and Johnson 2021). To pinpoint the 'true' m<sup>6</sup>A residues, RNA-seq from the identical replicates as the 'input' was initially employed to normalize IP enrichment. This step was implemented to exclude false positive peaks not resulting from C-to-T mutations or RT stall during PCR induced by anti-m<sup>6</sup>A antibodies, ensuring the identification of specific m<sup>6</sup>A sites. Further, the input reflecting the gene expression was also utilized to exclude the expressional difference within the DMSO and CP groups. This way, the exact change in the number of m<sup>6</sup>A positions could be compared in these two groups, providing a more accurate picture of the m<sup>6</sup>A RNA modification state in CP-treated HeLa cells. After normalization, the correlation coefficient between three replicates of samples (CP\_IPvsInput and DMSO\_IPvsInput) was calculated using the Pearson correlation test. The correlation scores were 0.87 and 0.86 for DMSO and CP, which ensured high reproducibility for all modification sites among replicates (Figure 3. 4A).

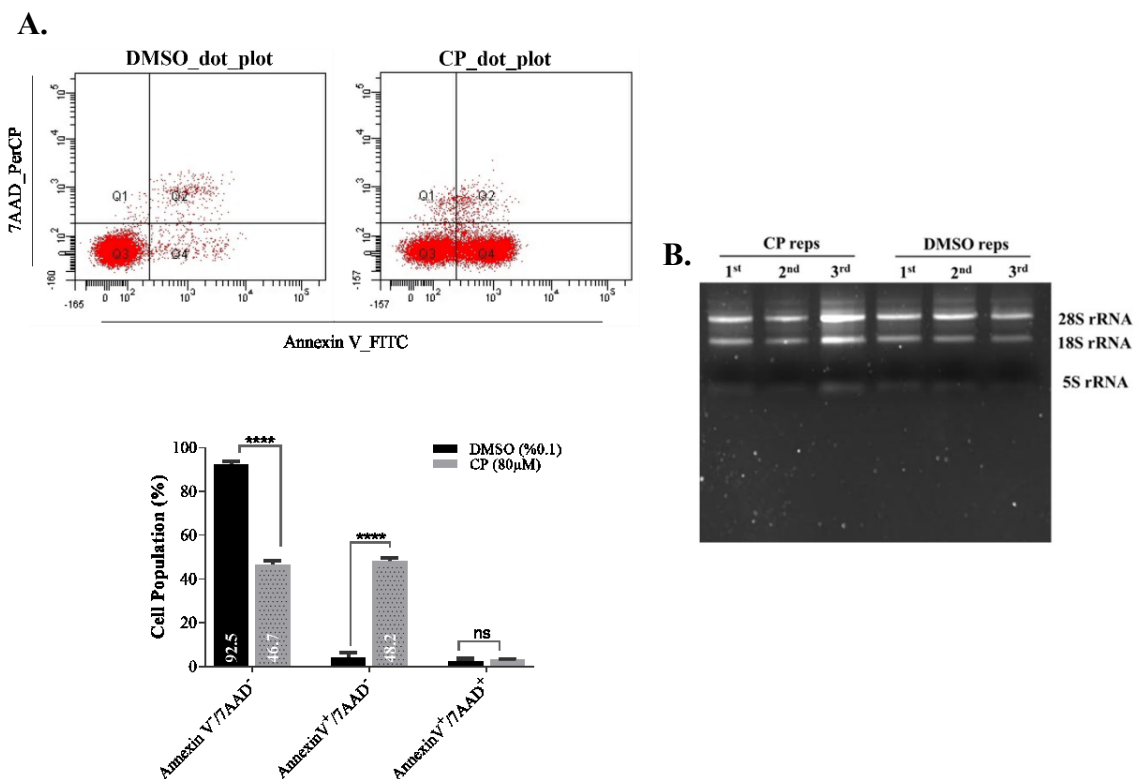


**Figure 3.3. The preparation of total RNA replicates for m<sup>6</sup>A-eCLIP-seq.** 0.5 x 10<sup>6</sup> HeLa cells were treated with 80 µM CP and 0.1% (v/v) DMSO for 16 hrs to obtain total RNA as three biological replicates for both groups. **A.** Distribution of cell populations was determined with Annexin V and 7AAD staining by flow cytometry. Dot-blot analysis shows the distribution of alive and apoptotic cells, where the percentage of live and early apoptosis. **B.** Agarose gel image demonstrated the integrity of RNAs. All experiments were executed as triplicates. (\*:  $p \leq 0.05$ , \*\*\*:  $p \leq 0.001$ , \*\*\*\*:  $p \leq 0.0001$ ). (Continues on next page)

In the absence of a reference to biologically validated m<sup>6</sup>A sites, the data was next assessed in the distribution of confidence and enrichment scores concerning the biological reproducibility to enhance confidence in detecting “true-positive” crosslink sites. The rationale behind this step was that “true” m<sup>6</sup>A sites were prone to reproduce across replicates, whereas “false-positive” sites were less likely to exhibit such consistency. The table below (Table 3.1) illustrates the total count number of crosslink sites (*n\_sites*) identified in all replicates and the distribution of these counts categorized by the reproducibility levels. Approximately 41% of DMSO and 36% of CP of all detected sites were reproducible in all three biological replicates. Similarly, the equivalent number of sites was detected in one replicate (40% of DMSO and 44% of CP) but not in the other two replicates. A smaller portion of sites (~20%) in both groups were reproducible between two replicates and not in the third. These results displayed that the crosslink sites were mainly divided into two: (i) potentially “true positive” methylated sites, which were consistently identified across all three biological replicates, and (ii) potentially “false positive” sites, which were only detected in one replicate.

**Table 3.1. m<sup>6</sup>A sites detected in all biological replicates**

<b>Sample</b>	<b>n_sites</b>	<b>In 1 Rep</b>	<b>In 2 Rep</b>	<b>In 3 Rep</b>
DMSO	197876	79525 (40.19%)	37595 (19%)	80756 (40.81%)
CP	165377	74135 (44.83%)	32340 (19.56%)	58902 (35.62%)

Since the “true positive” m<sup>6</sup>A sites were expected to reflect high confidence and IP-v-Input enrichment scores, the distribution of these scores relative to biological reproducibility was tested. Notably, it was observed that higher PureCLIP and IP-v-Input enrichment scores in sites were detected across all biological triplicates compared to those identified in only two replicates or a single replicate. This observation also showed that reproducible sites were more inclined to represent “true positives” than those lacking reproducibility (Figure 3. 4B-C).

Although a list of validated m<sup>6</sup>A sites is not available as a simple positive control, it has been known that the m<sup>6</sup>A sites tend to be positioned in the context of the DRACH motif (where D represents an A, G, or U, R represents an A or G, and H represents an A, C, or U based on IUPAC nucleotide codes) (Linder et al. 2015). Since the PureCLIP analysis does not impute in sequence context when calling crosslink sites, the presence of the DRACH motif enriched at the detected crosslink sites served as another

confirmation for biological validity. Indeed, the motif analysis of each replicate displayed an enrichment of “K-mers” containing the DRACH motif positioned at -2 relative to crosslink sites, which corresponds to the “A” in the DRACH motif. Moreover, this enrichment was more notable in sites observed in all three replicates (Figure 3.4D). To identify the enriched sequence motifs within the peaks at m<sup>6</sup>A sites, the HOMER motif algorithm was applied to “true positive” sites determined by the above analysis. The motif enrichment calculation used 6236 sites in DMSO and 1422 sites in CP. According to the results, the top-ranked (ranked by p-value) motif word at crosslink sites was “GGACU” in both DMSO (71% of targets) and CP (58% of targets) samples, which further confirmed the obtained crosslinked sites from triplicates representing “true positives” (Figure 3.4E).

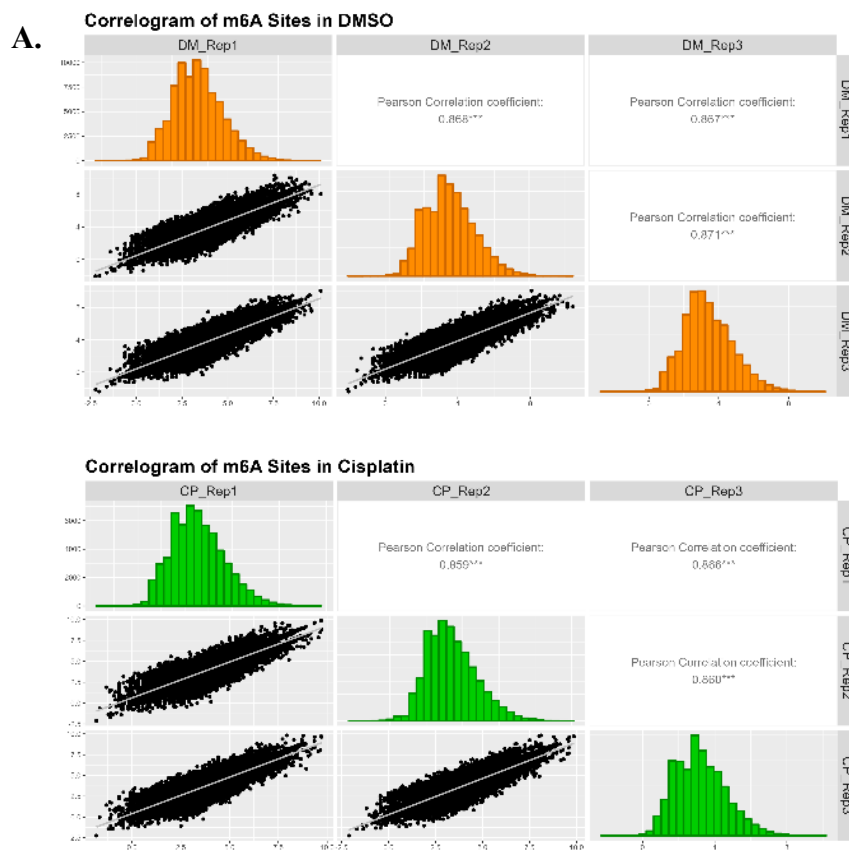
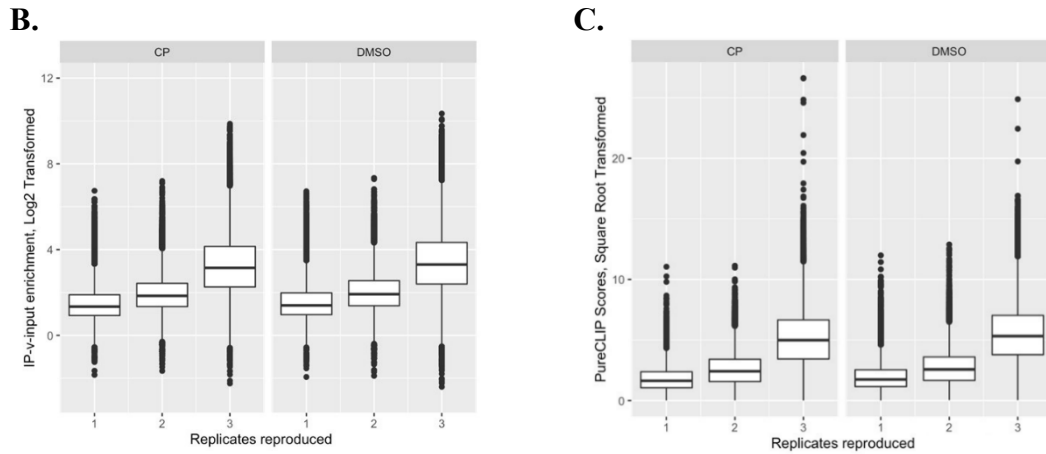
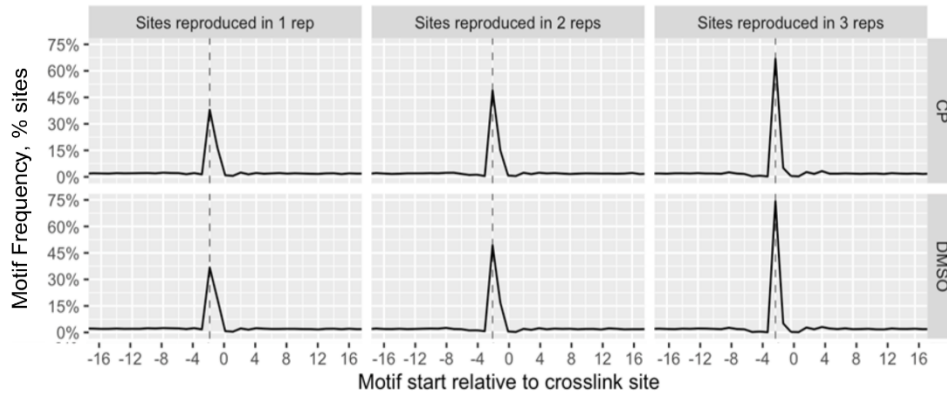


**Figure 3.4. The validation of m<sup>6</sup>A peaks and crosslink sites in CP and DMSO samples.** The determination and validation of m<sup>6</sup>A sites were performed utilizing Clipper and PureCLIP tools by ECLIPSE Bio., explained in the Material and Methods section. **A.** Pearson correlation test comparing three replicates reflected the high reproducibility between replicates for DMSO and CP samples, respectively. **B.** IP-v-input enrichment and **C.** PureCLIP scores indicated that detected sites in all three replicates were higher than detected sites in two or only one replicate. **D.** Combined frequency of words comprising DRACH motif. 70% of sites in CP and 75% in DMSO were detected in tree replicates. **E.** HOMER motif analysis confirmed the highest-ranking word, “GGACU,” for both CP and DMSO. (Continues on next page)



**D.** Combined Frequency of DRACH Motif Words at Crosslink Sites  
For reproduced sites, motif frequency is shown as average between replicates



**E.**

**DMSO**

Total target sequences = 6236  
Total background sequences = 40005

\* - possible false positive

Rank	Motif	P-value	log P-value	% of Targets	% of Background	STD(Bg STD)
1		1e-413	-9.527e+02	71.02%	43.73%	48.0bp (71.0bp)
2		1e-132	-3.046e+02	40.43%	26.14%	56.4bp (71.6bp)
3		1e-110	-2.553e+02	35.84%	23.22%	52.9bp (72.5bp)
4		1e-107	-2.472e+02	21.47%	11.62%	55.0bp (70.1bp)
5		1e-89	-2.068e+02	32.12%	21.14%	56.1bp (68.6bp)

**CP**

Total target sequences = 1422  
Total background sequences = 43314

\* - possible false positive

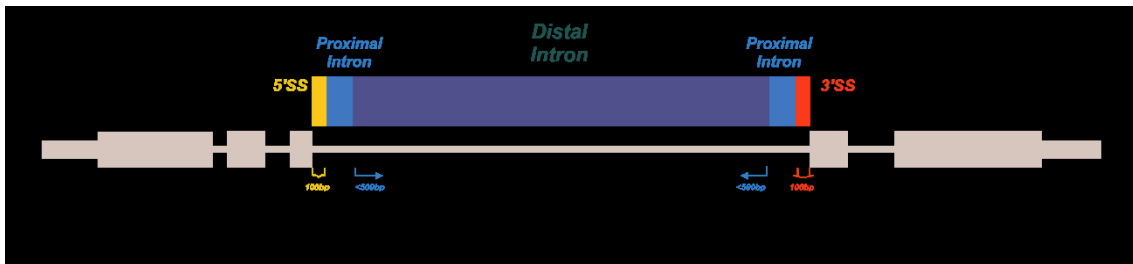
Rank	Motif	P-value	log P-value	% of Targets	% of Background	STD(Bg STD)
1		1e-106	-2.462e+02	57.52%	29.37%	45.4bp (73.6bp)
2		1e-36	-8.359e+01	1.34%	0.01%	51.7bp (70.3bp)
3		1e-31	-7.311e+01	0.98%	0.00%	55.4bp (0.0bp)
4		1e-31	-7.311e+01	0.98%	0.00%	51.3bp (61.6bp)
5		1e-29	-6.705e+01	0.91%	0.00%	53.5bp (51.3bp)

Figure 3.4. (Cont.)

Following the validation of the m<sup>6</sup>A sites detected in both DMSO and CP samples, the peaks and single-nucleotide sites were annotated utilizing transcript information sourced from Ensembl or GENECODE databases. Each annotated transcript region was categorized with specific annotation feature types, initially divided by coding and non-coding transcripts and subsequently split by intron/exon proximity regions. The definitions of the feature types are explained in Table 3.2. and Figure 3.5.

**Table 3.2. The feature types where m<sup>6</sup>A sites were annotated**

<b>Feature Type</b>	<b>Definition</b>
CDS	Coding Sequence
5' UTR	5' Untranslated Region
3' UTR	3' Untranslated Region
miRNA proximal	Within 500 bp of an annotated miRNA
5' splice site (5' SS)	Within the first 100 bp of an intron (5' to 3')
3' splice site (3' SS)	Within the last 100 bp of an intron (5' to 3')
Proximal intron	Within 100 bp to 500 bp of the nearest exon
Distal intron	Greater than 500 bp away from the nearest exon



**Figure 3. 5. Schematic representation of each feature location in a gene.**

The relative frequency of peaks annotated to each feature above was further quantified to elucidate the differential location of the m<sup>6</sup>A modification across the transcriptome in response to CP treatment. The m<sup>6</sup>A peaks/sites identified in the DMSO control group were designated as decreased (or absent) sites in the CP samples. The rationale was predicated on the presumption that the distribution of m<sup>6</sup>A modification is typically consistent in cells originating from the same tissue (Murakami and Jaffrey, 2022). The mapping results revealed more heterogeneous localization of m<sup>6</sup>A peaks across various genomic regions upon CP treatment compared to the DMSO control.

Specifically, m<sup>6</sup>A peaks were increased in the distal intronic region (18%), 3'UTR (17%), CDS (12.6%), 5'UTR (12.6%), noncoding exons (12%), and proximal introns (11.5%) following the CP treatment. In contrast, the predominant verification of m<sup>6</sup>A peaks was noted in CDS (52.4%) and 3'UTR (23%) in the DMSO group (Figure 3.6A-B). The central regions of mature mRNAs were emphasized to assess the direct impact of CP on mRNA fate via m<sup>6</sup>A modification. Metagene plots generated from peak info and m<sup>6</sup>A sites pinpointed a notable shift in m<sup>6</sup>A abundance from the 3'UTR to 5'UTR in HeLa cells, particularly following CP treatment (Figure 3.6C-D).

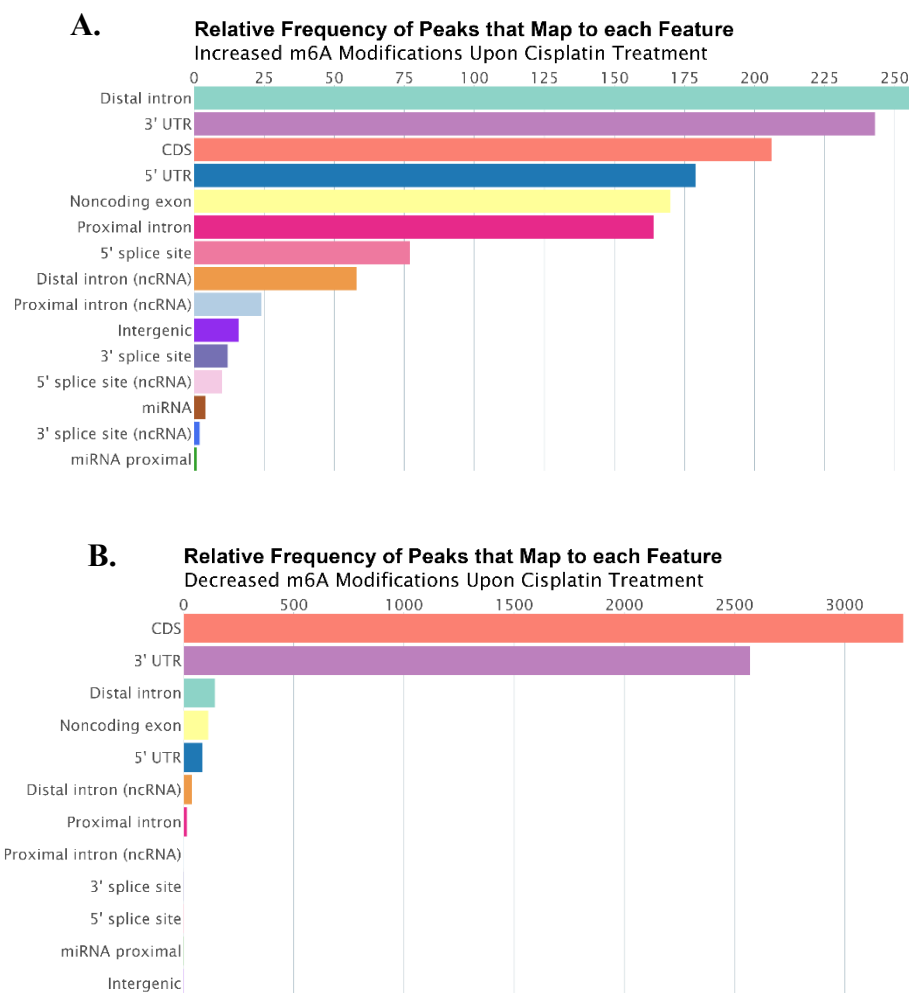


**Figure 3.6. The m<sup>6</sup>A RNA modification profile of HeLa cells upon CP treatment.** All analyses were conducted using data obtained from ECLIPSE Bio, as explained in the Material and Methods section. Relative frequencies of **A.** elevated, and **B.** reduced m<sup>6</sup>A peaks were mapped to each feature. Metagene Plot analysis demonstrated relative localization of m<sup>6</sup>A **C.** peaks and **D.** sites that were annotated to 5'UTR, CDS, and 3'UTR on a transcript. Venn diagram of differential m<sup>6</sup>A pattern **E.** per transcript and **F.** per m<sup>6</sup>A site. **G.** Representative graph for 33 genes containing both upregulated and downregulated m<sup>6</sup>A sites. (**Continues on next page**)

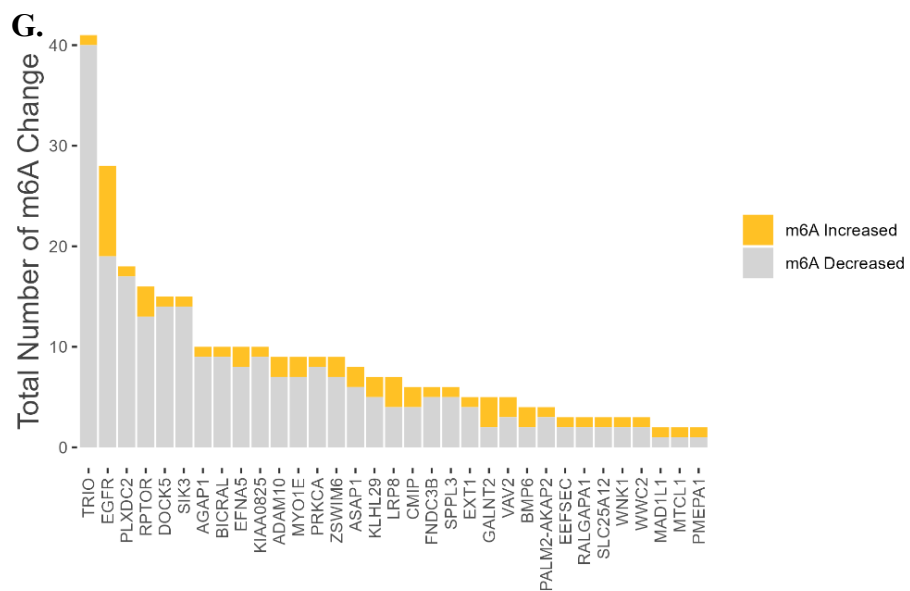
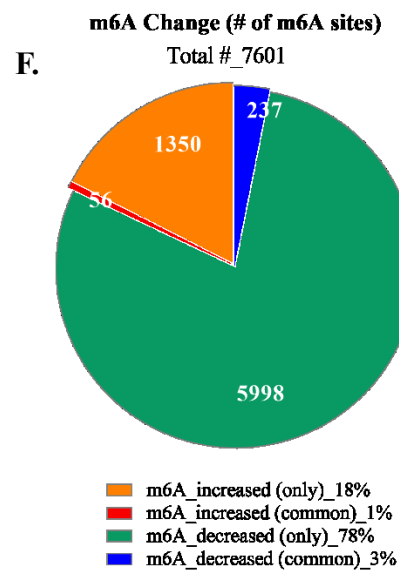
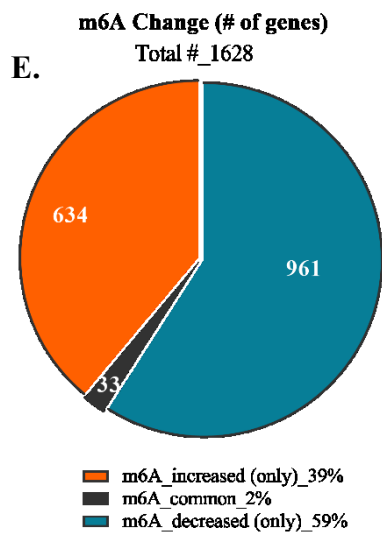
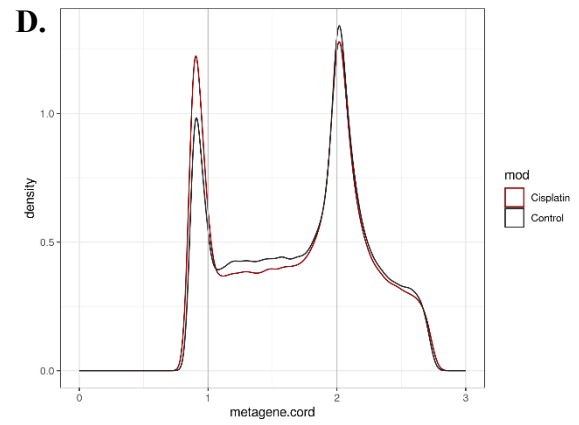
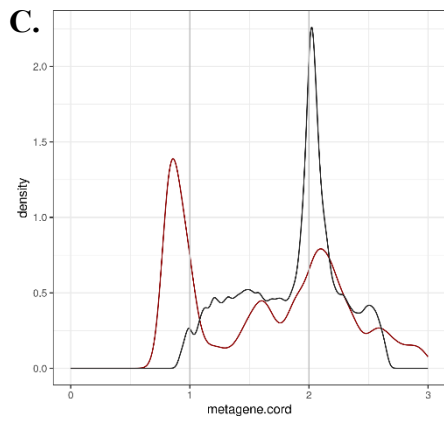


**Figure 3.6. (Cont.)**

Utilizing a fusion of peak and single-nucleotide data aligned to the reference genome, the impact of CP was further assessed on the alteration of m<sup>6</sup>A extent on genes. The analysis demonstrated that 7601 differential m<sup>6</sup>A residues were detected in 1628 genes. Of these, 961 genes displayed only a reduction of 6235 m<sup>6</sup>A positions, while 634 genes exhibited only the elevation of 1406 m<sup>6</sup>A sites. Furthermore, we noted concurrent decreases and increases in specific m<sup>6</sup>A sites within 33 genes (Figure 3.6E-G).

### **3.3. Pathway Analysis Demonstrates m<sup>6</sup>A RNA Modification as a Part of CP Response**

In order to enhance the efficacy and simplify the interpretation of variations in the m<sup>6</sup>A extent following CP treatment, the m<sup>6</sup>A data was integrated into existing pathway analysis tools, including GO enrichment and KEGG. The pathway analysis was initially conducted with two distinct data sets: m<sup>6</sup>A increased (referring to CP sample normalized with DMSO) and m<sup>6</sup>A decreased (referring to DMSO sample normalized with CP). The GO pathway analysis tool mapped the genes exhibiting differential m<sup>6</sup>A patterns according to their participation in biological processes and molecular function. Figures 3.7 A and B demonstrate the top ten processes and functions of genes containing elevated (Figure 3.7A) and reduced (Figure 3.7B) upon CP treatment. The results indicated that m<sup>6</sup>A abundance significantly escalated in genes involved in proliferation, nucleic acid metabolism, programmed cell death, and cell cycle events and functioning as kinases, nucleic acid binding proteins, and transcription factors. On the other hand, the genes participating in the signal transduction, specifically cyclic-AMP, PI3-K, and GTPase-activated signaling cascades, carry lesser or no m<sup>6</sup>A modifications compared to the DMSO control.

Furthermore, the KEGG analysis was performed using the datasets above to corroborate previous findings. As a different database, KEGG offers more refined pathways, thereby facilitating the visualization of genes and their involvement in specific signaling cascades. Like GO analysis, the m<sup>6</sup>A-increased group was involved in signaling cascades such as MAPK, TNF, NF $\kappa$ -B, and HF-1, regulating proliferation, cell death, and stress response. Additionally, it was observed that the genes participating in PI3K-Akt, Rap, Ras, WNT, and cGMP-PKG signaling pathways lost their m<sup>6</sup>A sites and abundance (Figure 3.7C-D).

The GO and KEGG analysis results exhibited similar patterns and indicated that m<sup>6</sup>A modification is an indispensable regulatory and response mechanism for cells exposed to CP.

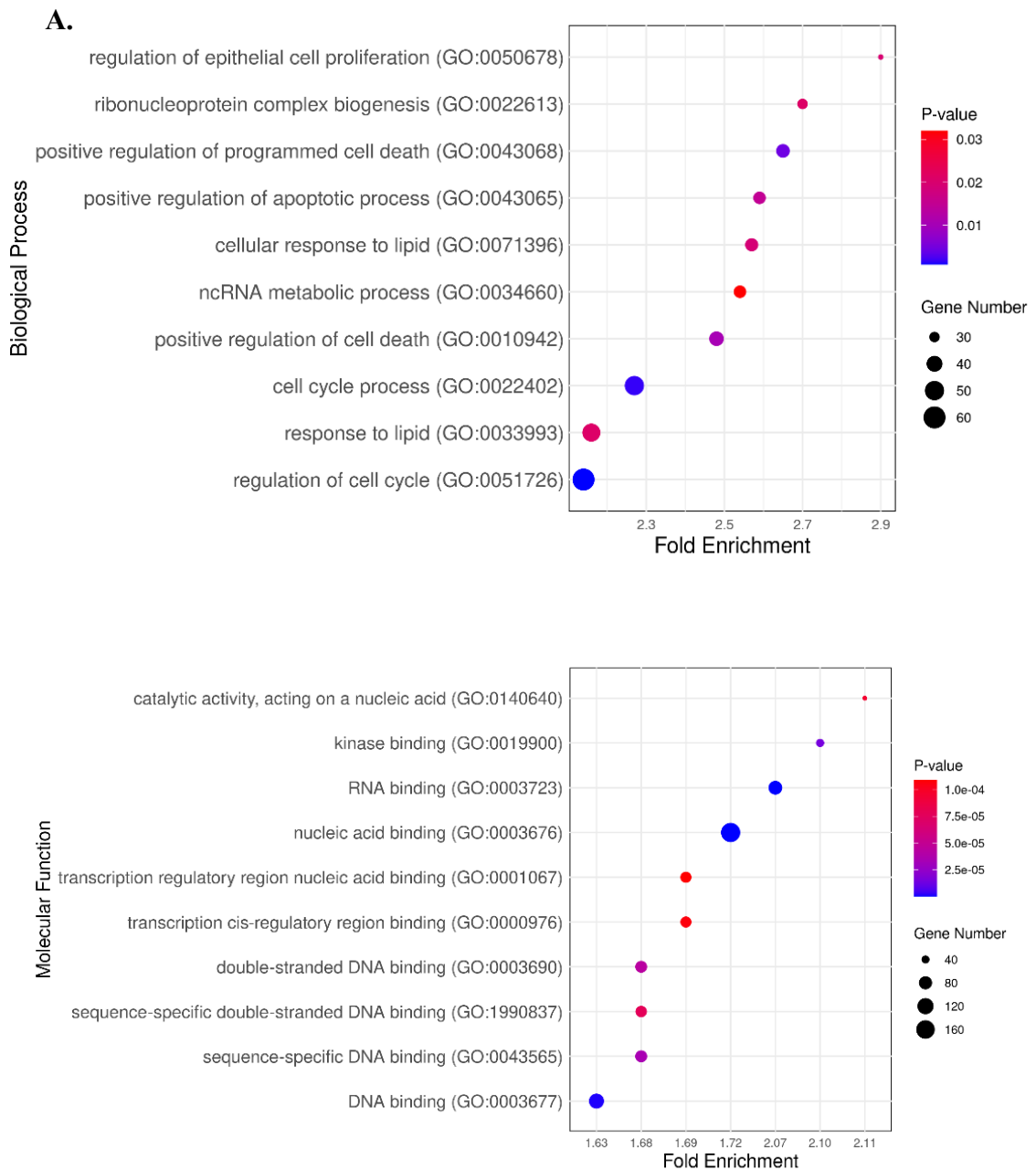


**Figure 3.7. The pathway analysis of genes exhibiting differential m<sup>6</sup>A modification.** All analyses were conducted using data obtained from ECLIPSE Bio, explained in the Material and Methods section. The GO enrichment analysis of genes containing **A.** elevated and **B.** reduced m<sup>6</sup>A peaks. The graphs display both the top ten biological processes and molecular functions. The top ten KEGG pathways of genes exhibiting **C.** increased, and **D.** decreased m<sup>6</sup>A peaks. (Continues on next pages)

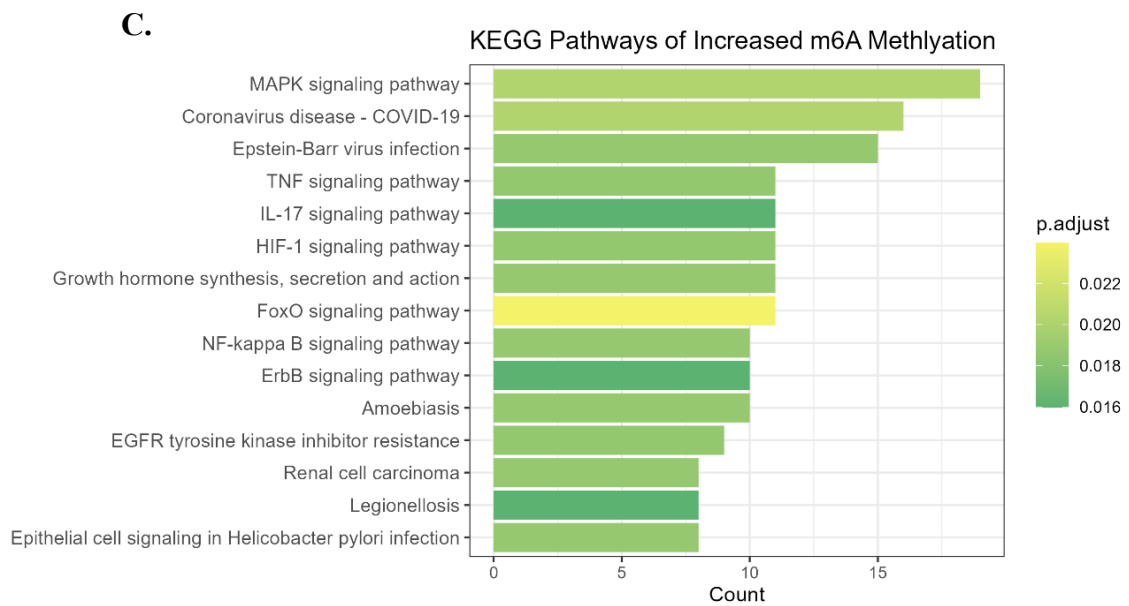
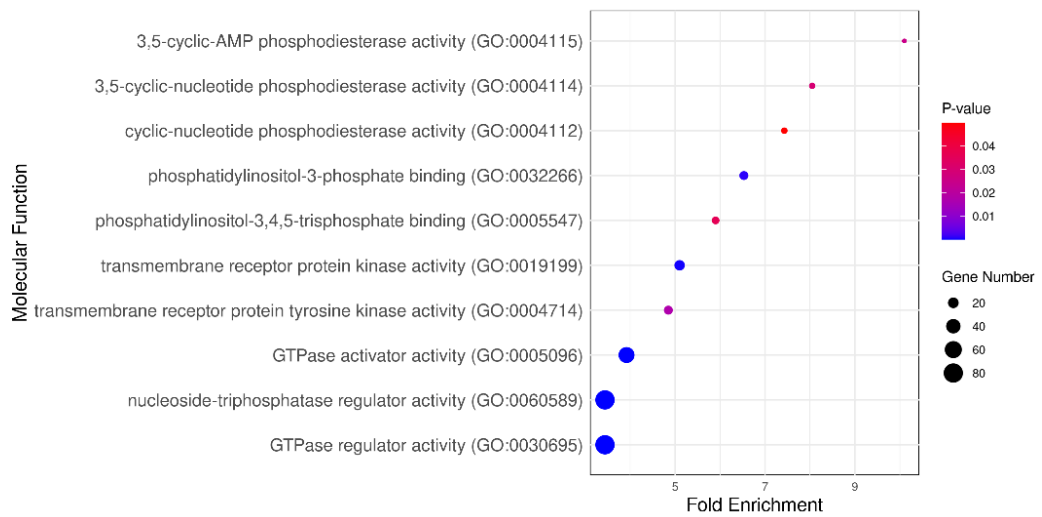
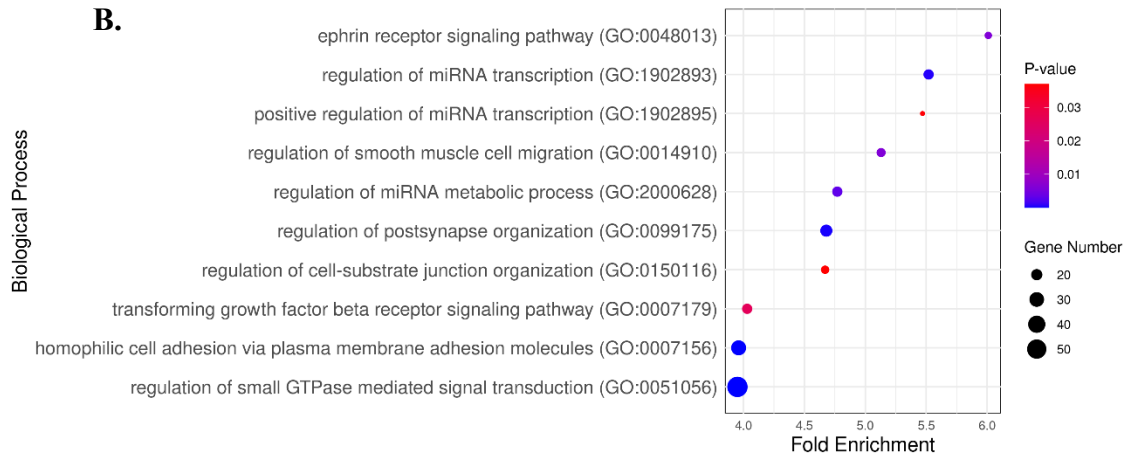
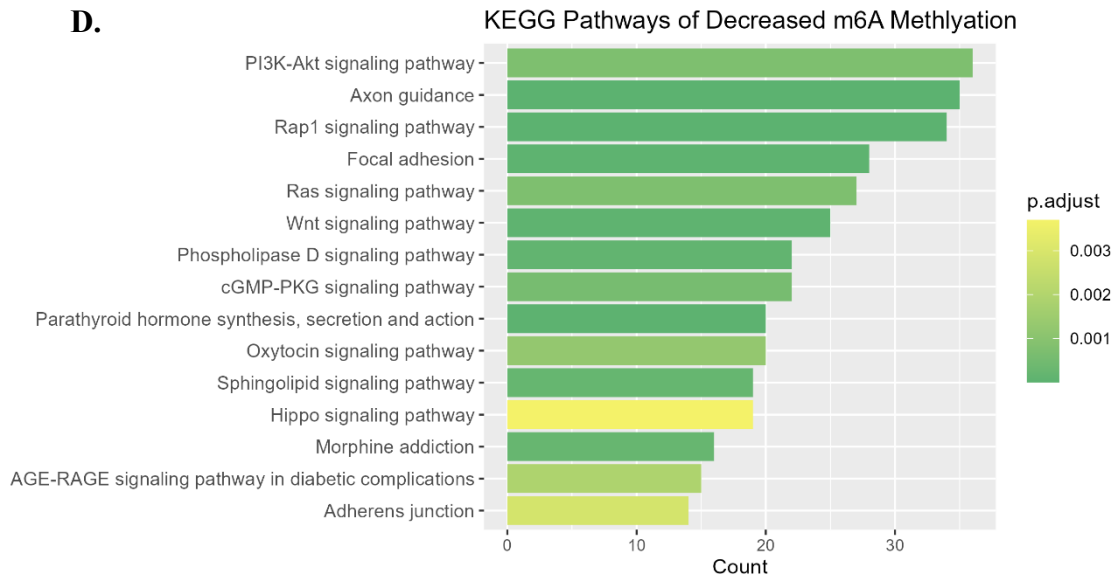


Figure 3.7. (Cont.)



**Figure 3.7. (Cont.)**

### **3.4. Integrative RNA-seq and m<sup>6</sup>A-eCLIP-seq Analysis Reveal Positive Correlation between RNA Abundance and m<sup>6</sup>A Levels in CP-Responsive Genes**

The RNA-seq used as “input” for the detection of m<sup>6</sup>A log<sub>2</sub>fold change upon “IP” was reanalyzed to describe the RNA expression patterns between CP and DMSO (control) groups. The genes that were expressed more (log<sub>2</sub>FC >1) or less (log<sub>2</sub>FC <1) than two-fold were selected for further analysis. A total of 8228 RNAs displayed significant differences following the CP treatment, including 3701 upregulated genes and 4527 downregulated genes (Figure 3.8A). The volcano and the hierarchical clustering analysis were further utilized to visualize the distribution of differentially expressed genes (DEGs) (Figure 3. 8B-C). The GO Enrichment analysis was conducted to identify and characterize the biological processes and molecular functions associated with the DEGs. The results demonstrated that DEGs were enriched in biological functions, including translation, DNA replication, and cell cycle processes, with tasks of kinase activity, GTPase binding, and RNA binding (Figure 3. 8D), suggesting the possible correlation between differential expression and methylation.

To uncover the correlation between differential expression and methylation, the Pearson correlation analysis was performed. A positive correlation was found between

RNA abundance and m<sup>6</sup>A levels (Figure 3.9A).

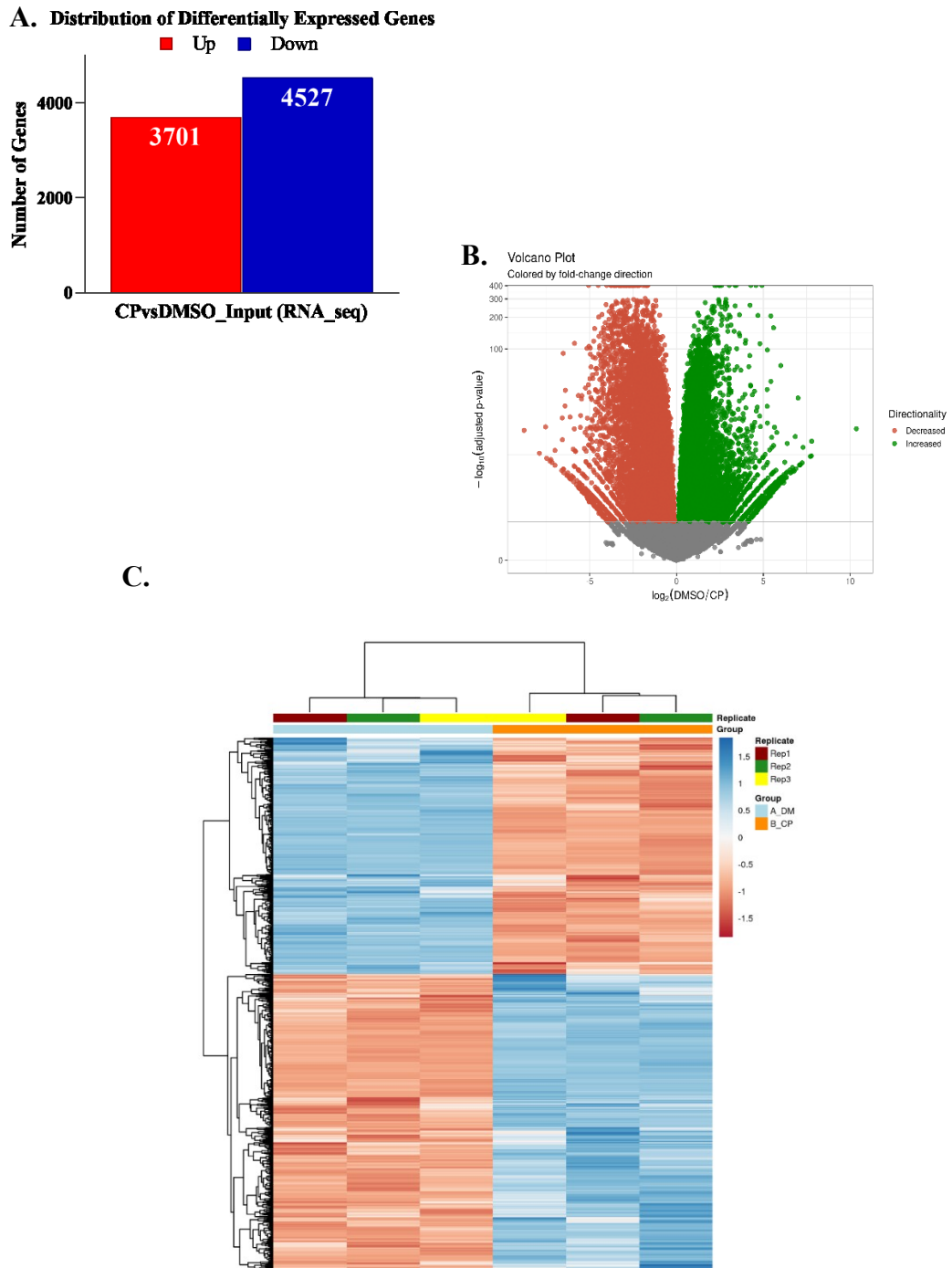


**Figure 3.8.** The analysis of RNA-seq was used as “input” for m<sup>6</sup>A enrichment. All analyses were conducted using raw data obtained from ECLIPSE Bio, as explained in the Material and Methods section. **A.** Bar graph representing the gene number with elevated and reduced transcript abundances. **B.** Volcano plot and **C.** heatmap analysis demonstrating the distribution of differentially expressed genes. **D.** The top ten GO pathways of genes exhibiting differential RNA levels. (Continues on next pages)

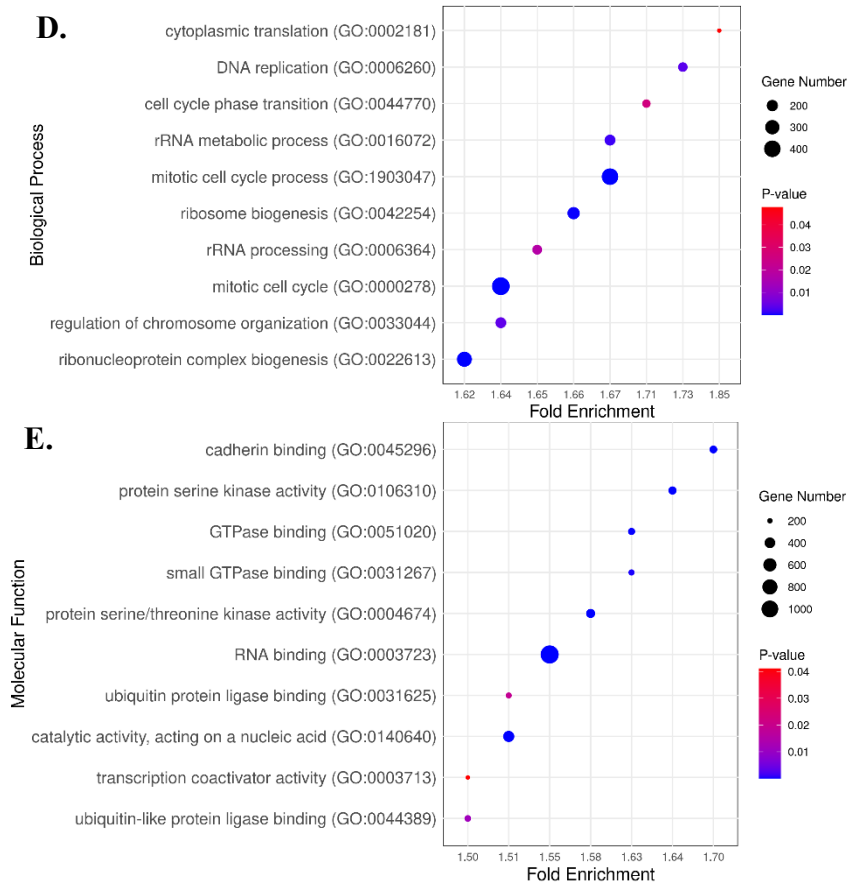


**Figure 3.8. (Cont.)**

As mentioned in section 3.2, 337 genes were identified with increased transcript abundance in 664 hyper-m<sup>6</sup>A (m<sup>6</sup>A increased) genes, termed “hyper-induced.” The 44 genes were determined to have hyper-m<sup>6</sup>A sites alongside decreased RNA levels, termed “hyper-reduced.” Similarly, among the 993 hypo-m<sup>6</sup>A (m<sup>6</sup>A decreased) peaks, 904 genes were identified with reduced transcript levels, which is “hypo-reduced.” Only one gene exhibited hypo-m<sup>6</sup>A sites with increased transcript, called “hypo-induced.” Moreover, 33 genes harboring both hyper- and hypo-m<sup>6</sup>A sites had reduced transcript levels (Figure 3.9B). Considerably, the analysis indicated a significant positive correlation in both m<sup>6</sup>A levels and RNA in CP-treated cells compared to the DMSO control, which might be inferred from the results that the number of “hyper-induced” and “hypo-reduced” genes was dominantly higher than those of “hyper-reduced” and “hypo-induced” transcripts.

Next, the relationship between the number of m<sup>6</sup>A sites per transcript and RNA levels was explored. As previously displayed in Figure 3.6E-F, the genes consisting of different numbers of m<sup>6</sup>A sites were classified. Combining this data with the relative transcript levels of those genes showed that the genes owing more than one increased

peak were gradually upregulated than the genes with one m<sup>6</sup>A point. Similarly, a slightly lesser transcript abundance was observed in the genes containing reduced m<sup>6</sup>A peaks at more than one site (Figure 3.9C-D).

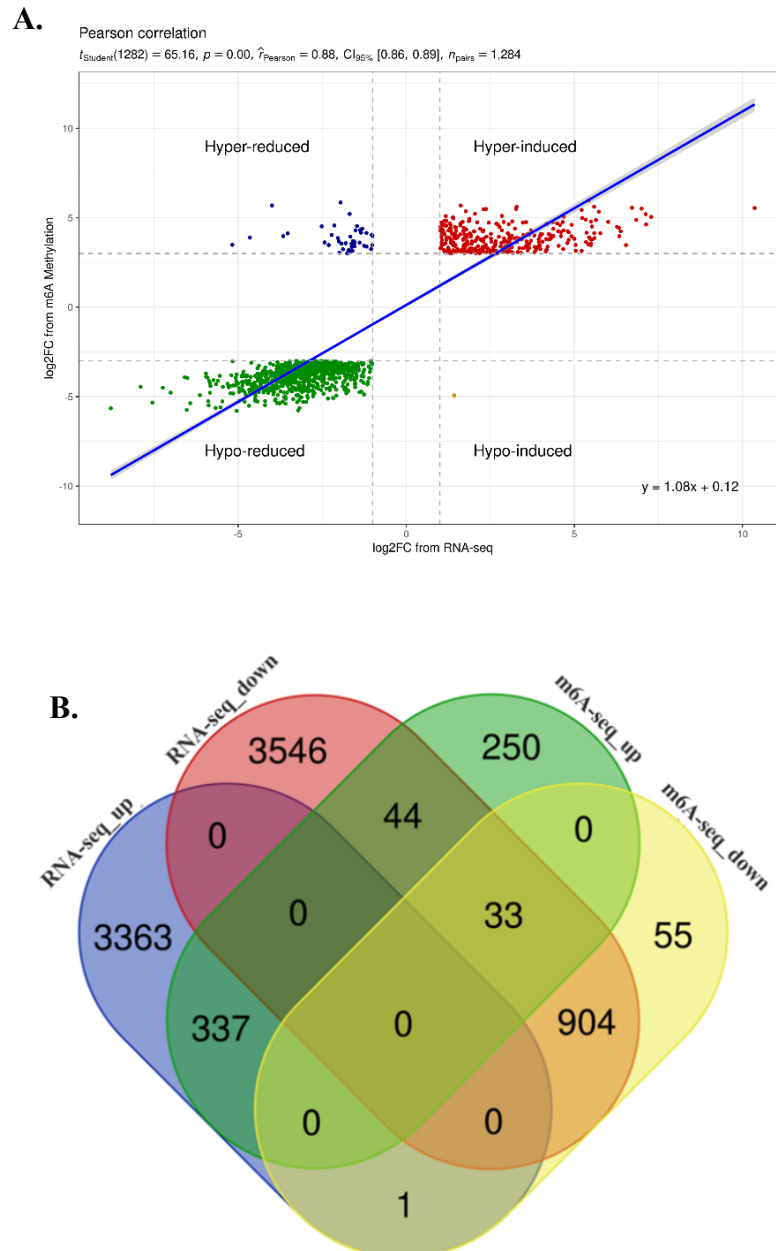


**Figure 3.9. The correlation analysis between “DMGs” and “DEGs.”** **A.** Distribution of genes with significant changes in both RNA abundance and m<sup>6</sup>A peaks. The terms, “Hyper” and “Hypo” indicate the increment or the decrement in m<sup>6</sup>A levels on a gene, respectively. The “induced” and “reduced” represent the upregulation or downregulation in transcript abundance, respectively. **B.** Categorization of genes according to the direction of differential methylation or expression patterns. RNA levels of genes exhibiting different numbers of m<sup>6</sup>A sites in **C.** CP-treated (upregulated) and **D.** DMSO (downregulated) groups. (Continues on next page)

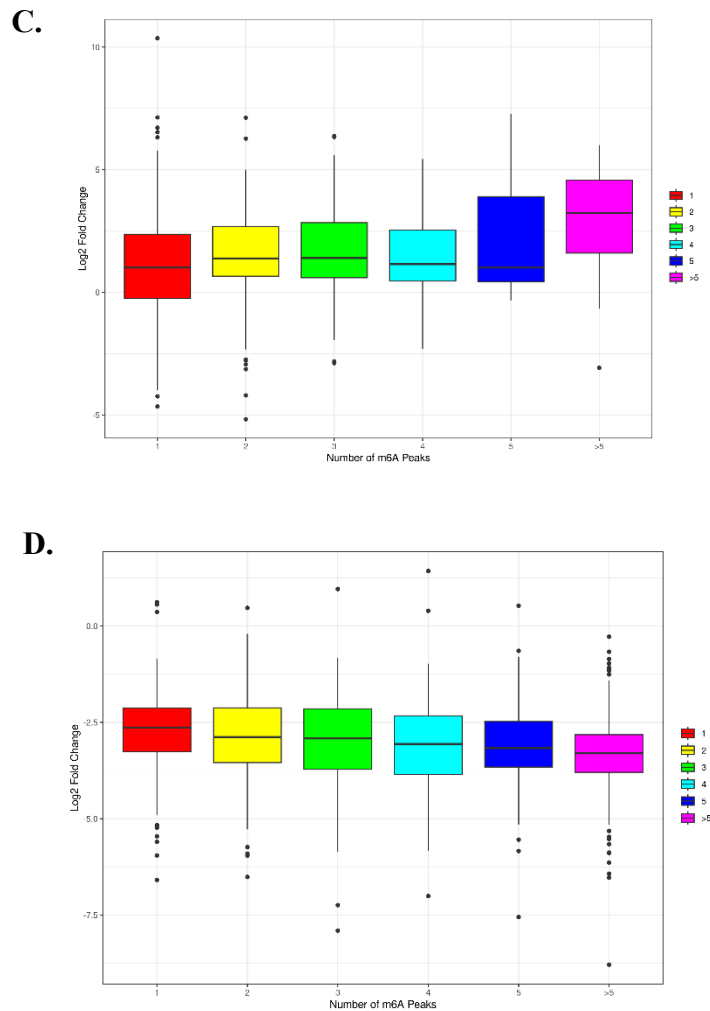


**Figure 3.9. (Cont.)**

To identify the association of “hyper-induced” and “hyper-reduced” genes with the phenotypes represented after CP treatment, the gene set enrichment analysis (GSEA) was applied. It was found that the genes enriched in the top five pathways were strongly correlated with CP response. These were TNF-alpha signaling ( $ES=0.72$ ,  $NES=5.75$ ,  $FDR < 0.0001$ ,  $p < 0.0001$ ), p53 pathway ( $ES=0.67$ ,  $NES=4.01$ ,  $FDR < 0.0001$ ,  $p < 0.0001$ ), apoptosis ( $ES=0.46$ ,  $NES=2.43$ ,  $FDR=0.01$ ,  $p < 0.0001$ ), hypoxia ( $ES=0.40$ ,  $NES=2.31$ ,  $FDR=0.013$ ,  $p < 0.0001$ ), and regulation of cell cycle ( $ES=0.13$ ,  $NES=1.64$ ,  $FDR=0.19$ ,  $p < 0.0001$ ), respectively (Figure 3. 10A-E). Controversially, the enrichment results indicate a significant depletion of genes GTPase, kinase activities, and macromolecule synthesis, consistent with the previous pathway analysis. Rho-GTPase cycle ( $ES=-0.34$ ,  $NES=-2.27$ ,  $FDR < 0.15$ ,  $p < 0.000$ ) and Transmembrane receptor protein kinase signaling ( $ES=-0.49$ ,  $NES=-2.21$ ,  $FDR < 0.13$ ,  $p < 0.000$ ) were the top two ranked cellular mechanisms which negatively regulated through transcriptional and post-transcriptional

processes in CP-treated HeLa cells (Figure 3.10F-G).

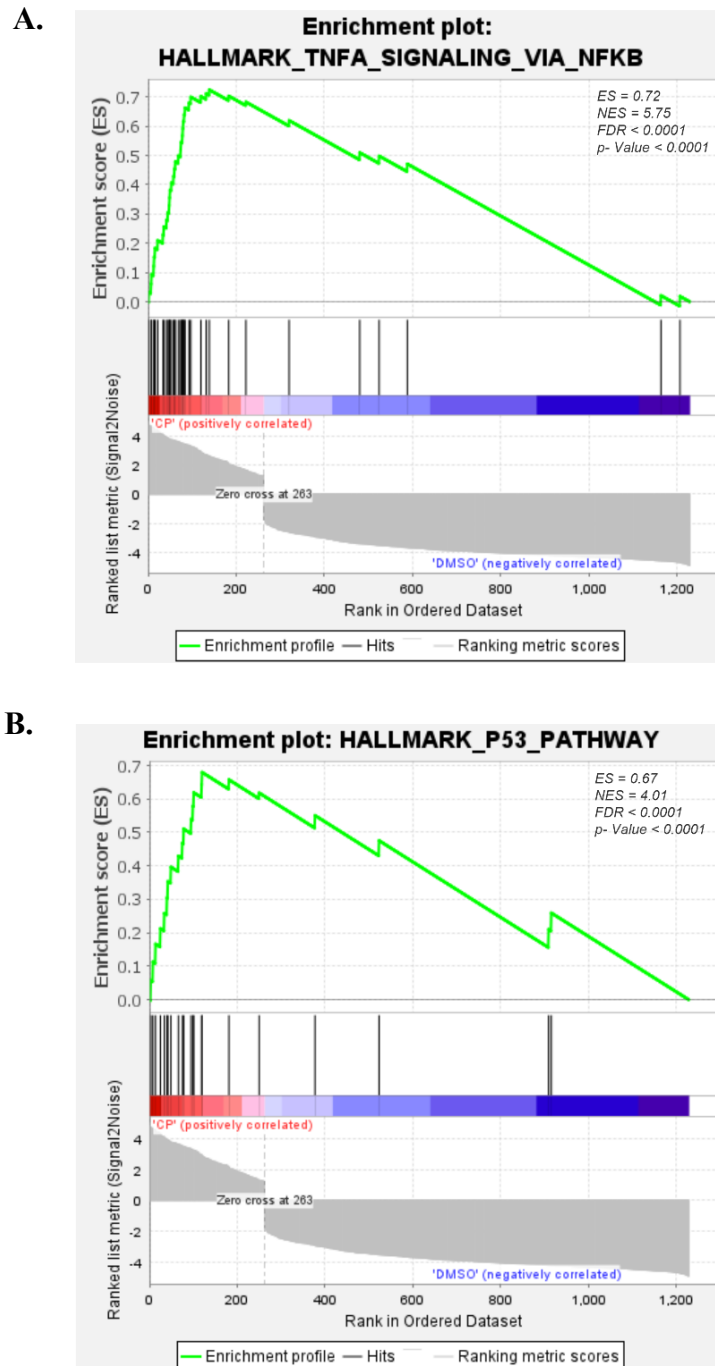


**Figure 3.10.** The GSEA plots showing the top five gene sets enriched in “hyper-induced” and “hyper-reduced” gene groups in HeLa cells. Enrichment plots for **A.** TNFA signaling via NFKB, **B.** p53 pathway, **C.** apoptosis, **D.** hypoxia, and **E.** cell cycle. Genes involved in these five pathways show a significant upregulation in response to CP treatment, as indicated in the score tables. Enrichment plots for **F.** Rho-GTPase cycle and **G.** transmembrane receptor protein kinase activity. The negative enrichment scores highlight a loss of m<sup>6</sup>A sites and reduced transcript levels of genes in these pathways in CP-treated HeLa cells. (Cont. on next page)

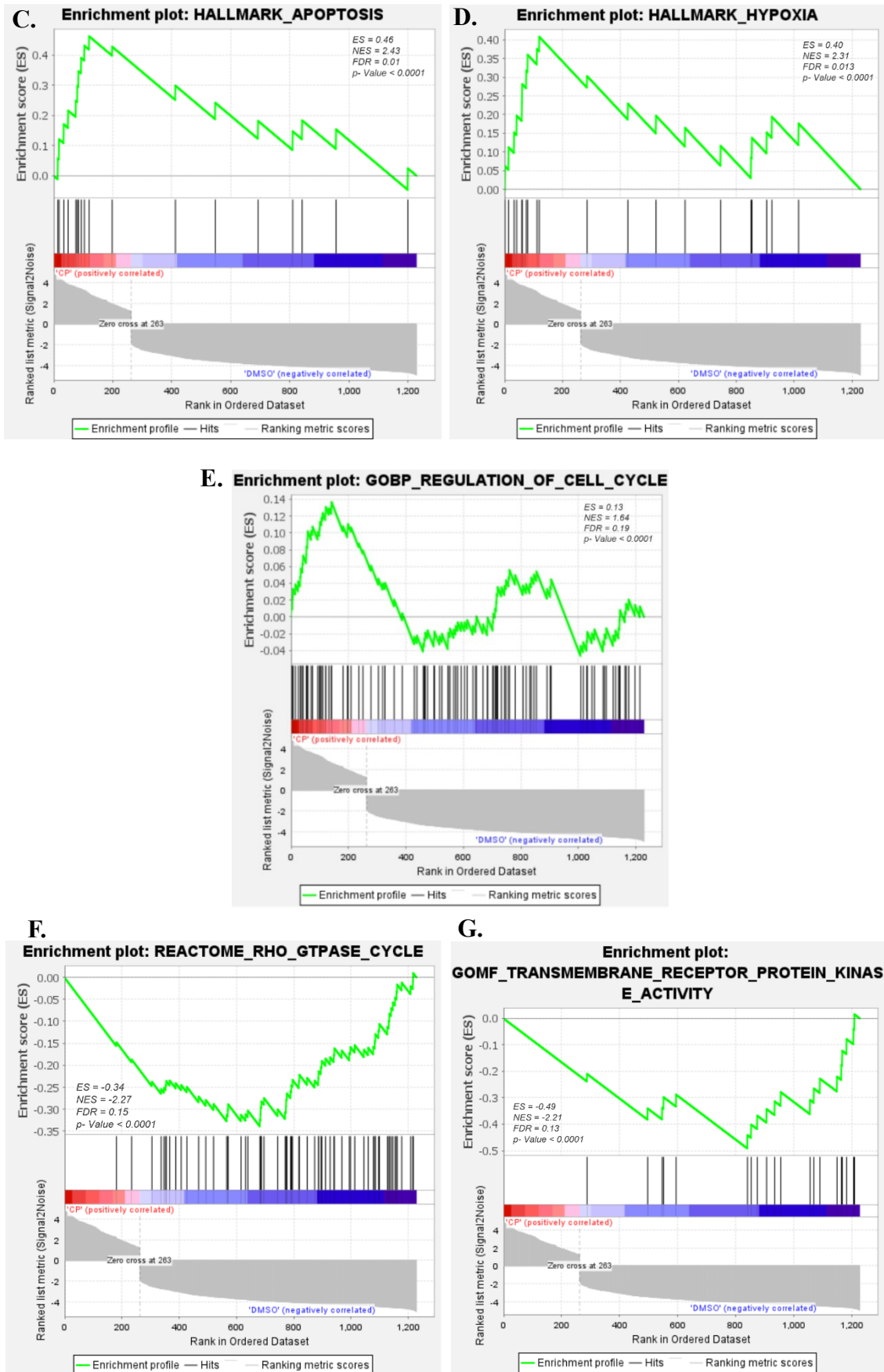
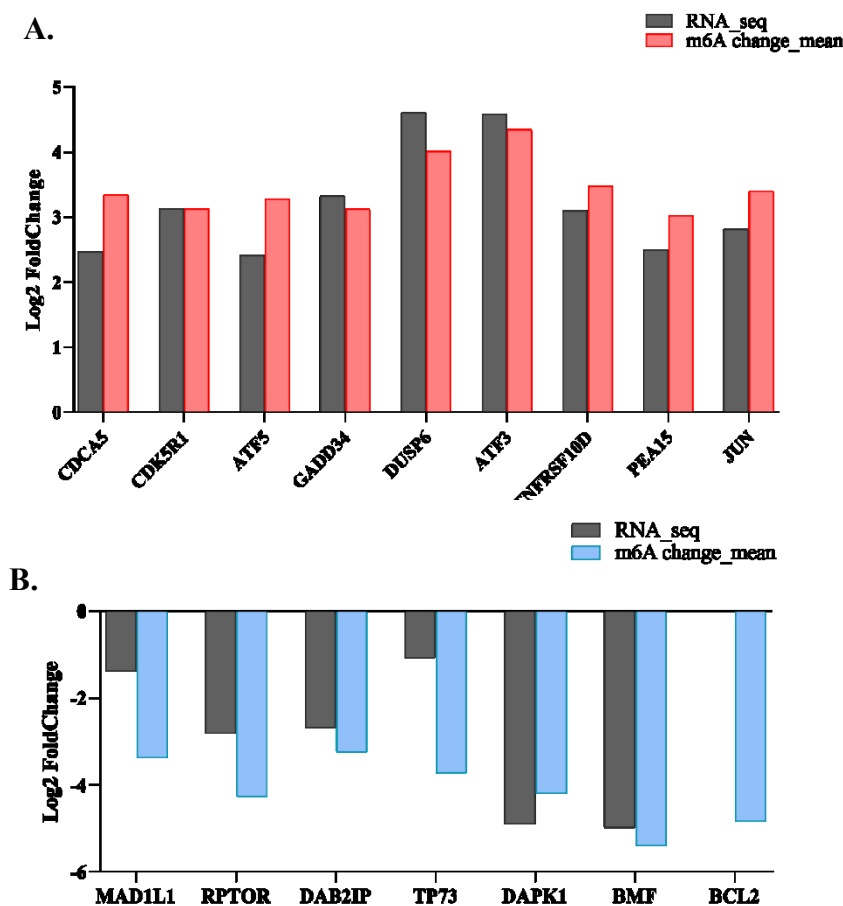


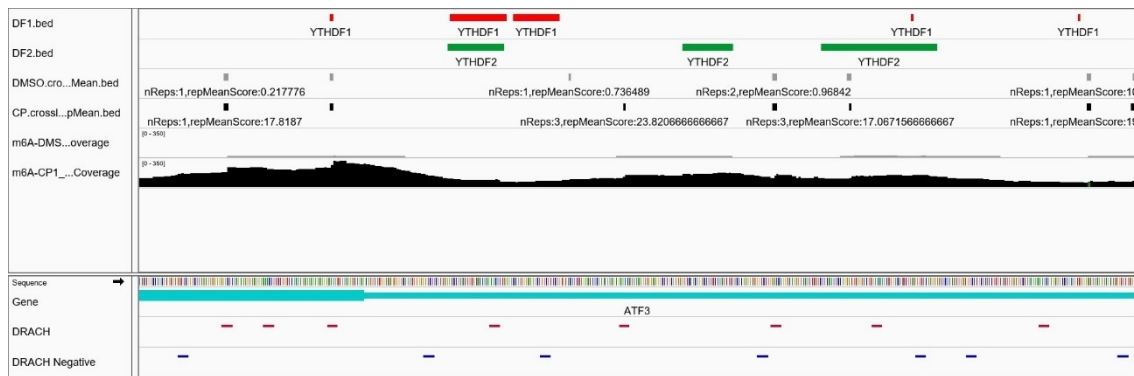
Figure 3.10. (Cont.)

Considering the differential methylation patterns, differential expression levels, and their annotation to pathways related to the CP response, 35 genes from the “hyper-induced” group and 17 genes from the “hypo-reduced” group were initially selected. In addition to these selections, two further steps were implemented to enhance the analysis of m<sup>6</sup>A modification impacts on the fate of those genes. First, genes with significant m<sup>6</sup>A peaks mapped to 5' UTR, CDS, and 3' UTR regions were prioritized over those mapped to other non-coding regions. Second, we ranked the genes based on their occupancy of YTHDF1 and YTHDF2 binding sites to facilitate further functional characterization. The nine genes (CDCA5, TNFRSF10D, JUN, GADD34, ATF5, PEA15, CDK5R1, DUSP6, ATF3) from the “hyper-induced,” six genes (MAD1L1, TP73, DAB2IP, RPTOR, DAPK1, BMF) from the “hypo-reduced,” and BCL2 with only significant decrease in methylation were finally determined for further analysis (Figure 3.11A-C, and Table 3.3).



**Figure 3.11. The selection criteria of candidate genes exhibiting differential methylation sites and mRNA levels.** Bar graphs demonstrate that the candidate genes **A.** upregulated and **B.** downregulated m<sup>6</sup>A sites, along with their transcript levels, changed in response to CP treatment. The visualization of methylation profile and YTHDF1-2 binding sites for the **C.** ATF3 gene representing the “hyper-induced” group and **D.** TP73 gene representing the “hypo-reduced” group. (Cont. on next page)

C.



D.

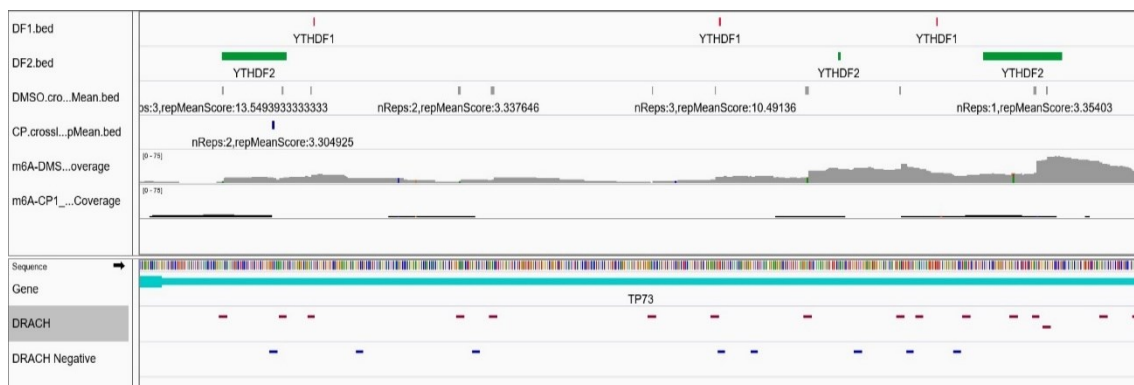


Figure 3.11. (Cont.)

### 3.5. METTL14 Knocking-down Influences Cell Proliferation and Sensitizes HeLa Cells to CP

Previous results in section 3.1. revealed a correlation between the downregulation of MTC expression and the concomitant decrease in global m<sup>6</sup>A abundance in HeLa cells after CP treatment. Our group previously demonstrated the effect of METTL3 as a catalytic domain of the METTL3:METTL14 heterodimer methyltransferase complex. (Alasar et al., 2022). To provide a more comprehensive and detailed view of the impact of m<sup>6</sup>A modification in both HeLa cells and their CP response, METTL14 was further investigated in this thesis. This focus was primarily predicated on the substantial downregulation of its protein level and its critical role as the activator of METTL3.

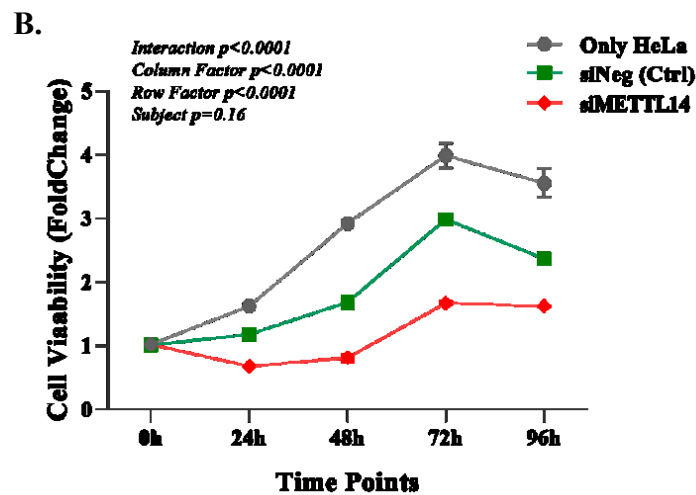
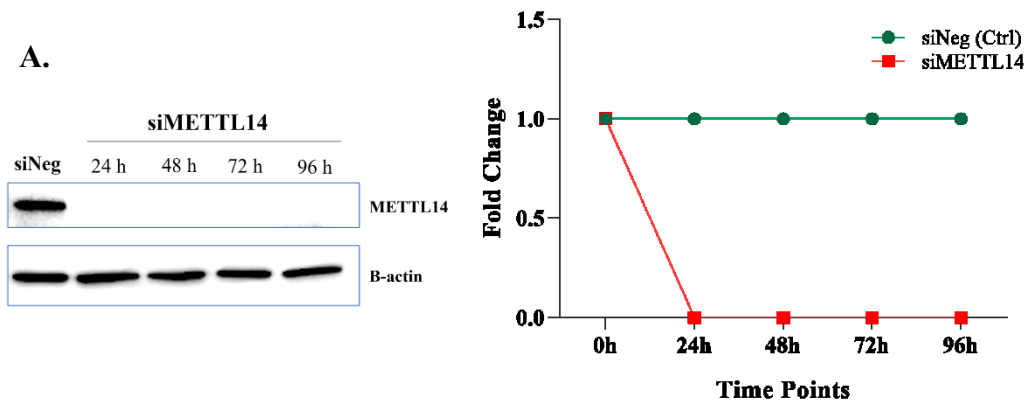
Gene Name	Pattern	Transcript ID	m6A_Info		Feature	mRNA_Info			YTHDFs Binding
			Peak_start-end			Fold Enrichment (Log2)	Fold Change (Log2)	P-value	
CDCAS	Hyper-induced	ENSGG000000146670	Chr11:65,083,989-65,083,042		5'UTR	3.34	2.47	0.00...	DF1
TNFRSF10D	Hyper-induced	ENSGG000000173530	Chr8:23,137,886-23,137,942		CDS	3.47	3.10	2.0972E-203	DF1, DF2
JUN	Hyper-induced	ENSGG000000177606	Chr1:58,783,976-58,784,042		5'UTR	3.40	2.81	2.2421E-278	DF1
GADD34	Hyper-induced	ENSGG000000087074	Chr19:48,873,639-48,873,671		CDS	3.09	3.12	3.2131E-148	DF1,DF2
ATF5	Hyper-induced	ENSGG000000169136	Chr19:49,929,210-49,929,284		5'UTR	3.30	2.41	6.8622E-114	DF2
PEA15	Hyper-induced	ENSGG000000162734	Chr1:160,214,485-160,214,586		3'UTR	3.05	2.50	0.00...	DF1
CDK5R1	Hyper-induced	ENSGG000000176749	Chr17:32,490,503-32,490,568		3'UTR	3.12	3.13	1.74655E-25	DF1, DF2
DUSP6	Hyper-induced	ENSGG000000139318	Chr12:89,349,316-89,349,531		CDS	4.30	4.58	8.7281E-26	DF1, DF2
ATF3	Hyper-induced	ENSGG000000162772	Chr1:212,608,763-212,608,843		5'UTR	5.62	4.58	0.00...	DF1, DF2
MAD1L1	Hypo-reduced	ENSGG000000002822	Chr7:1,815,864-1,816,033		3'UTR	-3.37	-1.38	1.89412E-15	DF1
TP73	Hypo-reduced	ENSGG000000078900	Chr1:3,733,113-3,733,189		3'UTR	-4.19	-1.08	0.00082	DF1, DF2
DAB2IP	Hypo-reduced	ENSGG000000136848	Chr9:121,782,628-121,782,665		3'UTR	-3.13	-2.68	1.53262E-91	DF2
RPTOR	Hypo-reduced	ENSGG000000141564	Chr17:80,965,754-80,965,802		3'UTR	-4.28	-2.81	1.28128E-86	
DAPK1	Hypo-reduced	ENSGG000000196730	Chr9:87,707,157-87,707,288		CDS	-4.19	-4.89	0.00073	DF1, DF2
BMF	Hypo-reduced	ENSGG000000104081	Chr15:40,090,336-40090416		3'UTR	-5.46	-4.97	1.1636E-102	DF1
BCL2	Hypo-methyl.	ENSGG000000171791	Chr18:63,127,661-63,127,758		CDS	-4.83	0.00	NA	DF1, DF2

METTL14 mRNA was transiently targeted utilizing siRNA cocktail, as explained in the Material and Methods section. Four different time points were selected (24<sup>th</sup>, 48<sup>th</sup>, 72<sup>nd</sup>, and 96<sup>th</sup> hrs) for further experiments to evaluate the effect of knocking down on cellular function throughout time. The protein levels starting in the 24<sup>th</sup> hour were utterly silenced in all time points, compared to the negative control group (siNeg) (Figure 3.12A). Subsequently, WST-8 analysis was performed to assess the effect of METTL14 on cell proliferation and viability. The viability difference for siMETTL14 was calculated as fold changes relative to siNeg (Ctrl), which was set to one-fold. The fold changes for siMETTL14 were 0.6 at the 24<sup>th</sup> hour, 0.5 at the 48<sup>th</sup> hr, 0.6 at the 72<sup>nd</sup> hr, and 0.7 at the 96<sup>th</sup> hr. These findings indicate that the suppression of METTL14 inhibits cell proliferation in a time-dependent manner compared to the siNeg group (Figure 3.12B). Based on these results, we further investigated whether METTL14 knockdown sensitizes HeLa cells to CP. Due to the existence of three different variables (silencing, time points, and CP), the normalization step for the silencing effect was first applied to calculate the significance between the hrs and CP for each siNeg and siMETTL14 group at each time point. Then, the ratio of each group (siMETTL14 vs. siNeg) was divided to determine the difference in viability results. Under the same conditions, the additional application of 40  $\mu$ M CP revealed that METTL14-silenced cells exhibited increased sensitivity starting at the 48-hour mark, with a 0.1-fold change. This sensitivity further increased to 0.3-fold at 72 hrs and 0.6-fold at 96 hrs. (Figure 3.12C-D).

The apoptosis analysis was performed to refine the target pathways and genes, leading to the CP sensitivity subsequent to METTL14 depletion. Cells from the negative control (siNeg) and siMETTL14 groups were stained with Annexin V and 7AAD antibodies following a 16-hour treatment with 40  $\mu$ M CP. Flow cytometry results indicated no significant difference in the living cell population (double-negative gate), with 47% in the siNeg + CP group and 46% in the siMETTL14 + CP group. However, 31% of cells in the siNeg group and 26% in the siMETTL14 + CP group were found in the Annexin V<sup>+</sup> quadrant, demonstrating a 5% reduction in apoptotic cells in the siMETTL14 + CP compared to the negative control. Notably, METTL14 silencing appeared to increase necrotic cell death by 7.7% compared to the siNeg group upon CP treatment (Figure 3.12E-F).

To evaluate the METTL14 effect on HeLa cell survival and proliferation, we proceeded to overexpress this gene by using an expression plasmid encompassing the METTL14 coding sequence. The protein expression grade compared to control

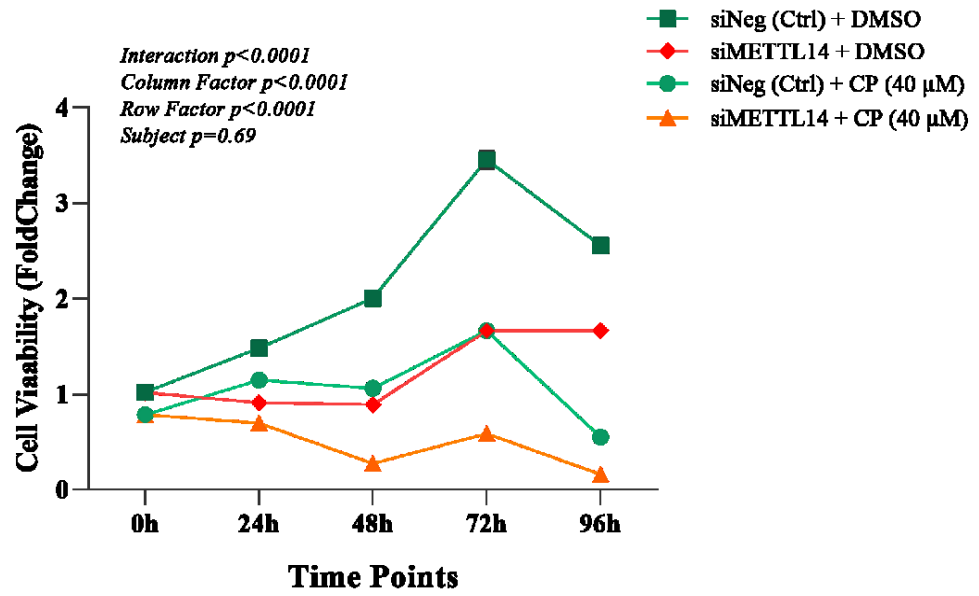
(pcDNA3.1) at 24<sup>th</sup>, 48<sup>th</sup>, 72<sup>nd</sup>, and 96<sup>th</sup> hrs was quantified as 2.7-, 3.5-, 3.6-, and 4-fold, respectively (Figure 3.13A).



**siMETTL14 vs siNeg**

Time Points	Mean_Ratio	P Value	Significance
0h	1	0.7720	ns
24h	0.58	<0.0001	****
48h	0.48	<0.0001	****
72h	0.56	<0.0001	****
96h	0.69	<0.0001	****

**Figure 3.12.** The functional analysis in only METTL14 depleted and cisplatin-treated METTL14 knockdown HeLa cells. METTL14 was silenced with siRNA technology, and 40  $\mu$ M CP and 0.1% DMSO (ctrl) were applied for 16 hrs for each time point. **A.** Western blot analysis reflecting the protein depletion of METTL14 for all time points compared to siNeg control. WST-8 assay results revealed that **B.** METTL14 silencing affected cell proliferation. **C.** Graph illustrating the cisplatin response patterns after METTL14 reduction. **D.** The CP sensitization in METTL14 KD cells compared to the siNeg control. **E.** Dot plots illustrated the distribution of the living, early apoptotic, and necrotic cell populations in METTL14 silenced and CP-applied cells. **F.** Graphical abstract showing the percentages of cell population in each quadrant. All experiments were executed as biological triplicates. (\*:  $p \leq 0.05$ , \*\*\*:  $p \leq 0.001$ , \*\*\*\*:  $p \leq 0.0001$ ). (Continues on next page)



siNeg (Ctrl) + CP vs. siNeg (Ctrl) + DMSO (40 μM)				siMETTL14 + CP vs. siMETTL14 + DMSO (40 μM)			
Time Points	Mean_Ratio	P Value	Significance	Time Points	Mean_Ratio	P Value	Significance
0h	0.78	0.0007	***	0h	0.78	0.0074	**
24h	0.78	0.0003	***	24h	0.78	0.004	**
48h	0.34	<0.0001	****	48h	0.31	<0.0001	****
72h	0.48	<0.0001	****	72h	0.35	<0.0001	****
96h	0.21	<0.0001	****	96h	0.10	<0.0001	****

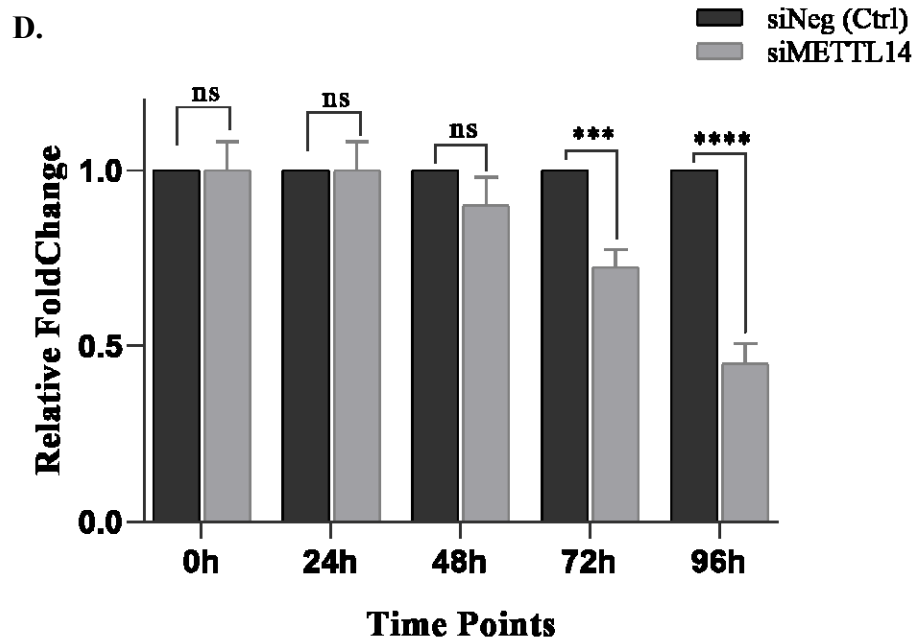


Figure 3.12. (Cont.)

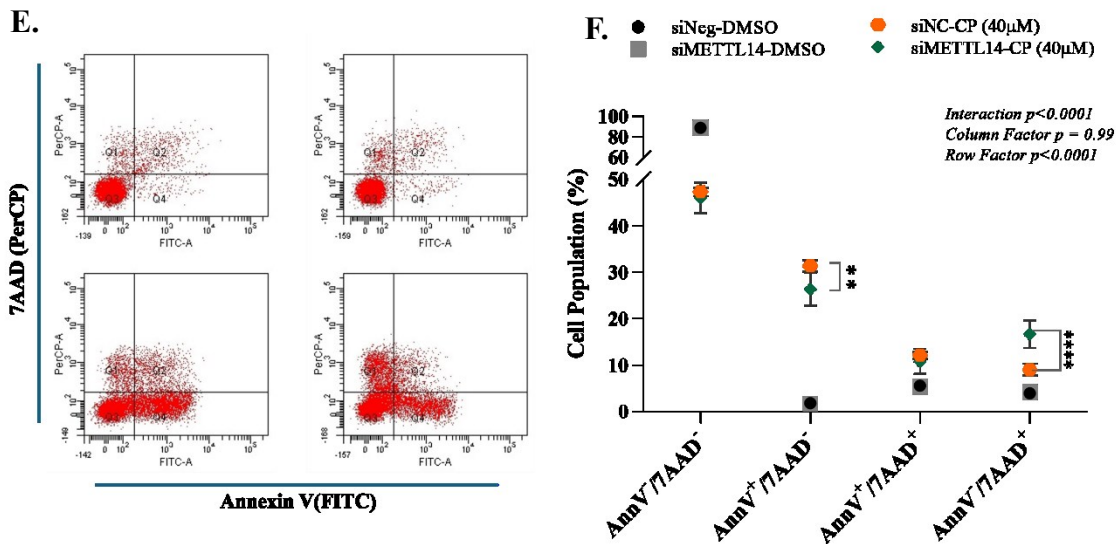
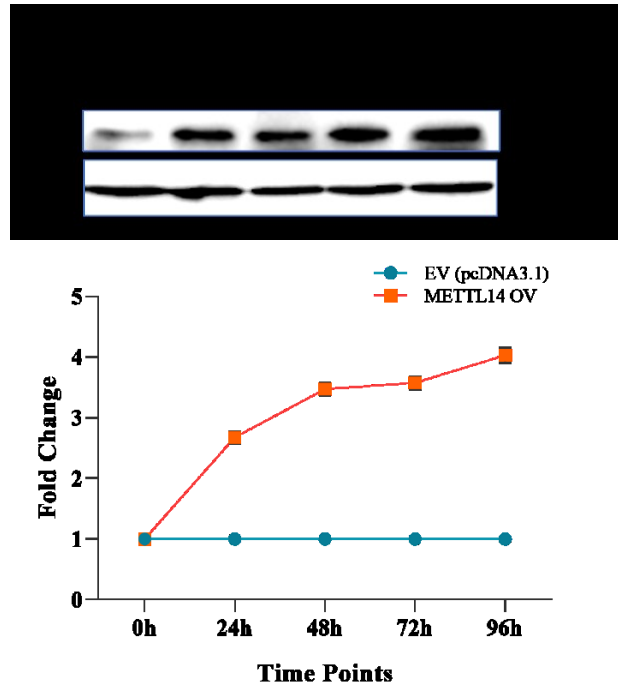


Figure 3.12. (Cont.)

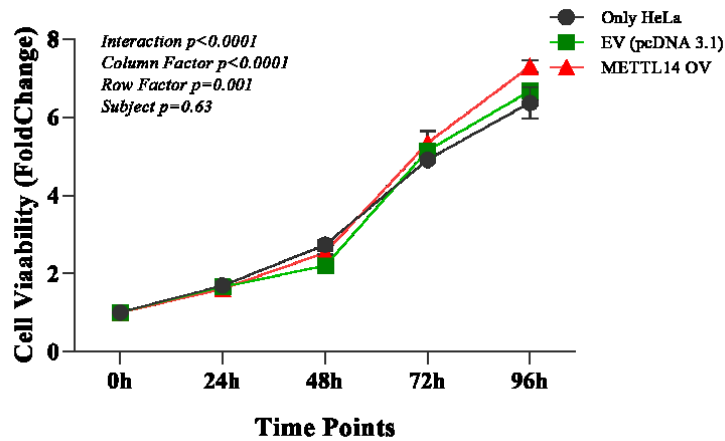
After validating protein overexpression, the proliferation status was analyzed using the WST-8 assay, the same as explained in the silencing procedure. Statistical analysis indicated significant differences at the 48<sup>th</sup> and 96<sup>th</sup> hrs post-transfection, showing 0.15- and 0.1-fold increases, respectively, in proliferation in METTL14 overexpressing cells compared to the control group. However, a significant elevation in proliferation was not observed at the 24<sup>th</sup> or 72<sup>nd</sup> hrs (Figure 3.13B). On the contrary, the relative resistance to CP was detected at the 24<sup>th</sup>-hour post-overexpression with a 0.2-fold increase in cell viability after 16-hour, 40  $\mu$ M CP treatment. Interestingly, METTL14 overexpressing cells became more sensitive to CP at the 72<sup>nd</sup> and 96<sup>th</sup> hrs, with 0.1- and 0.15-fold decrease in viability (Figure 3.13C-D).

### 3.6. m<sup>6</sup>A RNA Modification Involves the Regulation of Key Transcripts Fate Linked to CP Response

Based on the previous results demonstrating the impact of METTL14 on CP response, or vice versa, the impact of METTL14 reduction on the candidate genes with altered m<sup>6</sup>A methylation was explored. Therefore, qPCR was performed to examine whether the mRNA levels of the previously identified genes were affected by METTL14 depletion, thereby contributing to the observed sensitization by affecting the transcript's fate.



B.

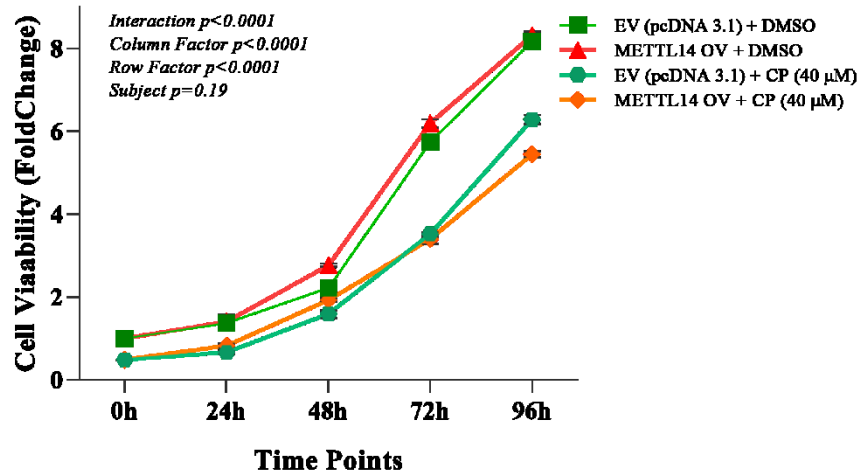


METTL14 OV vs EV (pcDNA 3.1)

Time Points	Mean_Ratio	P Value	Significance
0h	1	>0.9999	ns
24h	0.97	0.7125	ns
48h	1.15	0.0006	***
72h	1.04	0.5131	ns
96h	1.1	0.0045	**

**Figure 3.13. The effect of METTL14 overexpression on cell proliferation and CP response in HeLa cells.** METTL14 was overexpressed using the expression plasmid containing METTL14 CDS, and 40  $\mu$ M cisplatin and 0.1% DMSO (ctrl) were applied for 16 hrs for each time point. **A.** The western blot results demonstrating METTL14 overexpression for all time points compared to the control group (EV-pcDNA3.1). WST-8 assay results demonstrated that **B.** METTL14 overexpression exhibited a significant effect on cell proliferation at the 48<sup>th</sup> and 96<sup>th</sup> hrs. **C.** The cisplatin response patterns after METTL14 overexpression. All experiments were executed as biological triplicates. (\*:  $p \leq 0.05$ , \*\*\*:  $p \leq 0.001$ , \*\*\*\*:  $p \leq 0.0001$ ). (Continues on next page)

C.



EV (pcDNA 3.1) + CP vs EV (pcDNA 3.1) + DMSO				METTL14 OV + CP vs METTL14 OV + DMSO			
Time Points	Mean_Ratio	P Value	Significance	Time Points	Mean_Ratio	P Value	Significance
0h	0.49	<0.0001	****	0h	0.48	<0.0001	****
24h	0.48	<0.0001	****	24h	0.59	0.02	*
48h	0.72	0.0005	***	48h	0.70	<0.0001	****
72h	0.61	<0.0001	****	72h	0.55	<0.0001	****
96h	0.77	<0.0001	****	96h	0.65	<0.0001	****

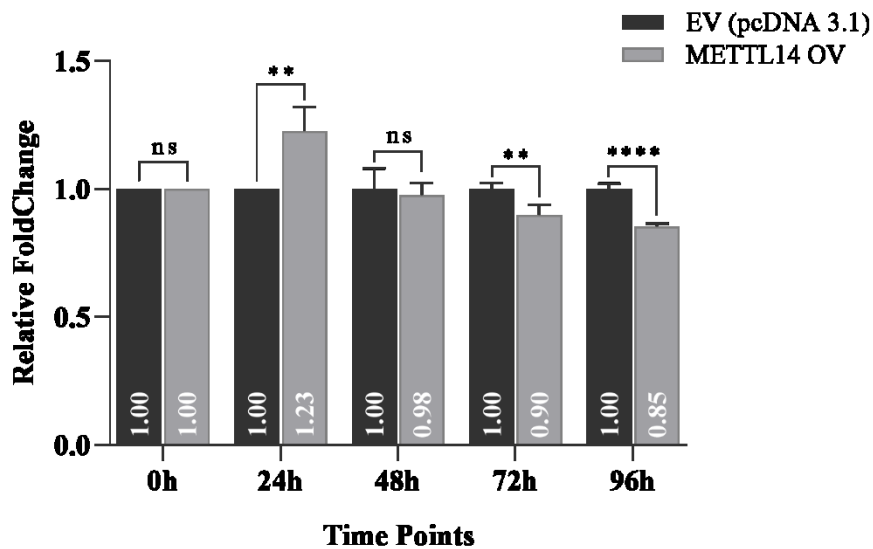
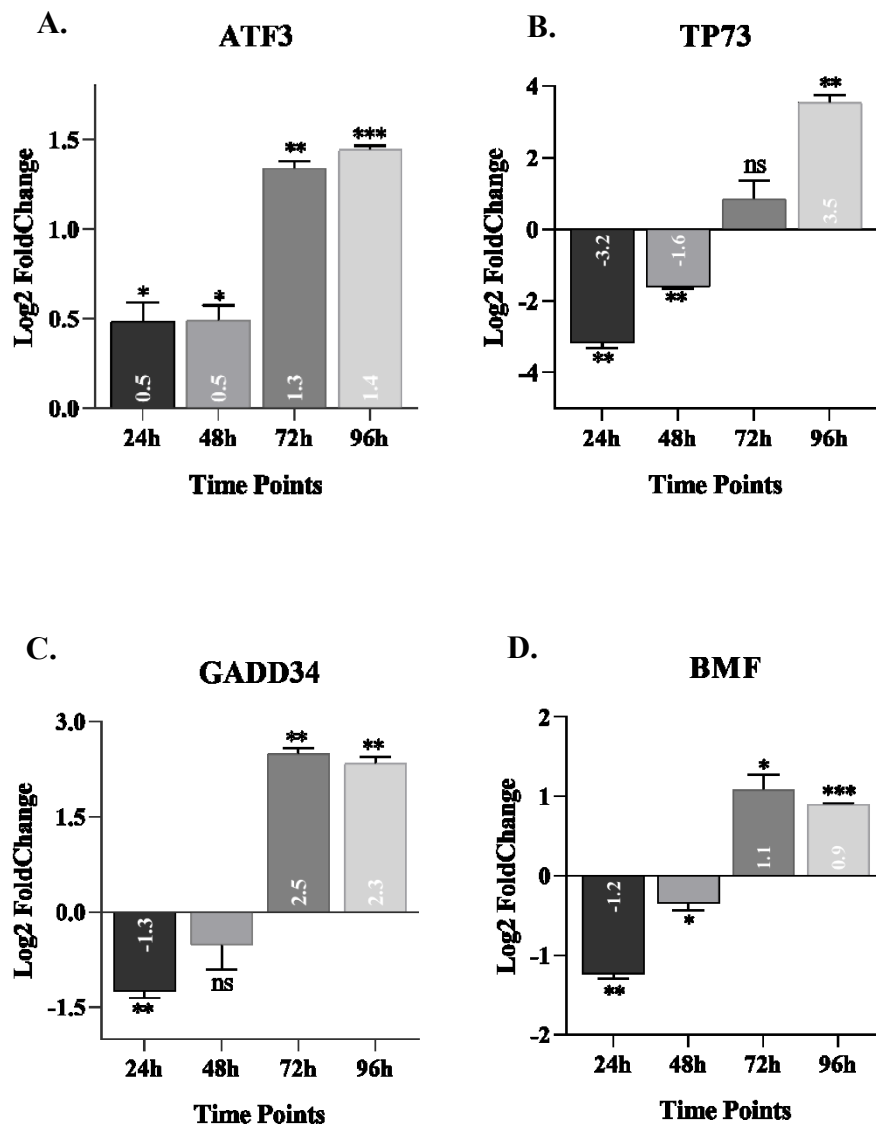


Figure 3.13. (Cont.)

To correlate with the METTL14 knockdown experiment described earlier, we performed qPCR analysis using total RNA collected from HeLa cells at 24-, 48-, 72-, and 96-hour post-transfection with METTL14 siRNA. The results, aligned with the CP sensitization and proliferation findings, revealed a complex pattern of gene expression changes. Pro-apoptotic genes such as ATF3, TP73, GADD34, BMF, DAPK1, and

DAB2IP showed significant upregulation at the 72<sup>nd</sup> and 96<sup>th</sup> hrs, while downregulation was observed at the 24<sup>th</sup> and 48<sup>th</sup> hrs, except for ATF3, which was consistently upregulated (Table 3.4 and Figure 3.14A-F). Among the pro-apoptotic genes, DUSP6 exhibited elevated transcript levels at all time points, with fold increases of 1.8, 1.6, 1.4, and 1.2, respectively (Table 3.4 and Figure 3.14G). Conversely, JUN mRNA levels decreased consistently across all time points (Table 3.4 and Figure 3.14H).



**Figure 3.14. The mRNA levels of pro-apoptotic genes and JUN in METTL14 silenced HeLa cells through time.** The total RNA was extracted from METTL14 silenced HeLa cells at 24<sup>th</sup>, 48<sup>th</sup>, 72<sup>nd</sup>, and 96<sup>th</sup> hrs post-transfection, then was subjected to the qPCR. The mRNA abundance of **A.** ATF3, **B.** TP73, **C.** GADD34, **D.** BMF, **E.** DAPK1, **F.** DAP2IP, **G.** DUSP6, and **H.** JUN among all time points. The Log2FoldChange was calculated via comparing with negative siRNA after GAPDH normalization. All experiments were executed as biological duplicates. (\*:  $p \leq 0.05$ , \*\*:  $p \leq 0.001$ , \*\*\*:  $p \leq 0.0001$ ). (Continues on next page)

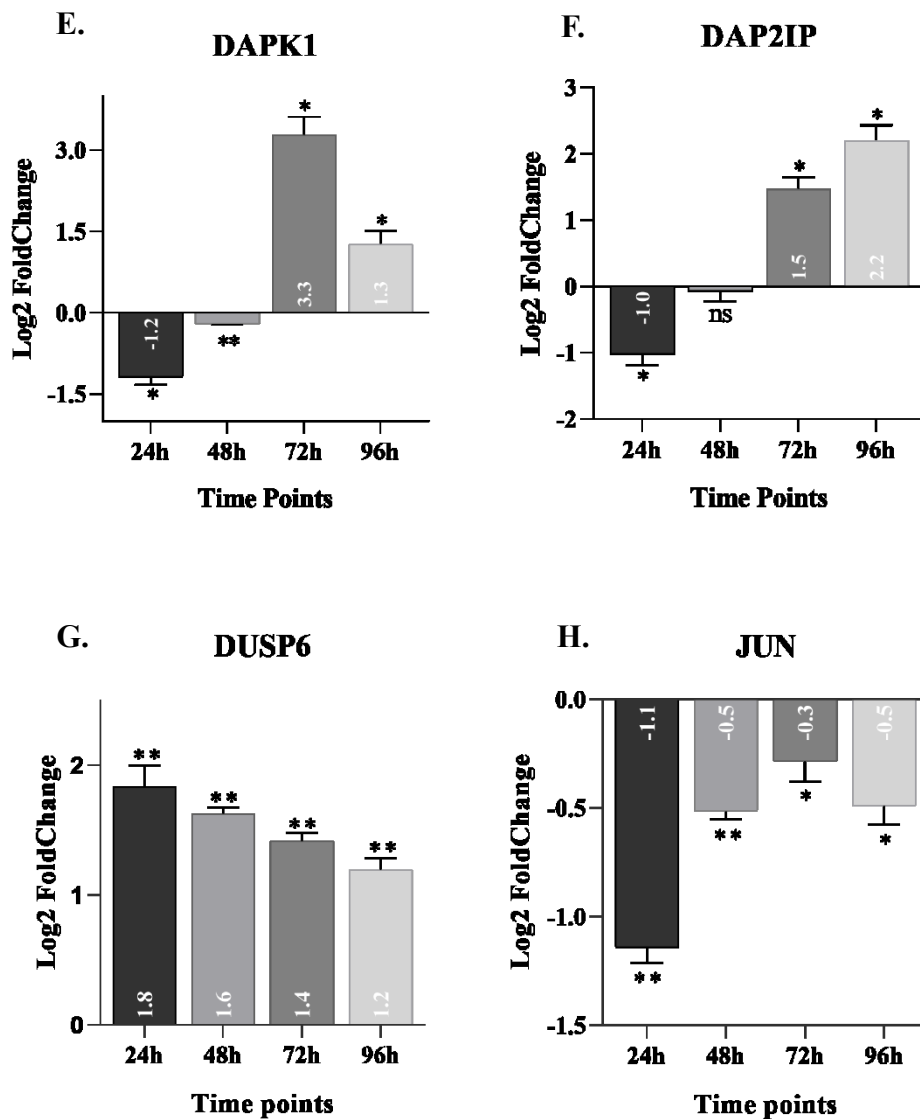


Figure 3.14. (Cont.)

Interestingly, the anti-apoptotic genes BCL2, ATF5, MAD1L1, and RPTOR showed a biphasic pattern, with decreased mRNA levels at the 24<sup>th</sup> and 48<sup>th</sup> hrs followed by increased levels at the 72<sup>nd</sup> and 96<sup>th</sup> hrs (Table 3.4 and Figure 3.15A-D). In contrast, the inhibitory proteins of extrinsic apoptosis, TNFRSF10D, and PEA15, were significantly upregulated at both the 24<sup>th</sup> and 48<sup>th</sup> hrs (Table 3.4 and Figure 3.15E-F). Additionally, CDCA5, a positive regulator of the cell cycle, showed a gradual increase in expression over time (Table 3.4 and Figure 3.15-G). These results suggest that METTL14 depletion leads to time-dependent modulation of both pro-apoptotic and anti-apoptotic gene expression, potentially contributing to enhanced CP sensitivity in HeLa cells.

Table 3.4. The list of candidate genes with the value of log2 fold change

	Gene Name	Log2FoldChange (mean±SD)			
		24h	48h	72h	96h
<b>PRO-APOPTOTIC</b>	ATF3	0.5±0,1	0.5±0.1	1.3±0	1.5±0
	TP73	-3.2±0.2	-1.6±0.1	0.9±0.5	3.5±0.1
	GADD34	-1.3±0.1	-0.5±0.4	2.5±0.1	2.3±0.1
	BMF	-1.2±0.1	-0.4±0.1	1.1±0.2	1±0
	DAPK1	-1.2±0.1	-0.2±0	3.3±0.3	1.3±0.2
	DAB2IP	-1±0.2	-0.1±0.1	1.5±0.2	2.2±0.2
	DUSP6	1.8±0.2	1.6±0	1.4±0.1	1.2±0.1
<b>DUAL</b>	ATF5	-0.7±0.1	-1±0.1	1.3±0.1	3.2±0.2
	JUN	-1.1±0.1	-0.5±0	-0.3±0.1	0.5±0.1
<b>ANTI-APOPTOTIC</b>	BCL2	-0.5±0.1	-2.4±0.5	1±0.1	1.9±0.2
	MAD1L1	-1.4±0.1	-0.2±0.1	0.1±0.3	1±0.1
	TNFRSF10D	3.2±0.2	4.4±0.2	-0.3±0.1	-0.5±0.1
	PEA15	1.3±0.1	1.8±0	1.5±0.1	-0.5±0.1
	CDCA5	0.1±0	1.3±0.2	1.3±0.1	4.3±0.3
	RPTOR	-0.4±0.1	-0.2±0.1	2.3±0.1	1.6±0.2

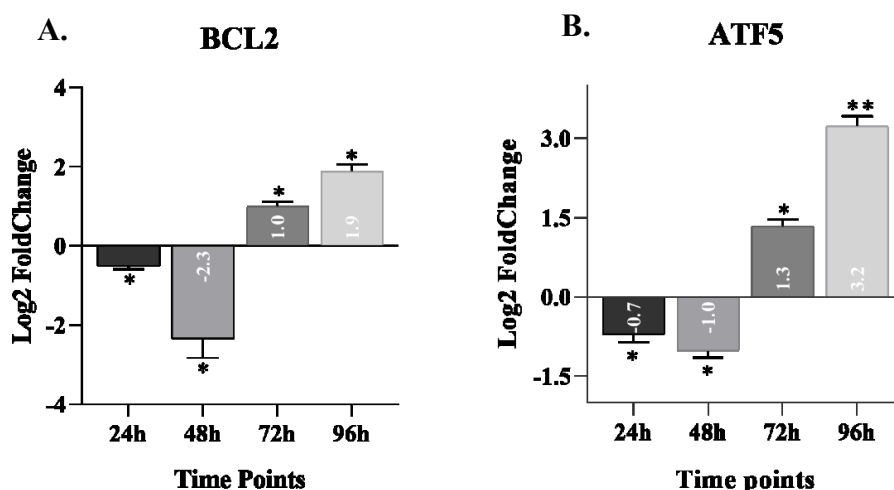


Figure 3.15. The mRNA levels of ATF5 and anti-apoptotic genes in METTL14 silenced HeLa cells through time. The total RNA was extracted from METTL14 silenced HeLa cells at 24<sup>th</sup>, 48<sup>th</sup>, 72<sup>nd</sup>, and 96<sup>th</sup> hrs post-transfection, then was subjected to the qPCR. The mRNA abundance of **A.** BCL2, **B.** ATF5, **C.** MAD1L1, **D.** RPTOR, **E.** TNFRSF10D, **F.** PEA15, and **G.** CDCA5 among all time points. The Log2FoldChange was calculated via comparing with negative siRNA after GAPDH normalization. All experiments were executed as biological duplicates. (\*:  $p \leq 0.05$ , \*\*\*:  $p \leq 0.001$ , \*\*\*\*:  $p \leq 0.0001$ ). (Continues on next page)

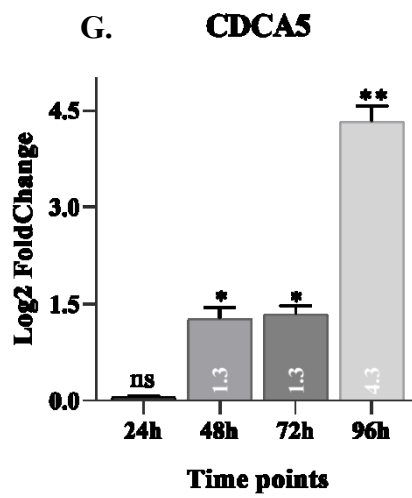
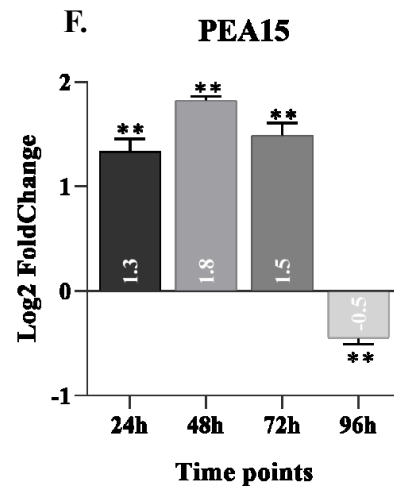
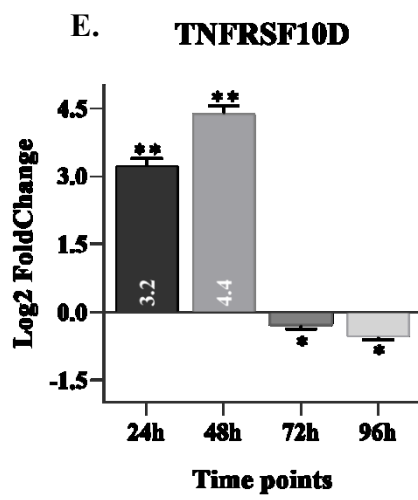
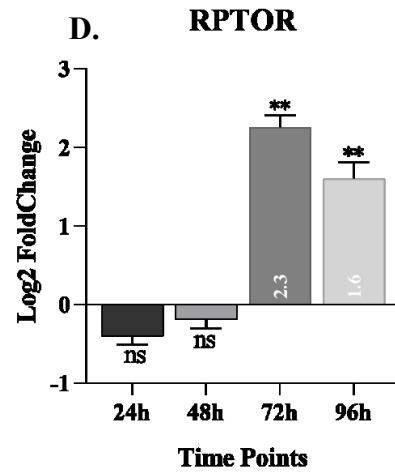
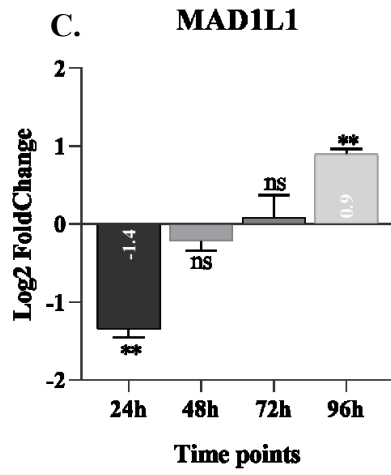


Figure 3.15. (Cont.)

### **3.7. Differential m<sup>6</sup>A Modification of Candidate Genes May Influence Transcript Fate via YTHDF2 under CP Exposure**

Based on the previous analysis demonstrating the influence of differential m<sup>6</sup>A methylation and METTL14 silencing on the transcript abundance of candidate genes involved in CP response, the functional relevance of m<sup>6</sup>A modification in these genes was further investigated. A cytoplasmic reader, YTHDF2, was selected for further experiments to test the binding affinity due to their dominance in regulating m<sup>6</sup>A methylated transcripts by its involvement in RNA decay compared to the rest of the readers (Sikorski et al. 2023). To achieve this, fCLIP-qPCR was performed to quantify the binding enrichment of YTHDF2 to the m<sup>6</sup>A sites in the presence and absence of CP treatment.

In the experimental setup, the Halo tag technology was used to increase the binding efficiency of magnetic beads, thereby reducing background signals. Then, the Halo tagged-YTHDF2 proteins were transfected to HeLa cells and later treated with DMSO or CP (80 $\mu$ M) for 16 hrs. Finally, cells were crosslinked and precipitated with Halo-tag-specific magnetic beads, and the associated RNAs were isolated for qPCR analysis. This approach enabled us to determine the differential binding enrichment of YTHDF2 to the m<sup>6</sup>A -modified candidate RNAs in both DMSO and CP-applied HeLa cells.

To obtain Halo-YTHDF2 expressed HeLa cells, YTHDF2 CDS was successfully cloned into pHTN-HaloTag CMV Neo plasmid, as explained in the Material and Methods section (Figure 3.16A). The western blot analysis indicated that the most efficient protein expression was at the 48<sup>th</sup> hr post-transfection with a 3.6-fold increment compared to the 24<sup>th</sup> and 72<sup>nd</sup> hrs (Figure 3.16B). Next, the effect of Halo-YTHDF2 overexpression on CP-induced apoptosis was investigated through flow cytometry analysis after 80  $\mu$ M CP treatment. It was found that there was no significant difference in apoptosis or cell death rate upon Halo-YTHDF2 overexpression compared to the EV control group, where 39% of cells in Halo-YTHDF2 + CP and 38% of cells in Halo-EV + CP were quantified in Annexin V<sup>+</sup>/7AAD<sup>-</sup> quadrant (Figure 3.16.C-D). Finally, the fCLIP-qPCR was performed with cells belonging to Neg Ctrl (pHTN Halo), Halo-YTHDF2 + DMSO, and Halo-YTHDF2 + CP groups. The input enrichment results for each gene indicated that the pull-down was efficiently completed. As shown in Table 3.5

and Figure 3.17A), ATF5, DAPK1, ATF3, BMF, GADD34, TP73, and DUSP6 were significantly enriched in the Halo-YTHDF2 + DMSO group, of which values were 8.1-, 9.2-, 9.3-, 11.9-, 5.2-, 0.3-, and 0.8-percent, respectively.

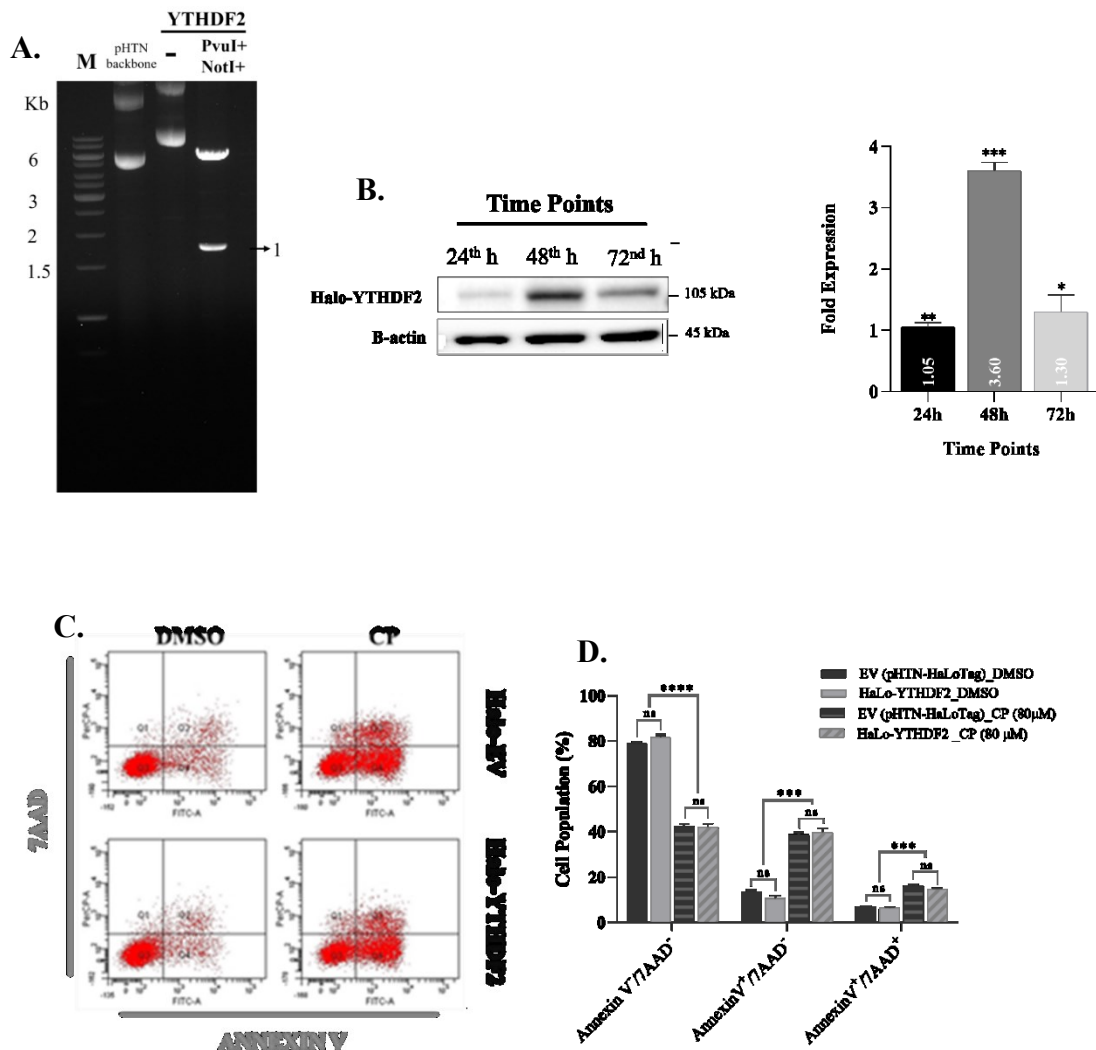


**Figure 3.16. The overexpression of HaLo-tagged YTHDF2 protein and impact on CP response.**

**A.** Agarose gel image displaying successful construction of pHTN-HaLo Tag + DF2 plasmid. **B.** WB analysis displaying the protein levels at 24<sup>th</sup>, 48<sup>th</sup>, and 72<sup>nd</sup> hrs after transfection. The expression folds for each time point were calculated after  $\beta$ -actin normalization. Flow cytometry analysis showing the Annexin V and 7AAD distribution via **C.** Dot plots and percentages via **D.** graph of EV (pHTN-HaLo) and HaLo-YTHDF2 expressed cells upon CP treatment. All experiments were executed as biological duplicates (WB) and triplicates (Flow cytometry). (\*:  $p \leq 0.05$ , \*\*\*:  $p \leq 0.001$ , \*\*\*\*:  $p \leq 0.0001$ ).

On the contrary, BCL2, MAD1L1, and DAB2IP displayed an elevated enrichment with 10.6, 6.7, and 10.1 percentages in HaLo-YTHDF2 + CP group. Consistent with the input percentage results, the fold enrichment of these genes displayed a similar pattern

(Table 3. 5 and Figure 3.17B). The fold enrichment of ATF5, DAPK1, ATF3, BMF, GADD34, TP73, and DUSP6 in the Halo-YTHDF2 + DMSO group were 10.4-, 8-, 7.6-, 4.9-, 4.4-, 4- and 3.8-fold, respectively, while BCL2, MAD1L1, and DAB2IP were enriched in CP group with 2.6-, 12, 8-, and 3.6- fold, respectively.

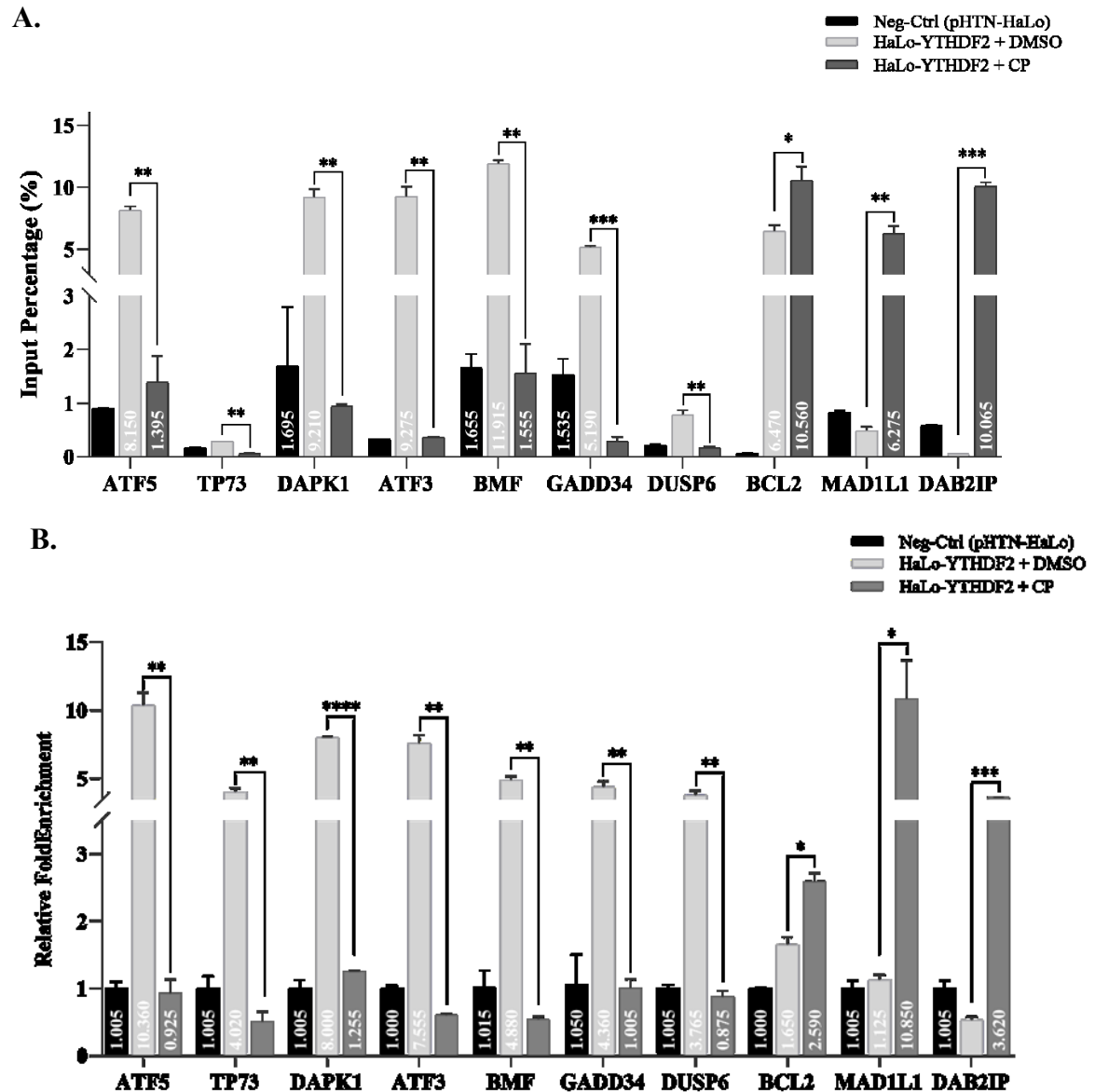


**Figure 3.17. The qPCR amplification of YTHDF2-bound mRNA of candidate genes obtained from fCLIP protocol.** The fCLIP protocol was performed with three groups of cell lysates as explained in Material and Methods. **A.** Input percentages of candidates demonstrating the efficiency of the pull-down. **B.** Relative fold enrichment of candidate genes indicating the binding affinity of HaLo-YTHDF2 in untreated and CP-treated HeLa cells. All experiments were executed as biological duplicates. (\*:  $p \leq 0.05$ , \*\*\*:  $p \leq 0.001$ , \*\*\*\*:  $p \leq 0.0001$ ).

By comparing the binding enrichment between the CP-treated and control

(DMSO) groups in HeLa cells, it was aimed to elucidate the role of YTHDF2 in mediating the effects of m<sup>6</sup>A methylation on the stability, thus, the function of transcripts involved in the cellular response to CP. Thereby, this analysis might provide insights into the dynamic interplay between m<sup>6</sup>A methylation, reader protein binding, and gene regulation in the context of CP sensitivity.

**Table 3.5. The list of candidate genes based on input percentages and fold enrichments**

<b>Gene Name</b>	<b>Input Percentage (%)</b>			<b>Fold Enrichment</b>		
	<b>pHTN-HaLo (Ctrl)</b>	<b>DMSO</b>	<b>CP</b>	<b>pHTN-HaLo (Ctrl)</b>	<b>DMSO</b>	<b>CP</b>
<b>ATF5</b>	<b>0.9</b>	<b>8.1</b>	<b>1.4</b>	<b>1.0</b>	<b>10.4</b>	<b>0.9</b>
TP73	0.2	0.3	0.1	1.0	4.0	0.5
<b>DAPK1</b>	<b>1.7</b>	<b>9.2</b>	<b>0.9</b>	<b>1.0</b>	<b>8.0</b>	<b>1.3</b>
ATF3	0.3	9.3	0.4	1.0	7.6	0.6
<b>BMF</b>	<b>1.7</b>	<b>11.9</b>	<b>1.6</b>	<b>1.0</b>	<b>4.9</b>	<b>0.5</b>
GADD34	1.5	5.2	0.3	1.0	4.4	1.0
<b>DUSP6</b>	<b>0.2</b>	<b>0.8</b>	<b>0.2</b>	<b>1.0</b>	<b>3.8</b>	<b>0.9</b>
BCL2	0.1	6.5	10.6	1.0	1.6	2.6
<b>MAD1L1</b>	<b>0.7</b>	<b>2.6</b>	<b>6.7</b>	<b>1.1</b>	<b>5.0</b>	<b>12.8</b>
DAB2IP	0.6	0.1	10.1	1.0	0.5	3.6

## CHAPTER 4

### DISCUSSION

m<sup>6</sup>A RNA methylation, a highly prevalent and efficient modification, holds a pivotal role in the fate of transcripts post-transcriptionally. Its influence spans numerous biological and pathological processes, making it a crucial regulatory mechanism. The functionality of m<sup>6</sup>A modification is intricately tied to the alteration in methyl profile via its modulator proteins, “writers” and “erasers,” and their recognition by the specific RNA binding proteins called “readers” (Balacco and Soller 2019; Y. Zhao et al. 2020). Notably, substantial alterations in the expression of these proteins, particularly writers, can modulate the transcriptome-wide m<sup>6</sup>A landscape, thereby shaping the cellular response to both internal and external stimuli (C. Zhang et al. 2020; Yao et al. 2022). These changes in m<sup>6</sup>A patterns can subsequently impact the stability or translation of critical transcripts involved in response pathways, such as cell cycle regulation, DNA damage response, ER stress response, and regulated cell death mechanisms (C. Zhang et al. 2020; Y. Fu and Zhuang 2020; Q. Y. Du et al. 2022; X. Chen et al. 2023).

CP, a platinum-based chemotherapeutic agent, has gained interest for its effectiveness in combating various forms of cancer, including ovarian, testicular, and head and neck cancers. Its primary mode of action involves the formation of DNA adducts that induce DNA damage, ultimately leading to apoptosis in rapidly dividing cancer cells (Basu and Krishnamurthy 2010; Brown, Kumar, and Tchounwou 2019). Furthermore, it has been extensively utilized to unveil the molecular mechanisms underlying the nature of cancer cells and the development of resistance against them. This study delves into the intriguing realm of the altering pattern of m<sup>6</sup>A status in response to CP treatment and the pivotal role of regulator proteins, particularly METTL14 and YTHDF2, in modulating this response.

Previous studies have underscored that the differential m<sup>6</sup>A landscape is primarily influenced by the expressional dynamics of writer proteins, particularly the METTL3:METTL14 heterodimer and WTAP (Schöller et al. 2018). Therefore, the protein levels of these key players were meticulously examined in HeLa cells exposed to CP. The initial step involved determining the impact of 80 μM CP on HeLa cell apoptosis

and caspase activation by cleavage for further investigations (Figure 3.1A-C). Subsequently, the mRNA levels of core writer proteins (METTL3, METTL14, WTAP) and eraser, FTO, were scrutinized using our previous RNA-seq data of CP-treated HeLa cells. Interestingly, METTL3 and WTAP levels slightly increased upon CP exposure, while METTL14 displayed no change in transcript abundance. In contrast, FTO mRNA reduced almost 3-fold upon the treatment (Figure 3.2A). To establish a correlation between this change and the protein function, the protein levels of these proteins under the same conditions were determined via western blotting. Strikingly, the protein levels of m<sup>6</sup>A writers, METTL3, METTL14, and WTAP were significantly decreased in CP-treated cells, particularly for METTL14, with an almost 70% reduction. A similar pattern was observed in the levels of FTO protein (Figure 3.2B-C). It was reported that the m<sup>6</sup>A modulators exhibited a cleavage site for caspases. The activation of caspase 3/7 resulted in cleaved modulators, in our case METTL3, METTL14, WTAP, and FTO, thus, the reduction in the original protein levels (K. Zhang et al. 2021). However, the bands showing cleaved parts of all these proteins did not appear in the blotting results. The proteolytic degradation of METTL14 might be caused by the duration of CP exposure, but it might not be dependent on caspase cleavage. The time kinetics for CP/protein levels were further examined to validate this hypothesis. Interestingly, the decrease in METTL14 protein levels was observed at the 2<sup>nd</sup> hr after CP treatment, while the pro-caspase 3 was reduced at the 4<sup>th</sup> hr (Figure 3.2D-E). This result suggests that the protein status of METTL14 might be regulated by other post-translational mechanisms, which might be activated upon CP exposure. Indeed, Zeng and colleagues showed that the METTL14 went under degradation via ubiquitinylation by E3 ligase, STUB1. Moreover, METTL3 was found to be a competitor of STUB1 and protected METTL14 from degradation (Zeng et al. 2023). Considering the decrease in METTL3 protein levels upon CP treatment (Figure 3.2B-C), the reduction in METTL14 levels might result from elevated availability of such ubiquitinating proteins.

Based on the dramatic decrease in writer proteins, the possible alteration in m<sup>6</sup>A extent upon CP treatment was further questioned. The m<sup>6</sup>A -eCLIP-seq was preferred to identify the differential changes in global m<sup>6</sup>A peaks and exact sites on transcripts. (Roberts, Porman, and Johnson 2021). In our experimental design, the total RNA of two groups, CP-treated HeLa versus DMSO control, was sequenced according to the m<sup>6</sup>A -eCLIP protocol. The Pearson correlation analysis and PureCLIP enrichment scores comparing the three biological replicates confirmed the reliability of the final output

(Table 3.1 and Figure 3.4A-D). DRACH is the signature motif for m<sup>6</sup>A modification, and the “word,” referring to one combination of DRACH, displays tissue-specificity (Grozhiik et al. 2017; Murakami and Jaffrey 2022). Consistent with this knowledge, our data demonstrates the same sequence, “GGACU,” for both CP and DMSO groups, indicating that the writers preferentially methylated this motif without affecting the CP exposure (Figure 3.4E).

The second key finding from the sequencing data was the localization of differentially methylated sites following CP treatment. This was determined by annotating the relative frequency of m<sup>6</sup>A modifications across various transcript features. It was known that the m<sup>6</sup>A RNA modification predominantly localizes in the last exons (3'UTR) and near-stop codon regions (Meyer et al. 2012; Ke et al. 2015). Interestingly, our results demonstrated that the majority of methylated residues were elevated in the distal intronic region in the CP-treatment group compared to the DMSO control (Figure 3.6A). Additionally, the decrement of the methylated sites was mainly observed in CDS and 3'UTR. The localization pattern of m<sup>6</sup>A residues depends not only on the sequence of the DRACH motif but also on the availability of this motif, leading us to the genome architecture and the location of transcription machinery. It has been found that the length of the terminal exon, the existence of an exon-exon junction near the stop codon, and the presence of RNA Pol II in the actively transcribed regions determine the frequency and localization of methylation (Dominissini et al. 2012; S. Ke et al. 2015; Nojima et al. 2015). Additionally, genome mapping of CP-treated ovarian cancer cell lines has identified that CP alters chromatin accessibility at intergenic regions, leading to alternative gene expression (Gallon et al. 2021). In this concept, our findings support and, most importantly, combine the information from the literature, increasing the significance of m<sup>6</sup>A modification considered a therapeutic target. However, the function of those transcribed intergenic regions and the role of m<sup>6</sup>A modification in those transcripts are further investigated to uncover their potential in cancer research and therapy. When limiting the regions placed only in the mature transcripts, the methylation peaks were dramatically upregulated in 5'UTR compared to the other regions, CDS and 3'UTR (Figure 3.6C-D). This pattern may also be attributable to the previously discussed factors.

CP also impacted the number of differentially methylated sites and genes. The results highlighted that 1350 m<sup>6</sup>A residues on 634 genes were gained, while 5998 on 1350 genes were lost upon CP treatment. Only 33 genes exhibited increased and decreased methylation sites, with elevation in 56 positions against reduction in 237 (Figure 3.6E-F).

This might be the consequence of CP, which stalls the expression of the genes related to regular cellular functions, such as cell metabolism, growth, biosynthesis, and cellular maintenance (Dasari and Bernard Tchounwou 2014; S. H. Chen and Chang 2019). Indeed, GO Pathway and KEGG analysis indicated that m<sup>6</sup>A peaks were primarily elevated in genes involving the cellular response to CP, such as regulation of proliferation and cell cycle and programmed cell death/apoptosis (Figure 3.7A-C). On the contrary, the reduction was observed in those genes regulating transcription, migration, adhesion, and growth signaling events (Figure 3.7B-D).

To acquire deeper insights, the RNA-seq, used as “input” for normalizing the relative exchange in m<sup>6</sup>A levels, was annotated to the reference genome to obtain the list of differentially expressed genes from the same RNA samples. The volcano plot and heatmap analysis revealed specific differences in the RNA levels of CP-treated HeLa cells against the DMSO control (Figure 3.8B-C). This result was consistent with the previously published RNA-seq data (Gurer et al. 2021). A correlation analysis of these two data was performed to investigate the link between differential gene expression and differential methylation. Intriguingly, the RNA abundance displayed a strong positive correlation with the m<sup>6</sup>A levels (Figure 3.9A). Furthermore, the number of differentially methylated sites was positively correlated with the differential gene expression patterns. The results indicated a positive regulatory role of m<sup>6</sup>A methylation in the transcript stability of genes related to the CP response. Despite the well-established function in cytoplasmic RNA degradation, our findings pointed to the function in RNA stability, and the pre-RNA processing influencing the localization and stability might become the dominant role of methylation in response to CP exposure (Uzonyi et al. 2023).

To explore the relationship between “hyper-induced” and “hyper-reduced” genes and the phenotypic changes observed following CP treatment, gene set enrichment analysis (GSEA) was performed. The analysis indicated a strong correlation between the genes enriched in the top five pathways, including the p53 pathway, apoptosis, and regulation of cell cycle and the cellular response to CP, suggesting that these genes play a crucial role in mediating the drug's effects (Figure 3.10A-G). The GSEA results were also used to determine candidate genes for further analysis. Nine genes (CDCA5, TNFRSF10D, JUN, GADD34, ATF5, PEA15, CDK5R1, DUSP6, ATF3) from the “hyper-induced” group, six genes (MAD1L1, TP73, DAB2IP, RPTOR, DAPK1, BMF) from the “hypo-reduced” group, and BCL2, which showed a significant decrease only in methylation, were selected with a collection of different steps. First, the genes were

categorized according to their differential methylation and gene expression status as defined in Results section 3.4. The genes belonging to these two groups were subsequently subjected to GSEA, as indicated above. An initial selection between those was made of 17 genes from the “hypo-reduced” group and 35 genes from the “hyper-induced” group, which were linked to the CP response. Finally, two additional criteria were applied to refine this selection further and enhance the analysis of m<sup>6</sup>A modification effects on gene fate. First, genes exhibiting significant m<sup>6</sup>A peaks within the 5' UTR, CDS, and 3' UTR regions were prioritized over those in other non-coding regions. Second, genes were ranked according to their occupancy of YTHDF1 and YTHDF2 binding sites for subsequent functional analysis (Table 3.3 and Figure 3.11A-C).

Among these 16 genes, ATF3 (D. Lu, Wolfgang, and Hai 2006; Sato et al. 2014), TP73 (K. C. Kim, Jung, and Choi 2006, 152–58), GADD34 (Holczer, Bánhegyi, and Kapuy 2016), BMF (Haolan Wang et al. 2023, 3760–67), DAPK1 (S. Wang et al. 2017, 4716–22), DAB2IP (J. Zhou et al. 2015, 1955–65), DUSP6 (Piya et al. 2012) and CDK5R1 (Wan Liu et al. 2017) are known to be pro-apoptotic genes, while BCL2 (Vaux, Cory, and Adams 1988), MAD1L1 (H. Luo et al. 2023), THNFRSF10D (Slattery et al. 2018), PEA15 (Renault et al. 2003), CDCA5 (W. Shen et al. 2022), and RPTOR (Ito et al. 2017) act as anti-apoptotic. Additionally, ATF5 (Y. Wei et al. 2008; Dluzen et al. 2011) and JUN (Dou et al. 2019) exhibit dual function in cell survival and apoptosis.

To evaluate the interplay between CP response and m<sup>6</sup>A modification, this study also examined the role of METTL14, an m<sup>6</sup>A writer, in regulating cell proliferation and its subsequent impact on CP sensitivity. METTL3 is the core protein that accomplishes the m<sup>6</sup>A deposition as the only writer exhibiting catalytic activity (Xiang Wang et al. 2016). The active SAM residue in METTL3 allows the addition of methyl group to the adenosine at the N<sup>6</sup> position. Even if it is absent or has lesser catalytic activity, METTL14 is undoubtedly required to activate METTL3 by providing conformational stability and increased affinity for the pre-RNA binding site to contact the substrate of METTL3 (P. Wang, Doxtader, and Nam 2016). Given its critical role in activating METTL3, METTL14 has emerged as a pivotal focus in functional studies on m<sup>6</sup>A modification. Relevant to this thesis, METTL14 has been found to support cell proliferation and migration in multiple cancer types (Sun et al. 2020; H. Zhou et al. 2021). Moreover, METTL14 knockdown advances the impact of CP by disturbing the ERK1/2 and mTOR signaling cascades and driving the cells to apoptosis in pancreatic cancer cells (Kong et al. 2020). The downregulation of METTL14 influences global m<sup>6</sup>A levels and extent via

deactivating the methyltransferase core complex (Miyake et al. 2023). Our results revealed that CP exposure significantly reduced METTL14 protein levels (Figure 3.2B-C). METTL14 expression was first manipulated by silencing (Figure 3.12A) and overexpressing (Figure 3.13A) to examine further the connection between changed m<sup>6</sup>A status and CP response. As expected, METTL14 downregulation stalled the HeLa cell proliferation with a consistent increment over time (Figure 3.12B). However, METTL14 overexpressed HeLa cells did not alter their proliferation pattern at the same duration compared to the negative control (Figure 3.13B). Interestingly, METTL14 knockdown did not influence the rate of apoptosis (Figure 3.1F), which pointed out that the METTL14 depletion might affect only the paths related to the cell cycle, growth, or other types of regulated cell death but not apoptosis in HeLa cells. A similar effect was observed after CP treatment in METTL14-depleted cells. Specifically, the sensitization to CP started at the 48<sup>th</sup> hr upon METTL14 silencing and significantly elevated gradually at the 72<sup>nd</sup> and 96<sup>th</sup> hrs (Figure 3.12D). Surprisingly, the sensitization to CP was not due to the increment in apoptosis. This finding suggested that the possible impact of METTL14-targeted m<sup>6</sup>A methylated transcripts might influence the stress-response mechanisms other than apoptosis (W. Yu et al. 2018, 1–12; Y. Yang et al. 2024, 1–17). The upregulation of METTL14 demonstrated a different pattern of CP impact. Time kinetics of METTL14 overexpression revealed that HeLa cells gained resistance to CP at the 24<sup>th</sup> hr after METTL14 overexpression. However, this effect was reversed between the 48<sup>th</sup> and 96<sup>th</sup> hrs. It was previously reported that both increments and decreases in METTL14 protein abundance have promoted the inhibition of proliferation via inducing regulated cell death mechanisms in brain tissue (Gao et al. 2022; Pomaville et al. 2024). Until now, a negative correlation between METTL14 levels and CP sensitivity has been reported in different studies (Kong et al. 2020; Gong, Wang, and Shao 2022). Nevertheless, this dual function of CP response and its mechanism remains uncovered. This thesis provided initial evidence about the dual effect of METTL14 abundance on CP response over time in HeLa cells for the first time.

To correlate the previous findings demonstrating the significant elevation or decrease in both methylation and RNA levels of candidate genes upon CP treatment and integrative impacts of both METTL14 and CP on each other in HeLa cells, we further explored the influence of METTL14 depletion on those candidate genes over time. The RNA levels of candidate genes were the priority in this study for two connected reasons: (i) the significant impact of m<sup>6</sup>A modification on the stability of cytosolic RNAs and (ii)

the existence of potential binding sites of those genes to YTHDF2, which was the final aim of this thesis.

Based on the decreased level of METTL14 upon CP treatment, the repercussions of METTL14-dependent m<sup>6</sup>A modification on candidate genes were further explored. The total RNA was extracted from METTL14 siRNA transfected cells at the 24<sup>th</sup>, 48<sup>th</sup>, 72<sup>nd</sup>, and 96<sup>th</sup> hrs. The results indicated that only ATF3, DUSP6, CDCA5, and PEA15 RNAs were consistently elevated, like sequencing data, after METTL14 silencing in all time points (Figure 3. 14A-G, Figure 3.15F-G). On the other hand, most of the candidates' transcripts constituted an elevation followed by a reduction, and vice versa, over time. For instance, TP73 exhibited a 3.2-fold reduction at the 24th-hour mark, followed by a 1.6-fold increment (but still less than the negative control). However, its RNA levels exceeded those of the control group at the 72<sup>nd</sup> and 96<sup>th</sup> hrs (Figure 3.14B). Additionally, two genes showed a different pattern than others. Even if the RNA abundance differed among all time points, JUN was consistently downregulated compared to the control group (Figure 3.14H). Secondly, TNFRSF10D was significantly upregulated at the first two hrs and slightly downregulated at the rest (Figure 3.1E).

METTL14 silencing affected the transcript status of some candidate RNAs dissimilar to the observed levels upon CP treatment. Still, the prediction can be made on the possible effects of prolonged METTL14 absence on the CP response. The significant sensitivity to CP followed by the METTL14 silencing was viewed at the 72<sup>nd</sup>- and 96<sup>th</sup>-hr mark (Figure 3.12C-D). Combining this result, the influence of the candidate genes might be interpreted. TP73 is a member of the p53 family of proteins, which act as a tumor suppressor. While the function of p73 overlaps with the role of p53, mutations on TP73 are rare in most cancers, unlike TP53 (Ikawa, Nakagawara, and Ikawa 1999). The p73 does not only induce apoptosis but also the stress response mechanisms and autophagy. The evidence highlighted that the initial response of p73 to stress conditions was the promotion of cell survival by arresting the cycle and initiating the ER stress response and autophagy, leading to cell death (Humbert, Federzoni, and Tschan 2017; Rozenberg et al. 2021). In the RNA-seq and m<sup>6</sup>A -seq data, TP73 displayed decreased levels in both methylation and transcript. These results suggest that the cells might escaped the killing effect of CP (46.7% of cells in our data) and suppressed the expression of this protein. Intriguingly, the TP73 showed consistency with the reduced mRNA levels upon CP treatment at the 24<sup>th</sup> and 48<sup>th</sup> hrs. However, the upregulation of p73 mRNA was started at the 72<sup>nd</sup> hr. and significantly elevated at the 96<sup>th</sup> hr., at which time the cells were

sensitized to CP the most due to the METTL14 depletion. Similar to the TP73 gene, DAPK1 displayed an upregulation at the 72<sup>nd</sup> and 96<sup>th</sup> hrs, except the most increment to be observed in the 72<sup>nd</sup> hr. (Figure 3. 14E). Indeed, this pattern might indicate that the combined impact of TP73/DAPK1 due to the kinase activity of DAPK1 targeting p53-family proteins and causing their activation (S. Wang et al. 2017). Another gene, DAB2IP, exhibited enhanced levels of its mRNA at the last two time points (Figure 3. 14F). DAB2IP, a member of the RAS-GTPase activating protein family, suppresses cell growth by inhibiting both RAS-GTPase and PI3K/Akt pathways, thus indirectly inducing apoptosis (Xie et al. 2009). The sensitivity to CP in METTL14 knockdown cells was additionally supported by the inactivation of the PI3K/Akt cascade and, therefore, the elevated level of DAP2IP (N. Wang et al. 2018).

To correlate the altered transcript levels and m<sup>6</sup>A modification, the binding affinity of YTHDF2 to candidates was explored. YTHDF2, a reader protein that directly recognizes the N<sup>6</sup> methylated adenosine residues, recruits the nuclease complexes, such as CNOT1, UPF1, and HRSP12 (H. Du et al. 2016; Boo et al. 2022). Based on its function, the differential binding of YTHDF2 to the candidate genes in untreated and CP-treated HeLa cells provided more mechanistic insights into the CP response and the influence of METTL14-derived m<sup>6</sup>A methylation.

HaLo-tagged YTHDF2 plasmid was constructed and subsequently transfected to HeLa cells (Figure 3. 16A). After determining the maximum expression time as 48 hrs (Figure 3.16B), 80  $\mu$ M CP was applied for 16 hrs. The apoptosis rate of negative control (EV) and HaLo-YTHDF2 overexpressed cells in DMSO and CP-treated HeLa cells was further detected. The results indicated that the YTHDF2 overexpression did not change the apoptosis ratio in the DMSO and CP-treated group compared to the negative control group (Figure 3.16C-D). Then, the YTHDF2-overexpressed HeLa cells under CP exposure were subjected to the fCLIP-qPCR procedure to identify the differential binding to the candidate genes. Due to the limited amount of precipitated RNA obtained, TP73, DAPK1, ATF3 ATF5, DUSP6, DAB2IP1, GADD34, and BMF were selected for their capacity to induce a stress response and apoptosis, while BCL2 and MAD1L1 were selected as survival genes. Excitingly, the elevated binding of YTHDF2 was observed in almost all cell death inducers in the DMSO control group compared to the CP-exposed cells and negative control of the IP experiment (empty vector or EV), except for DAB2IP. Controversially, BCL2 and MAD1L1 were enriched in CP-applied cells.

The decreased binding of YTHDF2 to anti-survival, pro-apoptotic genes in the CP

group suggested that the stability, thus the protein expression of these mRNAs might raise as a response to CP. The same rationale might be applied to BCL2 and MAD1L1, which bind to YTHDF2 enriched upon CP treatment.

Even if this pattern of YTHDF2 binding enrichment seemed to be correlated with the CP response, it might not be applicable for ATF3, ATF5, GADD34, DAB2IP, BCL2, and MAD1L1 due to their differential m<sup>6</sup>A methylation and RNA abundance, based on our sequencing data. For example, the methylation and mRNA abundance of ATF3 were upregulated upon CP treatment (Figure 3.11A). Nevertheless, the binding affinity was significantly enriched in the DMSO group. Thus, it is possible that the increased RNA abundance might be dependent on other factors, such as m<sup>6</sup>A -mediated or other regulatory mechanisms.

In line with our RNA and m<sup>6</sup>A -seq data, three genes, TP73, DAPK1, and BMF, demonstrated a strong correlation with the regulatory role of YTHDF2 on the RNA abundance. The sequencing data revealed that genes showed significant downregulation in both RNA abundance and m<sup>6</sup>A methylation (Figure 3.11B). fCLIP-qPCR results of YTHDF2 further suggested that YTHDF2 targeted the 3'UTR of TP73 and DAPK1 and the CDS region of BMF, thereby accelerating their transcript degradation in an m<sup>6</sup>A -dependent manner in HeLa cells. Their mRNA levels were dramatically elevated due to the m<sup>6</sup>A depletion on the YTHDF2 binding site as a part of the CP response in HeLa cells.

## CHAPTER 5

### CONCLUSION

N<sup>6</sup>-methyladenosine (m<sup>6</sup>A) modification is one of the most abundant, dynamic RNA modifications, directly influencing transcripts' fate post-transcriptionally. This dynamic regulatory system is directly involved in the response mechanisms to internal or external stimuli. Thus, it was hypothesized in this study that m<sup>6</sup>A RNA modification participated in regulating CP response in HeLa cells.

In the exploration of this theory, we embarked on a novel approach. First, we detected the status of core m<sup>6</sup>A modulators upon CP exposure, followed by the analysis of the transcriptome-wide extent of m<sup>6</sup>A methylation. Our findings revealed that CP treatment significantly alters the m<sup>6</sup>A RNA methylation landscape, driven by changes in the expression of crucial m<sup>6</sup>A writer proteins, particularly METTL14. The reduction of METTL14 expression following CP exposure was significant and might be correlated with a global decrease in m<sup>6</sup>A modification levels. These novel insights open up new avenues for further research in this field.

METTL14, as an activator of methyltransferase core, positively influenced cell proliferation and survival; thereby, its depletion caused the incremental elevation of CP sensitivity. Indeed, METTL14 silencing significantly impacted the elevated RNA levels of cell-death-related genes, notably at 72<sup>nd</sup> and 96<sup>th</sup> hrs. Interestingly, some of the candidates, such as ATF3, ATF5, DUSP6, and PEA15, displayed similar expression patterns, while TP73, BMF, DAPK1, and DAB2IP exhibited the mRNA levels in the opposite direction to those identified in CP RNA-seq. These results provided initial data for the interplay between METTL14 and CP response, indicating that some candidates' mRNA status might be influenced by METTL14-directed methylation. However, the differential gene expression landscape of METTL14-depleted HeLa cells might be further investigated via RNA sequencing to obtain more accurate and transcriptome-wide information. Additionally, the transcript abundance of those candidates might be determined in HeLa cells upon METTL14 silencing, followed by CP treatment.

The fate of cytoplasmic mRNAs is mainly regulated through the binding of YTHDF proteins in an m<sup>6</sup>A -dependent manner. YTHDF2 is the primary regulator

influencing mRNA abundance because it recruits different nucleases to its bound region. Notably, the enriched binding of YTHDF2 to pro-apoptotic candidate genes (TP73, DAPK1, ATF3, and BMF, etc.) in the control group rather than CP-treated cells suggests that the expression of these genes might be post-transcriptionally regulated by YTHDF2-derived mRNA decay. The binding pattern of YTHDF2 to some candidates appeared to be independent from the differential methylation pattern of CP-exposed HeLa cells. For example, ATF3 was identified as a “hyper-induced” gene with elevation in mRNA and m<sup>6</sup>A levels upon CP treatment. Thus, it is expected that the YTHDF2 binding will be enriched in the CP group, leading to a reduction in mRNA abundance. Thus, the binding capacities of other readers functioning in the fate of mRNA stability, such as YTHDF3 or IGF2BPs, should be further explored via LC-MS/MS followed by location-specific-methylated RNA pulldown or CLIP-qPCR to obtain more mechanistic insights about the involvement of reader proteins to CP response.

## REFERENCES

- Aas, Aleksander, Pauline Isakson, Christian Bindesbøll, Endalkachew A. Alemu, Arne Klungland, and Anne Simonsen. 2017. “Nucleocytoplasmic Shuttling of FTO Does Not Affect Starvation-Induced Autophagy.” *PLoS ONE* 12 (3). <https://doi.org/10.1371/JOURNAL.PONE.0168182>.
- Agarwala, Sudeep D., Hannah G. Blitzblau, Andreas Hochwagen, and Gerald R. Fink. 2012. “RNA Methylation by the MIS Complex Regulates a Cell Fate Decision in Yeast.” *PLoS Genetics* 8 (6). <https://doi.org/10.1371/JOURNAL.PGEN.1002732>.
- Aik, Weishen, John S. Scotti, Hwanho Choi, Lingzhi Gong, Marina Demetriades, Christopher J. Schofield, and Michael A. McDonough. 2014. “Structure of Human RNA N<sup>6</sup>-Methyladenine Demethylase ALKBH5 Provides Insights into Its Mechanisms of Nucleic Acid Recognition and Demethylation.” *Nucleic Acids Research* 42 (7): 4741–54. <https://doi.org/10.1093/NAR/GKU085>.
- Ajay, Amrendra K., Avtar S. Meena, and Manoj K. Bhat. 2012. “Human Papillomavirus 18 E6 Inhibits Phosphorylation of P53 Expressed in HeLa Cells.” *Cell & Bioscience* 2 (1): 2. <https://doi.org/10.1186/2045-3701-2-2>.
- Akçaöz Alasar, Azime, Buket Sağlam, İpek Erdoğan Vatansever, and Bünyamin Akgül. 2023. “Expression Patterns of M<sup>6</sup>A RNA Methylation Regulators under Apoptotic Conditions in Various Human Cancer Cell Lines.” *Turkish Journal of Biology = Turk Biyoloji Dergisi* 48 (1): 24–34. <https://doi.org/10.55730/1300-0152.2679>.
- Alarcón, Claudio R., Hyeseung Lee, Hani Goodarzi, Nils Halberg, and Sohail F. Tavazoie. 2015. “N<sup>6</sup>-Methyladenosine Marks Primary MicroRNAs for Processing.” *Nature* 519 (7544): 482–85. <https://doi.org/10.1038/NATURE14281>.
- Alasar, Azime Akçaöz, Özge Tüncel, Ayşe Bengisu Gelmez, Buket Sağlam, İpek Erdoğan Vatansever, and Bünyamin Akgül. 2022. “Genomewide M<sup>6</sup>A Mapping Uncovers Dynamic Changes in the M<sup>6</sup>A Epitranscriptome of Cisplatin-Treated Apoptotic HeLa Cells.” *Cells* 11 (23): 3905. <https://doi.org/10.3390/CELLS11233905/S1>.

- Anita, Ramesh, Arumugam Paramasivam, Jayaseelan Vijayashree Priyadharsini, and Srinivasan Chitra. 2020. "The M<sup>6</sup>A Readers YTHDF1 and YTHDF3 Aberrations Associated with Metastasis and Predict Poor Prognosis in Breast Cancer Patients." *American Journal of Cancer Research* 10 (8): 2546. /pmc/articles/PMC7471347/.
- Aubrey, Brandon J., Gemma L. Kelly, Ana Janic, Marco J. Herold, and Andreas Strasser. 2018. "How Does P53 Induce Apoptosis and How Does This Relate to P53-Mediated Tumour Suppression?" *Cell Death and Differentiation* 25 (1): 104–13. <https://doi.org/10.1038/CDD.2017.169>.
- Balacco, Dario L., and Matthias Soller. 2019. "The M<sup>6</sup>A Writer: Rise of a Machine for Growing Tasks." Review-article. *Biochemistry* 58 (5): 363–78. <https://doi.org/10.1021/acs.biochem.8b01166>.
- Baltimore, David. 1970. "RNA-Dependent DNA Polymerase in Virions of RNA Tumour Viruses." *Nature* 226 (5252): 1209–11. <https://doi.org/10.1038/2261209A0>.
- Bansal, H., Q. Yihua, S. P. Iyer, S. Ganapathy, D. Proia, L. O. Penalva, P. J. Uren, et al. 2014. "WTAP Is a Novel Oncogenic Protein in Acute Myeloid Leukemia." *Leukemia* 2014 28:5 28 (5): 1171–74. <https://doi.org/10.1038/leu.2014.16>.
- Basak, Debasish, Scott Arrighi, Yasenya Darwiche, and Subrata Deb. 2022. "Comparison of Anticancer Drug Toxicities: Paradigm Shift in Adverse Effect Profile." *Life* 12 (1). <https://doi.org/10.3390/LIFE12010048>.
- Basu, Alakananda, and Soumya Krishnamurthy. 2010. "Cellular Responses to Cisplatin-Induced DNA Damage." *Journal of Nucleic Acids* (1): 201367. <https://doi.org/10.4061/2010/201367>.
- Bawankar, Praveen, Tina Lence, Chiara Paolantoni, Irmgard U. Haussmann, Migle Kazlauskienė, Dominik Jacob, Jan B. Heidelberger, et al. 2021. "Hakai Is Required for Stabilization of Core Components of the M<sup>6</sup>A mRNA Methylation Machinery." *Nature Communications* 12 (1): 1–15. <https://doi.org/10.1038/s41467-021-23892-5>.
- Bertero, Alessandro, Stephanie Brown, Pedro Madrigal, Anna Osnato, Daniel Ortmann, Loukia Yiangou, Juned Kadiwala, et al. 2018. "The SMAD2/3 Interactome Reveals That TGFβ Controls M<sup>6</sup>A mRNA Methylation in Pluripotency." *Nature* 555 (7695): 256–59. <https://doi.org/10.1038/NATURE25784>.

- Bhattacharjee, Rahul, Tanima Dey, Lamha Kumar, Sulagna Kar, Ritayan Sarkar, Mimosa Ghorai, Sumira Malik, et al. 2022. “Cellular Landscaping of Cisplatin Resistance in Cervical Cancer.” *Biomedicine & Pharmacotherapy* 153 (September):113345. <https://doi.org/10.1016/J.BIOPHA.2022.113345>.
- Bkownlee, G. G., F. Sanger, and B. G. Barrell. 1968. “The Sequence of 5 s Ribosomal Ribonucleic Acid.” *Journal of Molecular Biology* 34 (3). [https://doi.org/10.1016/0022-2836\(68\)90168-X](https://doi.org/10.1016/0022-2836(68)90168-X).
- Boo, Sung Ho, Hongseok Ha, Yujin Lee, Min Kyung Shin, Sena Lee, and Yoon Ki Kim. 2022. “UPF1 Promotes Rapid Degradation of M<sup>6</sup>A -Containing RNAs.” *Cell Reports* 39 (8): 110861. <https://doi.org/10.1016/j.celrep.2022.110861>.
- Brown, Andrea, Sanjay Kumar, and Paul B Tchounwou. 2019. “Cisplatin-Based Chemotherapy of Human Cancers.” *Journal of Cancer Science & Therapy* 11 (4). <https://doi.org/10.1016/j.jcst.2019.04.001>. /pmc/articles/PMC7059781/.
- Brumberger, Zachary L., Mary E. Branch, Max W. Klein, Austin Seals, Michael D. Shapiro, and Sujethra Vasu. 2022. “Cardiotoxicity Risk Factors with Immune Checkpoint Inhibitors.” *Cardio-Oncology* 8 (1): 1–8. <https://doi.org/10.1186/S40959-022-00130-5/FIGURES/1>.
- Cai, Xiaoli, Xiao Wang, Can Cao, Yuen Gao, Shuqin Zhang, Zhe Yang, Yunxia Liu, Xiaodong Zhang, Weiying Zhang, and Lihong Ye. 2018. “HBXIP-Elevated Methyltransferase METTL3 Promotes the Progression of Breast Cancer via Inhibiting Tumor Suppressor Let-7g.” *Cancer Letters* 415 (February):11–19. <https://doi.org/10.1016/J.CANLET.2017.11.018>.
- Calls, Aina, Abel Torres-Espin, Xavier Navarro, Victor J. Yuste, Esther Udina, and Jordi Bruna. 2021. “Cisplatin-Induced Peripheral Neuropathy Is Associated with Neuronal Senescence-like Response.” *Neuro-Oncology* 23 (1): 88. <https://doi.org/10.1093/NEUONC/NOAA151>.
- Chai, Jijie, Chunying Du, Jia Wei Wu, Saw Kyin, Xiaodong Wang, and Yigong Shi. 2000. “Structural and Biochemical Basis of Apoptotic Activation by Smac/DIABLO.” *Nature* 406 (6798): 855–62. <https://doi.org/10.1038/35022514>.
- Chao, C.C. 1994. “Decreased Accumulation as a Mechanism of Resistance to Cis-Diamminedichloroplatinum (II) in Cervix Carcinoma HeLa Cells : Relation to DNA

RepairChao.” *Molec. Pharmacol.* 45:1137–44.  
<https://cir.nii.ac.jp/crid/1571135651675469440>.

Chaudhary, Priya, Pracheta Janmeda, Anca Oana Docea, Balakyz Yeskaliyeva, Ahmad Faizal Abdull Razis, Babagana Modu, Daniela Calina, and Javad Sharifi-Rad. 2023. “Oxidative Stress, Free Radicals and Antioxidants: Potential Crosstalk in the Pathophysiology of Human Diseases.” *Frontiers in Chemistry* 11 (May):1158198. <https://doi.org/10.3389/FCHEM.2023.1158198/BIBTEX>.

Chen, Hengyu, Yuanhang Yu, Ming Yang, Haohao Huang, Shenghui Ma, Jin Hu, Zihan Xi, et al. 2022. “YTHDF1 Promotes Breast Cancer Progression by Facilitating FOXM1 Translation in an M<sup>6</sup>A -Dependent Manner.” *Cell and Bioscience* 12 (1): 1–16. <https://doi.org/10.1186/S13578-022-00759-W/FIGURES/8>.

Chen, Jiandong. 2016. “The Cell-Cycle Arrest and Apoptotic Functions of P53 in Tumor Initiation and Progression.” *Cold Spring Harbor Perspectives in Medicine* 6 (3). <https://doi.org/10.1101/CSHPERSPECT.A026104>.

Chen, Jianhua, Lemeng Zhang, Hui Zhou, Wei Wang, Yongzhong Luo, Hua Yang, and Huihuang Yi. 2018. “Inhibition of Autophagy Promotes Cisplatin-Induced Apoptotic Cell Death through Atg5 and Beclin 1 in A549 Human Lung Cancer Cells.” *Molecular Medicine Reports* 17 (5): 6859–65. <https://doi.org/10.3892/MMR.2018.8686/HTML>.

Chen, Jiaxin, Chan Wang, Weiqiang Fei, Xiao Fang, and Xiaotong Hu. 2019. “Epitranscriptomic M<sup>6</sup>A Modification in the Stem Cell Field and Its Effects on Cell Death and Survival.” *American Journal of Cancer Research* 9 (4): 752. [/pmc/articles/PMC6511641/](https://pmc/articles/PMC6511641/).

Chen, Shang Hung, and Jang Yang Chang. 2019. “New Insights into Mechanisms of Cisplatin Resistance: From Tumor Cell to Microenvironment.” *International Journal of Molecular Sciences* 20 (17). <https://doi.org/10.3390/IJMS20174136>.

Chen, Xiao Yu, Rui Liang, You Cai Yi, Hui Ning Fan, Ming Chen, Jing Zhang, and Jin Shui Zhu. 2021. “The M<sup>6</sup>A Reader YTHDF1 Facilitates the Tumorigenesis and Metastasis of Gastric Cancer via USP14 Translation in an M<sup>6</sup>A -Dependent Manner.” *Frontiers in Cell and Developmental Biology* 9 (March):647702. <https://doi.org/10.3389/FCELL.2021.647702/BIBTEX>.

- Chen, Xiao Yu, Yan Ling Yang, Yi Yu, Zhao Yu Chen, Hui Ning Fan, Jing Zhang, and Jin Shui Zhu. 2024. "CircUGGT2 Downregulation by METTL14-Dependent M<sup>6</sup>A Modification Suppresses Gastric Cancer Progression and Cisplatin Resistance through Interaction with MiR-186-3p/MAP3K9 Axis." *Pharmacological Research* 204 (June):107206. <https://doi.org/10.1016/J.PHRS.2024.107206>.
- Chen, Xun, Lejia Zhang, Yi He, Siyuan Huang, Shangwu Chen, Wei Zhao, and Dongsheng Yu. 2023. "Regulation of M<sup>6</sup>A Modification on Ferroptosis and Its Potential Significance in Radiosensitization." *Cell Death Discovery* 9 (1): 1–11. <https://doi.org/10.1038/s41420-023-01645-1>.
- Chen, Yuping, Jinhuan Wu, Guang Liang, Guohe Geng, Fei Zhao, Ping Yin, Somaira Nowsheen, et al. 2020. "CHK2-FOXK Axis Promotes Transcriptional Control of Autophagy Programs." *Science Advances* 6 (1). <https://doi.org/10.1126/SCIADV.AAX5819>.
- Chen, Zhen Hua, Tian Qi Chen, Zhan Cheng Zeng, Dan Wang, Cai Han, Yu Meng Sun, Wei Huang, et al. 2020. "Nuclear Export of Chimeric MRNAs Depends on an LncRNA-Triggered Autoregulatory Loop in Blood Malignancies." *Cell Death & Disease* 11 (7). <https://doi.org/10.1038/S41419-020-02795-1>.
- Cheng, Emily H.Y., Michael C. Wei, Solly Weiler, Richard A. Flavell, Tak W. Mak, Tullia Lindsten, and Stanley J. Korsmeyer. 2001. "BCL-2, BCL-X(L) Sequester BH3 Domain-Only Molecules Preventing BAX- and BAK-Mediated Mitochondrial Apoptosis." *Molecular Cell* 8 (3): 705–11. [https://doi.org/10.1016/S1097-2765\(01\)00320-3](https://doi.org/10.1016/S1097-2765(01)00320-3).
- Choi, Yong Min, Han Kyul Kim, Wooyoung Shim, Muhammad Ayaz Anwar, Ji Woong Kwon, Hyuk Kwon Kwon, Hyung Joong Kim, et al. 2015. "Mechanism of Cisplatin-Induced Cytotoxicity Is Correlated to Impaired Metabolism Due to Mitochondrial ROS Generation." *PLoS ONE* 10 (8). <https://doi.org/10.1371/JOURNAL.PONE.0135083>.
- Ciarimboli, Giuliano. 2012. "Membrane Transporters as Mediators of Cisplatin Effects and Side Effects." *Scientifica* 2012:473829. <https://doi.org/10.6064/2012/473829>.
- Coker, Heather, Guifeng Wei, Benoit Moindrot, Shabaz Mohammed, Tatyana Nesterova, and Neil Brockdorff. 2020. "The Role of the Xist 5' M<sup>6</sup>A Region and RBM15 in X

Chromosome Inactivation.” *Wellcome Open Research* 5.  
<https://doi.org/10.12688/WELLCOMEOPENRES.15711.1>.

Correia, Ana Luísa, and Mina J. Bissell. 2012. “The Tumor Microenvironment Is a Dominant Force in Multidrug Resistance.” *Drug Resistance Updates : Reviews and Commentaries in Antimicrobial and Anticancer Chemotherapy* 15 (1–2): 39–49.  
<https://doi.org/10.1016/J.DRUP.2012.01.006>.

Courtney, David G., Edward M. Kennedy, Rebekah E. Dumm, Hal P. Bogerd, Kevin Tsai, Nicholas S. Heaton, and Bryan R. Cullen. 2017. “Epitranscriptomic Enhancement of Influenza A Virus Gene Expression and Replication.” *Cell Host & Microbe* 22 (3): 377–386.e5. <https://doi.org/10.1016/J.CHOM.2017.08.004>.

CRICK, F H. 1958. “On Protein Synthesis.” *Symposia of the Society for Experimental Biology* 12:138–63.

Dasari, Shaloam, and Paul Bernard Tchounwou. 2014. “Cisplatin in Cancer Therapy: Molecular Mechanisms of Action.” *European Journal of Pharmacology* 740 (October):364–78. <https://doi.org/10.1016/J.EJPHAR.2014.07.025>.

Deng, Xiaolan, Rui Su, Hengyou Weng, Huilin Huang, Zejuan Li, and Jianjun Chen. 2018. “RNA N6-Methyladenosine Modification in Cancers: Current Status and Perspectives.” *Cell Research* 28 (5): 507–17. <https://doi.org/10.1038/S41422-018-0034-6>.

DeOcesano-Pereira, Carlos, Fernando Janczur Velloso, Ana Claudia Carreira, Oliveira, Carolina Simões Pires Ribeiro, Sheila Maria Winnischofer, Brochado, et al. 2018. “Post-Transcriptional Control of RNA Expression in Cancer.” In *Gene Expression and Regulation in Mammalian Cells - Transcription From General Aspects*, edited by Fumiaki (Tokyo University of Science) Uchiumi. IntechOpen. <https://doi.org/10.5772/INTECHOPEN.71861>.

Desrosiers, R., K. Friderici, and F. Rottman. 1974. “Identification of Methylated Nucleosides in Messenger RNA from Novikoff Hepatoma Cells.” *Proceedings of the National Academy of Sciences of the United States of America* 71 (10): 3971–75. <https://doi.org/10.1073/PNAS.71.10.3971>.

- Dilruba, Shahana, and Ganna V. Kalayda. 2016. "Platinum-Based Drugs: Past, Present and Future." *Cancer Chemotherapy and Pharmacology* 77 (6): 1103–24. <https://doi.org/10.1007/S00280-016-2976-Z>.
- Dluzen, Douglas, Guangfu Li, Diana Tacelosky, Matthew Moreau, and David X. Liu. 2011. "BCL-2 Is a Downstream Target of ATF5 That Mediates the Prosurvival Function of ATF5 in a Cell Type-Dependent Manner." *Journal of Biological Chemistry* 286 (9): 7705–13. <https://doi.org/10.1074/jbc.M110.207639>.
- Doherty, B., D. Lawlor, J. P. Gillet, M. Gottesman, J. J. O’Leary, and B. Stordal. 2014. "Collateral Sensitivity to Cisplatin in KB-8-5-11 Drug-Resistant Cancer Cells. No Title." *Anticancer Research* 34 (1): 503–7.
- Dominissini, Dan, Sharon Moshitch-Moshkovitz, Mali Salmon-Divon, Ninette Amariglio, and Gideon Rechavi. 2013. "Transcriptome-Wide Mapping of N(6)-Methyladenosine by m(6)A-Seq Based on Immunocapturing and Massively Parallel Sequencing." *Nature Protocols* 8 (1): 176–89. <https://doi.org/10.1038/NPROT.2012.148>.
- Dominissini, Dan, Sharon Moshitch-Moshkovitz, Schraga Schwartz, Mali Salmon-Divon, Lior Ungar, Sivan Osenberg, Karen Cesarkas, et al. 2012. "Topology of the Human and Mouse M<sup>6</sup>A RNA Methylomes Revealed by M<sup>6</sup>A -Seq." *Nature* 485 (7397): 201–6. <https://doi.org/10.1038/NATURE11112>.
- Dong, Hiep Phuc, Arild Holth, Lilach Kleinberg, Marit Gunhild Ruud, Mari Bunkholt Elstrand, Claes G. Tropé, Ben Davidson, and Björn Risberg. 2009. "Evaluation of Cell Surface Expression of Phosphatidylserine in Ovarian Carcinoma Effusions Using the Annexin-V/7-AAD Assay: Clinical Relevance and Comparison With Other Apoptosis Parameters." *American Journal of Clinical Pathology* 132 (5): 756–62. <https://doi.org/10.1309/AJCPAVFA8J3KHPRS>.
- Dou, Yingyu, Xiaoyan Jiang, Hui Xie, Junyu He, and Songshu Xiao. 2019. "The Jun N-Terminal Kinases Signaling Pathway Plays a ‘Seesaw’ Role in Ovarian Carcinoma: A Molecular Aspect." *Journal of Ovarian Research* 12 (1): 1–11. <https://doi.org/10.1186/S13048-019-0573-6/FIGURES/3>.
- Du, Hao, Ya Zhao, Jinqiu He, Yao Zhang, Hairui Xi, Mofang Liu, Jinbiao Ma, and Ligang Wu. 2016. "YTHDF2 Destabilizes M<sup>6</sup>A -Containing RNA through Direct

- Recruitment of the CCR4–NOT Deadenylation Complex.” *Nature Communications* 7 (1): 1–11. <https://doi.org/10.1038/ncomms12626>.
- Du, Qiu Ying, Fu Chun Huo, Wen Qi Du, Xiao Lin Sun, Xin Jiang, Lan Sheng Zhang, and Dong Sheng Pei. 2022. “METTL3 Potentiates Progression of Cervical Cancer by Suppressing ER Stress via Regulating M<sup>6</sup>A Modification of TXNDC5 mRNA.” *Oncogene* 41 (39): 4420–32. <https://doi.org/10.1038/s41388-022-02435-2>.
- Duan, Hong Chao, Lian Huan Wei, Chi Zhang, Ye Wang, Lin Chen, Zhike Lu, Peng R. Chen, Chuan He, and Guifang Jia. 2017. “ALKBH10B Is an RNA N<sup>6</sup>-Methyladenosine Demethylase Affecting Arabidopsis Floral Transition.” *The Plant Cell* 29 (12): 2995–3011. <https://doi.org/10.1105/TPC.16.00912>.
- Dudgeon, Crissy, Wei Qiu, Quanhong Sun, Lin Zhang, and Jian Yu. 2009. “Transcriptional Regulation of Apoptosis.” *Essentials of Apoptosis: A Guide for Basic and Clinical Research*, 239–60. [https://doi.org/10.1007/978-1-60327-381-7\\_10/COVER](https://doi.org/10.1007/978-1-60327-381-7_10/COVER).
- Edens, Brittany M., Caroline Vissers, Jing Su, Saravanan Arumugam, Zhaofa Xu, Han Shi, Nimrod Miller, et al. 2019. “FMRP Modulates Neural Differentiation through M<sup>6</sup>A - Dependent mRNA Nuclear Export.” *Cell Reports* 28 (4): 845-854.e5. <https://doi.org/10.1016/J.CELREP.2019.06.072>.
- Edupuganti, Raghu R., Simon Geiger, Rik G.H. Lindeboom, Hailing Shi, Phillip J. Hsu, Zhike Lu, Shuang Yin Wang, et al. 2017. “N<sup>6</sup>-Methyladenosine (M<sup>6</sup>A ) Recruits and Repels Proteins to Regulate mRNA Homeostasis.” *Nature Structural & Molecular Biology* 24 (10): 870–78. <https://doi.org/10.1038/NSMB.3462>.
- Eljack, Nasma D., Ho Yu M. Ma, Janine Drucker, Clara Shen, Trevor W. Hambley, Elizabeth J. New, Thomas Friedrich, and Ronald J. Clarke. 2014. “Mechanisms of Cell Uptake and Toxicity of the Anticancer Drug Cisplatin.” *Metallomics : Integrated Biometal Science* 6 (11): 2126–33. <https://doi.org/10.1039/C4MT00238E>.
- Engel, Mareen, Carola Eggert, Paul M. Kaplick, Matthias Eder, Simone Röh, Lisa Tietze, Christian Namendorf, et al. 2018. “The Role of M<sup>6</sup>A /m-RNA Methylation in Stress Response Regulation.” *Neuron* 99 (2): 389-403.e9. <https://doi.org/10.1016/j.neuron.2018.07.009>.
- Feng, Panpan, Dawei Chen, Xia Wang, Yanxia Li, Zhenyu Li, Boya Li, Yupeng Zhang, et al. 2022. “Inhibition of the M<sup>6</sup>A Reader IGF2BP2 as a Strategy against T-Cell Acute

- Lymphoblastic Leukemia.” *Leukemia* 36 (9): 2180–88.  
<https://doi.org/10.1038/s41375-022-01651-9>.
- Fish, Lisa, Albertas Navickas, Bruce Culbertson, Yichen Xu, Hoang C.B. Nguyen, Steven Zhang, Myles Hochman, et al. 2019. “Nuclear TARBP2 Drives Oncogenic Dysregulation of RNA Splicing and Decay.” *Molecular Cell* 75 (5): 967-981.e9.  
<https://doi.org/10.1016/J.MOLCEL.2019.06.001>.
- Fu, Minyang, Yuan Hu, Tianxia Lan, Kun Liang Guan, Ting Luo, and Min Luo. 2022. “The Hippo Signalling Pathway and Its Implications in Human Health and Diseases.” *Signal Transduction and Targeted Therapy* 7 (1): 1–20.  
<https://doi.org/10.1038/s41392-022-01191-9>.
- Fu, Ye, and Xiaowei Zhuang. 2020. “M<sup>6</sup>A -Binding YTHDF Proteins Promote Stress Granule Formation.” *Nature Chemical Biology* 16 (9): 955–63.  
<https://doi.org/10.1038/s41589-020-0524-y>.
- Fuertes, M., J. Castilla, C. Alonso, and J. Pérez. 2003. “Cisplatin Biochemical Mechanism of Action: From Cytotoxicity to Induction of Cell Death through Interconnections between Apoptotic and Necrotic Pathways.” *Current Medicinal Chemistry* 10 (3): 257–66. <https://doi.org/10.2174/09298670333368484>.
- Furlan, Mattia, Eugenia Galeota, Stefano de Pretis, Michele Caselle, and Mattia Pelizzola. 2019. “M<sup>6</sup>A -Dependent RNA Dynamics in T Cell Differentiation.” *Genes* 10 (1).  
<https://doi.org/10.3390/GENES10010028>.
- Gallon, John, Erick Loomis, Edward Curry, Nicholas Martin, Leigh Brody, Ian Garner, Robert Brown, and James M. Flanagan. 2021. “Chromatin Accessibility Changes at Intergenic Regions Are Associated with Ovarian Cancer Drug Resistance.” *Clinical Epigenetics* 13 (1): 1–15. <https://doi.org/10.1186/S13148-021-01105-6/FIGURES/8>.
- Galluzzi, L., L. Senovilla, I. Vitale, J. Michels, I. Martins, O. Kepp, M. Castedo, and G. Kroemer. 2012. “Molecular Mechanisms of Cisplatin Resistance.” *Oncogene* 31 (15): 1869–83. <https://doi.org/10.1038/ONC.2011.384>.
- Gan, Gregory N., John P. Wittschieben, Birgitte Wittschieben, and Richard D. Wood. 2007. “DNA Polymerase Zeta (Pol ζ) in Higher Eukaryotes.” *Cell Research* 18 (1): 174–83.  
<https://doi.org/10.1038/cr.2007.117>.

- Gao, Gang, Yufen Duan, Feng Chang, Ting Zhang, Xinhu Huang, and Chen Yu. 2022. "METTL14 Promotes Apoptosis of Spinal Cord Neurons by Inducing EEF1A2 M<sup>6</sup>A Methylation in Spinal Cord Injury." *Cell Death Discovery* 8 (1). <https://doi.org/10.1038/S41420-021-00808-2>.
- Giri, Khem Raj, Laurence de Beaurepaire, Dominique Jegou, Margot Lavy, Mathilde Mosser, Aurelien Dupont, Romain Fleurisson, et al. 2020. "Molecular and Functional Diversity of Distinct Subpopulations of the Stressed Insulin-Secreting Cell's Vesiculome." *Frontiers in Immunology* 11 (September):1814. <https://doi.org/10.3389/FIMMU.2020.01814/FULL>.
- Goeman, Jelle J., and Aldo Solari. 2014. "Multiple Hypothesis Testing in Genomics." *Statistics in Medicine* 33 (11): 1946–78. <https://doi.org/10.1002/SIM.6082>.
- Gong, Shulei, Shiyang Wang, and Mingrui Shao. 2022. "Mechanism of METTL14-Mediated M<sup>6</sup>A Modification in Non-Small Cell Lung Cancer Cell Resistance to Cisplatin." *Journal of Molecular Medicine* 100 (12): 1771–85. <https://doi.org/10.1007/S00109-022-02268-2/FIGURES/8>.
- Grozhhik, Anya V., Bastian Linder, Anthony O. Olarerin-George, and Samie R. Jaffrey. 2017. "Mapping M<sup>6</sup>A at Individual-Nucleotide Resolution Using Crosslinking and Immunoprecipitation (MiCLIP)." *Methods in Molecular Biology (Clifton, N.J.)* 1562:55. [https://doi.org/10.1007/978-1-4939-6807-7\\_5](https://doi.org/10.1007/978-1-4939-6807-7_5).
- Gu, Yinmin, Shaoxi Niu, Yang Wang, Liqiang Duan, Yongbo Pan, Zhou Tong, Xu Zhang, et al. 2021. "DMDRMR-Mediated Regulation of M<sup>6</sup>A -Modified CDK4 by M<sup>6</sup>A Reader IGF2BP3 Drives CcRCC Progression." *Cancer Research* 81 (4): 923–34. [https://doi.org/10.1158/0008-5472.CAN-20-1619/662491/AM/DMDRMR-MEDIATED-REGULATION-OF-M<sup>6</sup>A -MODIFIED-CDK4-BY](https://doi.org/10.1158/0008-5472.CAN-20-1619/662491/AM/DMDRMR-MEDIATED-REGULATION-OF-M6A-MODIFIED-CDK4-BY).
- Guo, Jialu, Jianfeng Zheng, Huizhi Zhang, and Jinyi Tong. 2021. "RNA M<sup>6</sup>A Methylation Regulators in Ovarian Cancer." *Cancer Cell International* 21 (1). <https://doi.org/10.1186/S12935-021-02318-8>.
- Gupta, Sonu Kumar, Priyanka Singh, Villayat Ali, and Malkhey Verma. 2020. "Role of Membrane-Embedded Drug Efflux ABC Transporters in the Cancer Chemotherapy." *Oncology Reviews* 14 (2): 144–51. <https://doi.org/10.4081/ONCOL.2020.448>.

- Gurer, Dilek Cansu, İpek Erdogan, Ulvi Ahmadov, Merve Basol, Osama Sweef, Gulcin Cakan-Akdogan, and Bünyamin Akgül. 2021. “Transcriptomics Profiling Identifies Cisplatin-Inducible Death Receptor 5 Antisense Long Non-Coding RNA as a Modulator of Proliferation and Metastasis in HeLa Cells.” *Frontiers in Cell and Developmental Biology* 9 (August). <https://doi.org/10.3389/FCELL.2021.688855>.
- Hammond, Ester M., Nicholas C. Denko, Mary Jo Dorie, Robert T. Abraham, and Amato J. Giaccia. 2002. “Hypoxia Links ATR and P53 through Replication Arrest.” *Molecular and Cellular Biology* 22 (6): 1834–43. <https://doi.org/10.1128/MCB.22.6.1834-1843.2002>.
- Han, Bing, Saisai Wei, Fengying Li, Jun Zhang, Zhongxiang Li, and Xiangwei Gao. 2021. “Decoding M<sup>6</sup>A mRNA Methylation by Reader Proteins in Cancer.” *Cancer Letters* 518 (October):256–65. <https://doi.org/10.1016/J.CANLET.2021.07.047>.
- Hastings, Michael H. 2013. “M(6)A mRNA Methylation: A New Circadian Pacesetter.” *Cell* 155 (4): 740. <https://doi.org/10.1016/J.CELL.2013.10.028>.
- Hausmann, Irmgard U., Zsuzsanna Bodi, Eugenio Sanchez-Moran, Nigel P. Mongan, Nathan Archer, Rupert G. Fray, and Matthias Soller. 2016. “M<sup>6</sup>A Potentiates Sxl Alternative Pre-mRNA Splicing for Robust Drosophila Sex Determination.” *Nature* 540 (7632): 301–4. <https://doi.org/10.1038/NATURE20577>.
- Hebbar, Sarita, and Elisabeth Knust. 2021. “Reactive Oxygen Species (ROS) Constitute an Additional Player in Regulating Epithelial Development.” *BioEssays* 43 (8): 2100096. <https://doi.org/10.1002/BIES.202100096>.
- Heinz, Sven, Christopher Benner, Nathanael Spann, Eric Bertolino, Yin C. Lin, Peter Laslo, Jason X. Cheng, Cornelis Murre, Harinder Singh, and Christopher K. Glass. 2010. “Simple Combinations of Lineage-Determining Transcription Factors Prime Cis-Regulatory Elements Required for Macrophage and B Cell Identities.” *Molecular Cell* 38 (4): 576–89. <https://doi.org/10.1016/J.MOLCEL.2010.05.004>.
- Holzner, Marianna, Gábor Bánhegyi, and Orsolya Kapuy. 2016. “GADD34 Keeps the MTOR Pathway Inactivated in Endoplasmic Reticulum Stress Related Autophagy.” *PloS One* 11 (12). <https://doi.org/10.1371/JOURNAL.PONE.0168359>.
- Holliday, Robin. 2006. “Epigenetics: A Historical Overview.” *Epigenetics* 1 (2): 76–80. <https://doi.org/10.4161/EPI.1.2.2762>.

- Hong, Ji Young, Geun Hong Kim, Jun Woo Kim, Soon Sung Kwon, Eisuke F. Sato, Kwang Hyun Cho, and Eun B. Shim. 2012. “Computational Modeling of Apoptotic Signaling Pathways Induced by Cisplatin.” *BMC Systems Biology* 6 (1): 1–16. <https://doi.org/10.1186/1752-0509-6-122/TABLES/7>.
- Hong, Lan, Xiuzhen Wang, Lang Zheng, Shengtian Wang, and Genhai Zhu. 2023. “Tumor-Associated Macrophages Promote Cisplatin Resistance in Ovarian Cancer Cells by Enhancing WTAP-Mediated N6-Methyladenosine RNA Methylation via the CXCL16/CXCR6 Axis.” *Cancer Chemotherapy and Pharmacology* 92 (1): 71–81. <https://doi.org/10.1007/S00280-023-04533-8/FIGURES/7>.
- Hou, Huaying, Huidong Zhao, Xiaoming Yu, Ping Cong, Yong Zhou, Yuhua Jiang, and Yufeng Cheng. 2020. “METTL3 Promotes the Proliferation and Invasion of Esophageal Cancer Cells Partly through AKT Signaling Pathway.” *Pathology, Research and Practice* 216 (9). <https://doi.org/10.1016/J.PRP.2020.153087>.
- Hsu, Phillip J., Yunfei Zhu, Honghui Ma, Yueshuai Guo, Xiaodan Shi, Yuanyuan Liu, Meijie Qi, et al. 2017. “Ythdc2 Is an N6-Methyladenosine Binding Protein That Regulates Mammalian Spermatogenesis.” *Cell Research* 27:9 27 (9): 1115–27. <https://doi.org/10.1038/cr.2017.99>.
- Hu, Jinchuan, Jason D. Lieb, Aziz Sancar, and Sheera Adar. 2016. “Cisplatin DNA Damage and Repair Maps of the Human Genome at Single-Nucleotide Resolution.” *Proceedings of the National Academy of Sciences of the United States of America* 113 (41): 11507–12. [https://doi.org/10.1073/PNAS.1614430113/SUPPL\\_FILE/PNAS.1614430113.SAPP.PDF](https://doi.org/10.1073/PNAS.1614430113/SUPPL_FILE/PNAS.1614430113.SAPP.PDF).
- Huang, Huilin, Hengyou Weng, and Jianjun Chen. 2020. “The Biogenesis and Precise Control of RNA M<sup>6</sup>A Methylation.” *Trends in Genetics* 36 (1): 44–52. <https://doi.org/10.1016/j.tig.2019.10.011>.
- Huang, Huilin, Hengyou Weng, Wenju Sun, Xi Qin, Hailing Shi, Huizhe Wu, Boxuan Simen Zhao, et al. 2018. “Recognition of RNA N6-Methyladenosine by IGF2BP Proteins Enhances mRNA Stability and Translation.” *Nature Cell Biology* 20 (3): 285–95. <https://doi.org/10.1038/s41556-018-0045-z>.

- Humbert, Magali, Elena A. Federzoni, and Mario P. Tschan. 2017. "Distinct TP73–DAPK2–ATG5 Pathway Involvement in ATO-Mediated Cell Death versus ATRA-Mediated Autophagy Responses in APL." *Journal of Leukocyte Biology* 102 (6): 1357–70. <https://doi.org/10.1189/JLB.1A0317-132R>.
- Ikawa, S., A. Nakagawara, and Y. Ikawa. 1999. "P53 Family Genes: Structural Comparison, Expression and Mutation." *Cell Death & Differentiation* 6 (12): 1154–61. <https://doi.org/10.1038/sj.cdd.4400631>.
- Ishida, Seiko, Jaekwon Lee, Dennis J. Thiele, and Ira Herskowitz. 2002. "Uptake of the Anticancer Drug Cisplatin Mediated by the Copper Transporter Ctr1 in Yeast and Mammals." *Proceedings of the National Academy of Sciences of the United States of America* 99 (22): 14298–302. <https://doi.org/10.1073/PNAS.162491399>.
- Ito, M., T. Yurube, K. Kakutani, K. Maeno, T. Takada, Y. Terashima, Y. Kakiuchi, et al. 2017. "Selective Interference of MTORC1/RAPTOR Protects against Human Disc Cellular Apoptosis, Senescence, and Extracellular Matrix Catabolism with Akt and Autophagy Induction." *Osteoarthritis and Cartilage* 25 (12): 2134–46. <https://doi.org/10.1016/J.JOCA.2017.08.019>.
- Jia, Guifang, Ye Fu, Xu Zhao, Qing Dai, Guanqun Zheng, Ying Yang, Chengqi Yi, et al. 2011. "N6-Methyladenosine in Nuclear RNA Is a Major Substrate of the Obesity-Associated FTO." *Nature Chemical Biology* 7 (12): 885–87. <https://doi.org/10.1038/NCHEMBIO.687>.
- Jia, Ruobing, Peiwei Chai, Shanzheng Wang, Baofa Sun, Yangfan Xu, Ying Yang, Shengfang Ge, Renbing Jia, Yun Gui Yang, and Xianqun Fan. 2019. "M<sup>6</sup>A Modification Suppresses Ocular Melanoma through Modulating HINT2 mRNA Translation." *Molecular Cancer* 18 (1). <https://doi.org/10.1186/S12943-019-1088-X>.
- Jiang, Xiulin, Baiyang Liu, Zhi Nie, Lincan Duan, Qiuxia Xiong, Zhixian Jin, Cuiping Yang, and Yongbin Chen. 2021. "The Role of M<sup>6</sup>A Modification in the Biological Functions and Diseases." *Signal Transduction and Targeted Therapy* 6 (1): 1–16. <https://doi.org/10.1038/s41392-020-00450-x>.
- Jin, Dan, Jiwei Guo, Yan Wu, Lijuan Yang, Xiaohong Wang, Jing Du, Juanjuan Dai, et al. 2020. "M<sup>6</sup>A Demethylase ALKBH5 Inhibits Tumor Growth and Metastasis by Reducing YTHDFs-Mediated YAP Expression and Inhibiting MiR-107/LATS2-

- Mediated YAP Activity in NSCLC.” *Molecular Cancer* 19 (1): 1–24. <https://doi.org/10.1186/S12943-020-01161-1/FIGURES/8>.
- Jin, Shouheng, Xiya Zhang, Yanyan Miao, Puping Liang, Kaiyu Zhu, Yuanchu She, Yaoxing Wu, et al. 2018. “M<sup>6</sup>A RNA Modification Controls Autophagy through Upregulating ULK1 Protein Abundance.” *Cell Research* 28 (9): 955. <https://doi.org/10.1038/S41422-018-0069-8>.
- Juan, Celia Andrés, José Manuel Pérez de la Lastra, Francisco J. Plou, and Eduardo Pérez-Lebeña. 2021. “The Chemistry of Reactive Oxygen Species (ROS) Revisited: Outlining Their Role in Biological Macromolecules (DNA, Lipids and Proteins) and Induced Pathologies.” *International Journal of Molecular Sciences* 22 (9): 4642. <https://doi.org/10.3390/IJMS22094642>.
- Jung, Yongwon, and Stephen J. Lippard. 2007. “Direct Cellular Responses to Platinum-Induced DNA Damage.” *Chemical Reviews* 107 (5): 1387–1407. <https://doi.org/10.1021/CR068207J>.
- Kaminsky, Vitaliy O., and Boris Zhivotovsky. 2014. “Free Radicals in Cross Talk between Autophagy and Apoptosis.” *Antioxidants & Redox Signaling* 21 (1): 86–102. <https://doi.org/10.1089/ARS.2013.5746>.
- Kan, Ryan L., Jianjun Chen, and Tamer Sallam. 2022. “Crosstalk between Epitranscriptomic and Epigenetic Mechanisms in Gene Regulation.” *Trends in Genetics* 38 (2): 182–93. <https://doi.org/10.1016/j.tig.2021.06.014>.
- Kanehisa, Minoru. 2019. “Toward Understanding the Origin and Evolution of Cellular Organisms.” *Protein Science : A Publication of the Protein Society* 28 (11): 1947–51. <https://doi.org/10.1002/PRO.3715>.
- Kanehisa, Minoru, Miho Furumichi, Yoko Sato, Masayuki Kawashima, and Mari Ishiguro-Watanabe. 2023. “KEGG for Taxonomy-Based Analysis of Pathways and Genomes.” *Nucleic Acids Research* 51 (D1): D587–92. <https://doi.org/10.1093/NAR/GKAC963>.
- Kanehisa, Minoru, and Susumu Goto. 2000. “KEGG: Kyoto Encyclopedia of Genes and Genomes.” *Nucleic Acids Research* 28 (1): 27–30. <https://doi.org/10.1093/NAR/28.1.27>.

- Kantari, Chahrazade, and Henning Walczak. 2011. “Caspase-8 and Bid: Caught in the Act between Death Receptors and Mitochondria.” *Biochimica et Biophysica Acta (BBA) - Molecular Cell Research* 1813 (4): 558–63. <https://doi.org/10.1016/J.BBAMCR.2011.01.026>.
- Ke, Jing, Chunming Gu, Heyan Zhang, Yang Liu, Wenhao Zhang, Huiling Rao, Shan Li, and Fuyun Wu. 2021. “Nucleolin Promotes Cisplatin Resistance in Cervical Cancer by the YB1-MDR1 Pathway.” *Journal of Oncology* <https://doi.org/10.1155/2021/9992218>.
- Ke, Shengdong, Endalkachew A. Alemu, Claudia Mertens, Emily Conn Gantman, John J. Fak, Aldo Mele, Bhagwattie Haripal, et al. 2015. “A Majority of M<sup>6</sup>A Residues Are in the Last Exons, Allowing the Potential for 3' UTR Regulation.” *Genes & Development* 29 (19): 2037–53. <https://doi.org/10.1101/GAD.269415.115>.
- Kelland, Lloyd. 2007. “The Resurgence of Platinum-Based Cancer Chemotherapy.” *Nature Reviews. Cancer* 7 (8): 573–84. <https://doi.org/10.1038/NRC2167>.
- Kim, Baekgyu, and V. Narry Kim. 2019. “FCLIP-Seq for Transcriptomic Footprinting of DsRNA-Binding Proteins: Lessons from DROSHA.” *Methods (San Diego, Calif.)* 152 (January):3–11. <https://doi.org/10.1016/J.YMETH.2018.06.004>.
- Kim, Keun Cheol, Chul Soo Jung, and Kyung Hee Choi. 2006. “Overexpression of P73 Enhances Cisplatin-Induced Apoptosis in HeLa Cells.” *Archives of Pharmacal Research* 29 (2): 152–58. <https://doi.org/10.1007/BF02974277>.
- Kirova, Dilyana Georgieva, Kristyna Judasova, Julia Vorhauser, Thomas Zerjatke, Jacky Kieran Leung, Ingmar Glauche, and Jörg Mansfeld. 2022. “A ROS-Dependent Mechanism Promotes CDK2 Phosphorylation to Drive Progression through S Phase.” *Developmental Cell* 57 (14): 1712-1727.e9. <https://doi.org/10.1016/J.DEVCEL.2022.06.008>.
- Kiss, Robert Csaba, Fen Xia, and Scarlett Acklin. 2021. “Targeting DNA Damage Response and Repair to Enhance Therapeutic Index in Cisplatin-Based Cancer Treatment.” *International Journal of Molecular Sciences* 22 (15): 8199. <https://doi.org/10.3390/IJMS22158199>.
- Kleih, Markus, Kathrin Böppele, Meng Dong, Andrea Gaißler, Simon Heine, Monilola A. Olayioye, Walter E. Aulitzky, and Frank Essmann. 2019. “Direct Impact of Cisplatin

on Mitochondria Induces ROS Production That Dictates Cell Fate of Ovarian Cancer Cells.” *Cell Death & Disease* 10 (11): 1–12. <https://doi.org/10.1038/s41419-019-2081-4>.

Knuckles, Philip, Sarah H. Carl, Michael Musheev, Christof Niehrs, Alice Wenger, and Marc Bühler. 2017. “RNA Fate Determination through Cotranscriptional Adenosine Methylation and Microprocessor Binding.” *Nature Structural & Molecular Biology* 24 (7): 561–69. <https://doi.org/10.1038/NSMB.3419>.

Knuckles, Philip, Tina Lence, Irmgard U. Haussmann, Dominik Jacob, Nastasja Kreim, Sarah H. Carl, Irene Masiello, et al. 2018. “Zc3h13/Flacc Is Required for Adenosine Methylation by Bridging the mRNA-Binding Factor Rbm15/Spenito to the M<sup>6</sup>A Machinery Component Wtap/Fl(2)d.” *Genes & Development* 32 (5–6): 415–29. <https://doi.org/10.1101/GAD.309146.117>.

Kong, Fanhua, Xi Liu, Yan Zhou, Xuyang Hou, Jun He, Qinglong Li, Xiongying Miao, and Leping Yang. 2020. “Downregulation of METTL14 Increases Apoptosis and Autophagy Induced by Cisplatin in Pancreatic Cancer Cells.” *The International Journal of Biochemistry & Cell Biology* 122 (May):105731. <https://doi.org/10.1016/J.BIOCEL.2020.105731>.

Krakau, Sabrina, Hugues Richard, and Annalisa Marsico. 2017. “PureCLIP: Capturing Target-Specific Protein-RNA Interaction Footprints from Single-Nucleotide CLIP-Seq Data.” *Genome Biology* 18 (1): 1–17. <https://doi.org/10.1186/S13059-017-1364-2/FIGURES/7>.

Lence, Tina, Junaid Akhtar, Marc Bayer, Katharina Schmid, Laura Spindler, Cheuk Hei Ho, Nastasja Kreim, et al. 2016. “M<sup>6</sup>A Modulates Neuronal Functions and Sex Determination in *Drosophila*.” *Nature* 540 (7632): 242–47. <https://doi.org/10.1038/NATURE20568>.

Li, Guo Min. 2007. “Mechanisms and Functions of DNA Mismatch Repair.” *Cell Research* 18 (1): 85–98. <https://doi.org/10.1038/cr.2007.115>.

Li, Jiexin, Feng Chen, Yanxi Peng, Ziyang Lv, Xinyao Lin, Zhuojia Chen, and Hongsheng Wang. 2020. “N<sup>6</sup>-Methyladenosine Regulates the Expression and Secretion of TGFβ1 to Affect the Epithelial-Mesenchymal Transition of Cancer Cells.” *Cells* 9 (2). <https://doi.org/10.3390/CELLS9020296>.

- Li, Qunhua, James B. Brown, Haiyan Huang, and Peter J. Bickel. 2011. "Measuring Reproducibility of High-Throughput Experiments" *Annals of Applied Statistics* (3): 1752–79. <https://doi.org/10.1214/11-AOAS466>.
- Li, Rui, Junfang Liu, Zekui Fang, Zhenyu Liang, and Xin Chen. 2020. "Identification of Mutations Related to Cisplatin-Resistance and Prognosis of Patients With Lung Adenocarcinoma." *Frontiers in Pharmacology* 11 (October):572627. <https://doi.org/10.3389/FPHAR.2020.572627/BIBTEX>.
- Li, Sheng, and Christopher E. Mason. 2014. "The Pivotal Regulatory Landscape of RNA Modifications." *Annual Review of Genomics and Human Genetics* 15:127–50. <https://doi.org/10.1146/annurev-genom-090413-025405>.
- Li, Tianxiang, Yanyan Yang, Hongzhao Qi, Weigang Cui, Lin Zhang, Xiuxiu Fu, Xiangqin He, Meixin Liu, Pei feng Li, and Tao Yu. 2023. "CRISPR/Cas9 Therapeutics: Progress and Prospects." *Signal Transduction and Targeted Therapy* 8 (1): 1–23. <https://doi.org/10.1038/s41392-023-01309-7>.
- Li, Yini, Mengying Zhou, Qi Hu, Xiao Chen Bai, Weiyun Huang, Sjors H.W. Scheres, and Yigong Shi. 2017. "Mechanistic Insights into Caspase-9 Activation by the Structure of the Apoptosome Holoenzyme." *Proceedings of the National Academy of Sciences of the United States of America* 114 (7): 1542–47. [https://doi.org/10.1073/PNAS.1620626114/SUPPL\\_FILE/PNAS.201620626SI.PDF](https://doi.org/10.1073/PNAS.1620626114/SUPPL_FILE/PNAS.201620626SI.PDF).
- Li, Zihan, Yanxi Peng, Jiexin Li, Zhuojia Chen, Feng Chen, Jian Tu, Shuibin Lin, and Hongsheng Wang. 2020. "N6-Methyladenosine Regulates Glycolysis of Cancer Cells through PDK4." *Nature Communications* 11 (1): 1–16. <https://doi.org/10.1038/s41467-020-16306-5>.
- Liang, Jianfeng, Hongshi Cai, Chen Hou, Fan Song, Yaoqi Jiang, Ziyi Wang, Danqi Qiu, et al. 2023. "METTL14 Inhibits Malignant Progression of Oral Squamous Cell Carcinoma by Targeting the Autophagy-Related Gene RB1CC1 in an M<sup>6</sup>A - IGF2BP2-Dependent Manner." *Clinical Science (London, England : 1979)* 137 (17): 1373–89. <https://doi.org/10.1042/CS20230219>.
- Liao, Yang, Gordon K. Smyth, and Wei Shi. 2014. "FeatureCounts: An Efficient General Purpose Program for Assigning Sequence Reads to Genomic Features."

- Bioinformatics* (Oxford, England) 30 (7): 923–30.  
<https://doi.org/10.1093/BIOINFORMATICS/BTT656>.
- Lin, Shuibin, Junho Choe, Peng Du, Robinson Triboulet, and Richard I. Gregory. 2016. “The m(6)A Methyltransferase METTL3 Promotes Translation in Human Cancer Cells.” *Molecular Cell* 62 (3): 335–45.  
<https://doi.org/10.1016/J.MOLCEL.2016.03.021>.
- Linder, Bastian, Anya V. Grozhik, Anthony O. Olarerin-George, Cem Meydan, Christopher E. Mason, and Samie R. Jaffrey. 2015. “Single-Nucleotide-Resolution Mapping of M<sup>6</sup>A and M<sup>6</sup>A m throughout the Transcriptome.” *Nature Methods* 12 (8): 767–72. <https://doi.org/10.1038/NMETH.3453>.
- Liu, Jia, Guoqiang Jiang, Ping Mao, Jing Zhang, Lin Zhang, Likun Liu, Jia Wang, et al. 2018. “Down-Regulation of GADD45A Enhances Chemosensitivity in Melanoma.” *Scientific Reports* 8 (1): 4111. <https://doi.org/10.1038/S41598-018-22484-6>.
- Liu, Jianzhao, Yanan Yue, Jun Liu, Xiaolong Cui, Jie Cao, Guanzheng Luo, Zezhou Zhang, et al. 2018. “VIRMA Mediates Preferential M<sup>6</sup>A mRNA Methylation in 3’UTR and near Stop Codon and Associates with Alternative Polyadenylation.” *Cell Discovery* 4 (1). <https://doi.org/10.1038/S41421-018-0019-0>.
- Liu, Jiqin, Dangli Ren, Zhenhua Du, Hekong Wang, Hua Zhang, and Ying Jin. 2018. “M<sup>6</sup>A Demethylase FTO Facilitates Tumor Progression in Lung Squamous Cell Carcinoma by Regulating MZF1 Expression.” *Biochemical and Biophysical Research Communications* 502 (4): 456–64. <https://doi.org/10.1016/J.BBRC.2018.05.175>.
- Liu, N., and T. Pan. 2017. *RNA Epigenetics (Epitranscriptomics). Translating Epigenetics to the Clinic*. Elsevier Inc. <https://doi.org/10.1016/B978-0-12-800802-7.00002-2>.
- Liu, Nian, Qing Dai, Guanqun Zheng, Chuan He, Marc Parisien, and Tao Pan. 2015. “N<sup>6</sup>-Methyladenosine-Dependent RNA Structural Switches Regulate RNA-Protein Interactions.” *Nature* 518 (7540): 560–64. <https://doi.org/10.1038/nature14234>.
- Liu, Tao, Qinglv Wei, Jing Jin, Qingya Luo, Yi Liu, Yu Yang, Chunming Cheng, et al. 2020. “The M<sup>6</sup>A Reader YTHDF1 Promotes Ovarian Cancer Progression via Augmenting EIF3C Translation.” *Nucleic Acids Research* 48 (7): 3816–31. <https://doi.org/10.1093/NAR/GKAA048>.

- Liu, Wan, Jun Li, Yu Shu Song, Yue Li, Yu Hong Jia, and Hai Dong Zhao. 2017. “Cdk5 Links with DNA Damage Response and Cancer.” *Molecular Cancer* 16 (1): 1–9. <https://doi.org/10.1186/S12943-017-0611-1/FIGURES/3>.
- Liu, Wei Wei, Zhong Yuan Zhang, Fei Wang, and Hao Wang. 2023. “Emerging Roles of M<sup>6</sup>A RNA Modification in Cancer Therapeutic Resistance.” *Experimental Hematology & Oncology* 12 (1): 1–22. <https://doi.org/10.1186/S40164-023-00386-2>.
- Liu, Weiwei, Chaoqun Liu, Jia You, Zilin Chen, Cheng Qian, Wandie Lin, Lina Yu, Lele Ye, Liang Zhao, and Rui Zhou. 2022. “Pan-Cancer Analysis Identifies YTHDF2 as an Immunotherapeutic and Prognostic Biomarker.” *Frontiers in Cell and Developmental Biology* 10 (August). <https://doi.org/10.3389/FCELL.2022.954214/FULL>.
- Liu, Xin, Hongjuan He, Fengwei Zhang, Xin Hu, Fanqi Bi, Kai Li, Haoran Yu, et al. 2022. “M<sup>6</sup>A Methylated EphA2 and VEGFA through IGF2BP2/3 Regulation Promotes Vasculogenic Mimicry in Colorectal Cancer via PI3K/AKT and ERK1/2 Signaling.” *Cell Death & Disease* 13 (5): 1–12. <https://doi.org/10.1038/s41419-022-04950-2>.
- Liu, Youqing, Hui Xing, Xiaobing Han, Xiaoyan Shi, Fengqi Liang, Gang Cheng, Yunping Lu, and Ding Ma. 2008. “Apoptosis of HeLa Cells Induced by Cisplatin and Its Mechanism.” *Journal of Huazhong University of Science and Technology. Medical Sciences = Hua Zhong Ke Ji Da Xue Xue Bao. Yi Xue Ying De Wen Ban = Huazhong Keji Daxue Xuebao. Yixue Yingdewen Ban* 28 (2): 197–99. <https://doi.org/10.1007/S11596-008-0221-7>.
- Love, Michael I., Wolfgang Huber, and Simon Anders. 2014. “Moderated Estimation of Fold Change and Dispersion for RNA-Seq Data with DESeq2.” *Genome Biology* 15 (12). <https://doi.org/10.1186/S13059-014-0550-8>.
- Lu, Dan, Curt D. Wolfgang, and Tsonwin Hai. 2006. “Activating Transcription Factor 3, a Stress-Inducible Gene, Suppresses Ras-Stimulated Tumorigenesis.” *Journal of Biological Chemistry* 281 (15): 10473–81. <https://doi.org/10.1074/JBC.M509278200>.
- Lu, Jiawei, Lanting Yu, Ni Xie, Ying Wu, and Baiwen Li. 2023. “METTL14 Facilitates the Metastasis of Pancreatic Carcinoma by Stabilizing LINC00941 in an M<sup>6</sup>A -

- IGF2BP2-Dependent Manner.” *Journal of Cancer* 14 (7): 1117–31. <https://doi.org/10.7150/JCA.84070>.
- Lu, Zengkui, Jianbin Liu, Chao Yuan, Meilin Jin, Kai Quan, Mingxing Chu, and Caihong Wei. 2021. “M<sup>6</sup>A mRNA Methylation Analysis Provides Novel Insights into Heat Stress Responses in the Liver Tissue of Sheep.” *Genomics* 113 (1): 484–92. <https://doi.org/10.1016/J.YGENO.2020.09.038>.
- Luo, Haitao, Kai Huang, Mengqi Cheng, Xiaoyan Long, Xingen Zhu, and Miaoqing Wu. 2023. “The HNF4A-CHPF Pathway Promotes Proliferation and Invasion through Interactions with MAD1L1 in Glioma.” *Aging* 15 (20): 11052–66. <https://doi.org/10.18632/AGING.205076>.
- Luo, Lin, Yingwei Zhen, Dazhao Peng, Cheng Wei, Xiaoyang Zhang, Xianzhi Liu, Lei Han, and Zhenyu Zhang. 2022. “The Role of N<sup>6</sup>-Methyladenosine-Modified Non-Coding RNAs in the Pathological Process of Human Cancer.” *Cell Death Discovery* 8 (1): 1–15. <https://doi.org/10.1038/s41420-022-01113-2>.
- Ma, Honghui, Xiaoyun Wang, Jiabin Cai, Qing Dai, S. Kundhavai Natchiar, Ruitu Lv, Kai Chen, et al. 2019. “N<sup>6</sup>-Methyladenosine Methyltransferase ZCCHC4 Mediates Ribosomal RNA Methylation.” *Nature Chemical Biology* 15 (1): 88–94. <https://doi.org/10.1038/S41589-018-0184-3>.
- Ma, Zhao, Qin Li, Peng Liu, Wei Dong, and Ying Zuo. 2020. “METTL3 Regulates M<sup>6</sup>A in Endometrioid Epithelial Ovarian Cancer Independently of METTL14 and WTAP.” *Cell Biology International* 44 (12): 2524–31. <https://doi.org/10.1002/cbin.11459>.
- Mao, Xiushan, Nan Hou, Zhenzhong Liu, and Jieqiang He. 2022. “Profiling of N<sup>6</sup>-Methyladenosine (M<sup>6</sup>a) Modification Landscape in Response to Drought Stress in Apple (*Malus Prunifolia* (Willd.) Borkh).” *Plants* 11 (1): 103. <https://doi.org/10.3390/PLANTS11010103/S1>.
- Martin, Marcel. 2011. “Cutadapt Removes Adapter Sequences from High-Throughput Sequencing Reads.” *EMBnet.Journal* 17 (1): 10–12. <https://doi.org/10.14806/EJ.17.1.200>.
- Martínez-Pérez, Mireya, Frederic Aparicio, Maria Pilar López-Gresa, Jose María Bellés, Jesus A. Sánchez-Navarro, and Vicente Pallás. 2017. “Arabidopsis M<sup>6</sup>A Demethylase Activity Modulates Viral Infection of a Plant Virus and the M<sup>6</sup>A Abundance in Its

- Genomic RNAs.” *Proceedings of the National Academy of Sciences of the United States of America* 114 (40): 10755–60. <https://doi.org/10.1073/PNAS.1703139114>.
- Maurmann, L., L. Belkacemi, N. R. Adams, P. M. Majmudar, S. Moghaddas, and R. N. Bose. 2015. “A Novel Cisplatin Mediated Apoptosis Pathway Is Associated with Acid Sphingomyelinase and FAS Proapoptotic Protein Activation in Ovarian Cancer.” *Apoptosis : An International Journal on Programmed Cell Death* 20 (7): 960–74. <https://doi.org/10.1007/S10495-015-1124-2>.
- Meng, Fanling, Chang Luo, Yuanlong Hu, Mingzhu Yin, Ming Lin, Ge Lou, and Rouli Zhou. 2010. “Overexpression of LAPTM4B-35 in Cervical Carcinoma: A Clinicopathologic Study.” *International Journal of Gynecological Pathology : Official Journal of the International Society of Gynecological Pathologists* 29 (6): 587–93. <https://doi.org/10.1097/PGP.0B013E3181E0898E>.
- Meng, Y., L. Wang, D. Chen, Y. Chang, M. Zhang, J. J. Xu, R. Zhou, and Q. Y. Zhang. 2016. “LAPTM4B: An Oncogene in Various Solid Tumors and Its Functions.” *Oncogene* 35 (50): 6359–65. <https://doi.org/10.1038/onc.2016.189>.
- Meyer, Kate D., Yogesh Saletore, Paul Zumbo, Olivier Elemento, Christopher E. Mason, and Samie R. Jaffrey. 2012. “Comprehensive Analysis of mRNA Methylation Reveals Enrichment in 3' UTRs and near Stop Codons.” *Cell* 149 (7): 1635–46. <https://doi.org/10.1016/j.cell.2012.05.003>.
- Micheau, Olivier, Eric Solary, Ariette Hammann, and Marie Thérèse Dimanche-Boitrel. 1999. “Fas Ligand-Independent, FADD-Mediated Activation of the Fas Death Pathway by Anticancer Drugs.” *The Journal of Biological Chemistry* 274 (12): 7987–92. <https://doi.org/10.1074/JBC.274.12.7987>.
- Milacic, Marija, Deidre Beavers, Patrick Conley, Chuqiao Gong, Marc Gillespie, Johannes Griss, Robin Haw, et al. 2024. “The Reactome Pathway Knowledgebase 2024.” *Nucleic Acids Research* 52 (D1): D672–78. <https://doi.org/10.1093/NAR/GKAD1025>.
- Miyake, Kotaro, Pedro Henrique Costa Cruz, Izumi Nagatomo, Yuki Kato, Daisuke Motooka, Shingo Satoh, Yuichi Adachi, Yoshito Takeda, Yukio Kawahara, and Atsushi Kumanogoh. 2023. “A Cancer-Associated METTL14 Mutation Induces

- Aberrant m<sup>6</sup>A Modification, Affecting Tumor Growth.” *Cell Reports* 42 (7).  
<https://doi.org/10.1016/J.CELREP.2023.112688>.
- Moon, Soo Park, Maryely De Leon, and Prasad Devarajan. 2002. “Cisplatin Induces Apoptosis in LLC-PK1 Cells via Activation of Mitochondrial Pathways.” *Journal of the American Society of Nephrology* 13 (4): 858–65.  
<https://doi.org/10.1681/ASN.V134858>.
- Murakami, Shino, and Samie R. Jaffrey. 2022. “Hidden Codes in mRNA: Control of Gene Expression by m<sup>6</sup>A .” *Molecular Cell* 82 (12): 2236–51.  
<https://doi.org/10.1016/J.MOLCEL.2022.05.029>.
- Nagane, Motoo, Alexander Levitzki, Aviv Gazit, Webster K. Cavenee, and H. J. Su Huang. 1998. “Drug Resistance of Human Glioblastoma Cells Conferred by a Tumor-Specific Mutant Epidermal Growth Factor Receptor through Modulation of Bcl-XL and Caspase-3-like Proteases.” *Proceedings of the National Academy of Sciences of the United States of America* 95 (10): 5724–29.  
<https://doi.org/10.1073/PNAS.95.10.5724>.
- Nehmé, A., R. Baskaran, S. Nebel, D. Fink, S. B. Howell, J. Y.J. Wang, and R. D. Christen. 1999. “Induction of JNK and C-Abl Signalling by Cisplatin and Oxaliplatin in Mismatch Repair-Proficient and -Deficient Cells.” *British Journal of Cancer* 1999 79:7 79 (7): 1104–10. <https://doi.org/10.1038/sj.bjc.6690176>.
- Niu, Yi, Ziyou Lin, Arabella Wan, Honglei Chen, Heng Liang, Lei Sun, Yuan Wang, et al. 2019. “RNA N<sup>6</sup>-Methyladenosine Demethylase FTO Promotes Breast Tumor Progression through Inhibiting BNIP3.” *Molecular Cancer* 18 (1).  
<https://doi.org/10.1186/S12943-019-1004-4>.
- Nojima, Takayuki, Tomás Gomes, Ana Rita Fialho Grosso, Hiroshi Kimura, Michael J. Dye, Somdutta Dhir, Maria Carmo-Fonseca, and Nicholas J. Proudfoot. 2015. “Mammalian NET-Seq Reveals Genome-Wide Nascent Transcription Coupled to RNA Processing.” *Cell* 161 (3): 526–40. <https://doi.org/10.1016/j.cell.2015.03.027>.
- Nostrand, Eric L. Van, Gabriel A. Pratt, Alexander A. Shishkin, Chelsea Gelboin-Burkhart, Mark Y. Fang, Balaji Sundararaman, Steven M. Blue, et al. 2016. “Robust Transcriptome-Wide Discovery of RNA Binding Protein Binding Sites with

- Enhanced CLIP (ECLIP).” *Nature Methods* 13 (6): 508.  
<https://doi.org/10.1038/NMETH.3810>.
- Olarerin-George, Anthony O., and Samie R. Jaffrey. 2017. “MetaPlotR: A Perl/R Pipeline for Plotting Metagenes of Nucleotide Modifications and Other Transcriptomic Sites.” *Bioinformatics (Oxford, England)* 33 (10): 1563–64.  
<https://doi.org/10.1093/BIOINFORMATICS/BTX002>.
- Orrenius, Sten, Vladimir Gogvadze, and Boris Zhivotovsky. 2015. “Calcium and Mitochondria in the Regulation of Cell Death.” *Biochemical and Biophysical Research Communications* 460 (1): 72–81.  
<https://doi.org/10.1016/J.BBRC.2015.01.137>.
- Panneerdoss, Subbarayalu, Vijay K. Eedunuri, Pooja Yadav, Santosh Timilsina, Subapriya Rajamanickam, Suryavathi Viswanadhapalli, Nourhan Abdelfattah, et al. 2018. “Cross-Talk among Writers, Readers, and Erasers of M<sup>6</sup>A Regulates Cancer Growth and Progression.” *Science Advances* 4 (10).  
<https://doi.org/10.1126/SCIADV.AAR8263>.
- Park, Ok Hyun, Hongseok Ha, Yujin Lee, Sung Ho Boo, Do Hoon Kwon, Hyun Kyu Song, and Yoon Ki Kim. 2019. “Endoribonucleolytic Cleavage of M<sup>6</sup>A -Containing RNAs by RNase P/MRP Complex.” *Molecular Cell* 74 (3): 494-507.e8.  
<https://doi.org/10.1016/j.molcel.2019.02.034>.
- Patil, Deepak P., Brian F. Pickering, and Samie R. Jaffrey. 2018. “Reading M<sup>6</sup>A in the Transcriptome: M<sup>6</sup>A -Binding Proteins.” *Trends in Cell Biology* 28 (2): 113.  
<https://doi.org/10.1016/J.TCB.2017.10.001>.
- Pendleton, Kathryn E., Beibei Chen, Kuanqing Liu, Olga V. Hunter, Yang Xie, Benjamin P. Tu, and Nicholas K. Conrad. 2017. “The U6 SnRNA M<sup>6</sup>A Methyltransferase METTL16 Regulates SAM Synthetase Intron Retention.” *Cell* 169 (5): 824.  
<https://doi.org/10.1016/J.CELL.2017.05.003>.
- Perevozchikov, A. P., O. K. Kuznetsov, and Y. P. Zerov. 1970. “Viral RNA-Dependent DNA Polymerase: RNA-Dependent DNA Polymerase in Virions of Rous Sarcoma Virus.” *Nature* 226 (5252): 1211–13. <https://doi.org/10.1038/2261211a0>.
- Perry, R. P., and D. E. Kelley. 1974. “Existence of Methylated Messenger RNA in Mouse L Cells.” *Cell* 1 (1): 37–42. [https://doi.org/10.1016/0092-8674\(74\)90153-6](https://doi.org/10.1016/0092-8674(74)90153-6).

- Pi, Jingnan, Wen Wang, Ming Ji, Xiaoshuang Wang, Xueju Wei, Jing Jin, Tao Liu, et al. 2021. “YTHDF1 Promotes Gastric Carcinogenesis by Controlling Translation of FZD7.” *Cancer Research* 81 (10): 2651–65. <https://doi.org/10.1158/0008-5472.CAN-20-0066/654088/AM/YTHDF1-PROMOTES-GASTRIC-CARCINOGENESIS-BY>.
- Pil, Pieter M., and Stephen J. Lippard. 1992. “Specific Binding of Chromosomal Protein HMG1 to DNA Damaged by the Anticancer Drug Cisplatin.” *Science (New York, N.Y.)* 256 (5054): 234–37. <https://doi.org/10.1126/SCIENCE.1566071>.
- Ping, Xiao Li, Bao Fa Sun, Lu Wang, Wen Xiao, Xin Yang, Wen Jia Wang, Samir Adhikari, et al. 2014. “Mammalian WTAP Is a Regulatory Subunit of the RNA N6-Methyladenosine Methyltransferase.” *Cell Research* 24 (2): 177–89. <https://doi.org/10.1038/CR.2014.3>.
- Piya, Sujana, Ji Young Kim, Jeehyeon Bae, Dai Wu Seol, Ae Ran Moon, and Tae Hyoung Kim. 2012. “DUSP6 Is a Novel Transcriptional Target of P53 and Regulates P53-Mediated Apoptosis by Modulating Expression Levels of Bcl-2 Family Proteins.” *FEBS Letters* 586 (23): 4233–40. <https://doi.org/10.1016/J.FEBSLET.2012.10.031>.
- Pomaville, Monica, Mohansrinivas Chennakesavalu, Pingluan Wang, Zhiwei Jiang, Hui Lung Sun, Peizhe Ren, Ryan Borchert, et al. 2024. “Small-Molecule Inhibition of the METTL3/METTL14 Complex Suppresses Neuroblastoma Tumor Growth and Promotes Differentiation.” *Cell Reports* 43 (5): 114165. <https://doi.org/10.1016/J.CELREP.2024.114165>.
- Rangel-Sosa, Martha Montserrat, Estuardo Aguilar-Córdova, and Augusto Rojas-Martínez. 2017. “Immunotherapy and Gene Therapy as Novel Treatments for Cancer.” *Colombia Médica: CM* 48 (3): 138. <https://doi.org/10.25100/CM.V48I3.2997>.
- Reinhardt, H. Christian, Aaron S. Aslanian, Jacqueline A. Lees, and Michael B. Yaffe. 2007. “P53-Deficient Cells Rely on ATM- and ATR-Mediated Checkpoint Signaling through the P38MAPK/MK2 Pathway for Survival after DNA Damage.” *Cancer Cell* 11 (2): 175–89. <https://doi.org/10.1016/J.CCR.2006.11.024>.
- Renault, François, Etienne Formstecher, Isabelle Callebaut, Marie Pierre Junier, and Hervé Chneiweiss. 2003. “The Multifunctional Protein PEA-15 Is Involved in the Control

- of Apoptosis and Cell Cycle in Astrocytes.” *Biochemical Pharmacology* 66 (8): 1581–88. [https://doi.org/10.1016/S0006-2952\(03\)00514-8](https://doi.org/10.1016/S0006-2952(03)00514-8).
- Roberts, Justin T., Allison M. Porman, and Aaron M. Johnson. 2021. “Identification of M<sup>6</sup>A Residues at Single-Nucleotide Resolution Using ECLIP and an Accessible Custom Analysis Pipeline.” *RNA* 27 (4): 527–41. <https://doi.org/10.1261/RNA.078543.120/-/DC1>.
- Rocha, Clarissa Ribeiro Reily, Matheus Molina Silva, Annabel Quinet, Januario Bispo Cabral-Neto, and Carlos Frederico Martins Menck. 2018. “DNA Repair Pathways and Cisplatin Resistance: An Intimate Relationship.” *Clinics* 73 (January):e478s. <https://doi.org/10.6061/CLINICS/2018/E478S>.
- Rosenberg, Barnett. 1973. “Platinum Coordination Complexes in Cancer Chemotherapy.” *Die Naturwissenschaften* 60 (9): 399–406. <https://doi.org/10.1007/BF00623551>.
- Rosenberg, Barnett, Loretta Van Camp, and Thomas Krigas. 1965. “Inhibition of Cell Division in Escherichia Coli by Electrolysis Products from a Platinum Electrode.” *Nature* 205 (4972): 698–99. <https://doi.org/10.1038/205698a0>.
- Roth, Patrick, Sebastian Winklhofer, Antonia M.S. Müller, Reinhard Dummer, Maximilian J. Mair, Dorothee Gramatzki, Emilie Le Rhun, Markus G. Manz, Michael Weller, and Matthias Preusser. 2021. “Neurological Complications of Cancer Immunotherapy.” *Cancer Treatment Reviews* 97 (June):102189. <https://doi.org/10.1016/J.CTRV.2021.102189>.
- Roundtree, Ian A., Guan Zheng Luo, Zijie Zhang, Xiao Wang, Tao Zhou, Yiquang Cui, Jiahao Sha, et al. 2017. “YTHDC1 Mediates Nuclear Export of N<sup>6</sup>-Methyladenosine Methylated MRNAs.” *ELife* 6 (October). <https://doi.org/10.7554/ELIFE.31311>.
- Rozenberg, Julian M., Svetlana Zvereva, Aleksandra Dalina, Igor Blatov, Ilya Zubarev, Daniil Luppov, Alexander Bessmertnyi, et al. 2021. “The P53 Family Member P73 in the Regulation of Cell Stress Response.” *Biology Direct* 16 (1): 1–21. <https://doi.org/10.1186/S13062-021-00307-5>.
- Ryu, Hyewon, Ik Chan Song, Yoon Seok Choi, Hwan Jung Yun, Deog Yeon Jo, Jin Man Kim, Young Bok Ko, and Hyo Jin Lee. 2017. “ERCC1 Expression Status Predicts the Response and Survival of Patients with Metastatic or Recurrent Cervical Cancer

- Treated via Platinum-Based Chemotherapy.” *Medicine* 96 (51).  
<https://doi.org/10.1097/MD.00000000000009402>.
- Sakai, Hiroyasu, Atsunobu Sagara, Kazuhiko Arakawa, Ryoto Sugiyama, Akiko Hirosaki, Kazuhide Takase, Ara Jo, et al. 2014. “Mechanisms of Cisplatin-Induced Muscle Atrophy.” *Toxicology and Applied Pharmacology* 278 (2): 190–99.  
<https://doi.org/10.1016/J.TAAP.2014.05.001>.
- Salehi, Fahimeh, Hossein Behboudi, Gholamreza Kavvoosi, and Sussan K. Ardestani. 2018. “Oxidative DNA Damage Induced by ROS-Modulating Agents with the Ability to Target DNA: A Comparison of the Biological Characteristics of Citrus Pectin and Apple Pectin.” *Scientific Reports* 8 (1): 1–16. <https://doi.org/10.1038/s41598-018-32308-2>.
- Saletore, Yogesh, Kate Meyer, Jonas Korlach, Igor D. Vilfan, Samie Jaffrey, and Christopher E. Mason. 2012. “The Birth of the Epitranscriptome: Deciphering the Function of RNA Modifications.” *Genome Biology* 13 (10): 175.  
<https://doi.org/10.1186/gb-2012-13-10-175>.
- Sambrook, Joseph, E. F. Fritsch, and Tom Maniatis. 1989. *Molecular Cloning: A Laboratory Manual*. 2nd ed. New York: Cold Spring Harbor Laboratory Press.
- Sanger, F., S. Nicklen, and A. R. Coulson. 1977. “DNA Sequencing with Chain-Terminating Inhibitors.” *Proceedings of the National Academy of Sciences of the United States of America* 74 (12): 5463–67.  
<https://doi.org/10.1073/PNAS.74.12.5463>.
- Sato, Akira, Kentaro Nakama, Hiroki Watanabe, Akito Satake, Akihiro Yamamoto, Takuya Omi, Akiko Hiramoto, Mitsuko Masutani, Yusuke Wataya, and Hye Sook Kim. 2014. “Role of Activating Transcription Factor 3 Protein ATF3 in Necrosis and Apoptosis Induced by 5-Fluoro-2'-Deoxyuridine.” *The FEBS Journal* 281 (7): 1892–1900.  
<https://doi.org/10.1111/FEBS.12752>.
- Satterwhite, Emily R., and Kyle D. Mansfield. 2022. “RNA Methyltransferase METTL16: Targets and Function.” *Wiley Interdisciplinary Reviews: RNA* 13 (2): e1681.  
<https://doi.org/10.1002/WRNA.1681>.
- Scaffidi, Carsten, Simone Fulda, Anu Srinivasan, Claudia Friesen, Feng Li, Kevin J. Tomaselli, Klaus Michael Debatin, Peter H. Krammer, and Marcus E. Peter. 1998.

“Two CD95 (APO-1/Fas) Signaling Pathways.” *The EMBO Journal* 17 (6): 1675–87.  
<https://doi.org/10.1093/EMBOJ/17.6.1675>.

Schöller, Eva, Franziska Weichmann, Thomas Treiber, Sam Ringle, Nora Treiber, Andrew Flatley, Regina Feederle, Astrid Bruckmann, and Gunter Meister. 2018. “Interactions, Localization, and Phosphorylation of the M<sup>6</sup>A Generating METTL3-METTL14-WTAP Complex.” *RNA (New York, N.Y.)* 24 (4): 499–512.  
<https://doi.org/10.1261/RNA.064063.117>.

Schwartz, Schraga, Sudeep D. Agarwala, Maxwell R. Mumbach, Marko Jovanovic, Philipp Mertins, Alexander Shishkin, Yuval Tabach, et al. 2013. “High-Resolution Mapping Reveals a Conserved, Widespread, Dynamic mRNA Methylation Program in Yeast Meiosis.” *Cell* 155 (6). <https://doi.org/10.1016/J.CELL.2013.10.047>.

Shaikh, Aisha. 2022. “Immunotherapies and Renal Injury.” *Current Opinion in Toxicology* 31 (September):100362. <https://doi.org/10.1016/J.COTOX.2022.100362>.

Shen, Ding Wu, Lynn M. Pouliot, Matthew D. Hall, and Michael M. Gottesman. 2012. “Cisplatin Resistance: A Cellular Self-Defense Mechanism Resulting from Multiple Epigenetic and Genetic Changes.” *Pharmacological Reviews* 64 (3): 706.  
<https://doi.org/10.1124/PR.111.005637>.

Shen, Wei, Dimin Tong, Jie Chen, Hongxiang Li, Zeyang Hu, Shuguang Xu, Sufang He, et al. 2022. “Silencing Oncogene Cell Division Cycle Associated 5 Induces Apoptosis and G1 Phase Arrest of Non-Small Cell Lung Cancer Cells via P53-P21 Signaling Pathway.” *Journal of Clinical Laboratory Analysis* 36 (5): e24396.  
<https://doi.org/10.1002/JCLA.24396>.

Shen, Xudong, Kui Zhao, Liming Xu, Guilian Cheng, Jianhong Zhu, Lei Gan, Yongyou Wu, and Zhixiang Zhuang. 2021. “YTHDF2 Inhibits Gastric Cancer Cell Growth by Regulating FOXC2 Signaling Pathway.” *Frontiers in Genetics* 11 (January):592042.  
<https://doi.org/10.3389/FGENE.2020.592042/BIBTEX>.

Shi, Hailing, Xiao Wang, Zhike Lu, Boxuan S. Zhao, Honghui Ma, Phillip J. Hsu, Chang Liu, and Chuan He. 2017. “YTHDF3 Facilitates Translation and Decay of N<sup>6</sup>-Methyladenosine-Modified RNA.” *Cell Research* 27 (3): 315–28.  
<https://doi.org/10.1038/CR.2017.15>.

- Shi, Hailing, Jiangbo Wei, and Chuan He. 2019. “Where, When, and How: Context-Dependent Functions of RNA Methylation Writers, Readers, and Erasers.” *Molecular Cell* 74 (4): 640–50. <https://doi.org/10.1016/J.MOLCEL.2019.04.025>.
- Shi, Yu, Chunlei Zheng, Yue Jin, Bowen Bao, Duo Wang, Kezuo Hou, Jing Feng, et al. 2020. “Reduced Expression of METTL3 Promotes Metastasis of Triple-Negative Breast Cancer by M<sup>6</sup>A Methylation-Mediated COL3A1 Up-Regulation.” *Frontiers in Oncology* 10 (July). <https://doi.org/10.3389/FONC.2020.01126>.
- Shima, Hiroki, Mitsuyo Matsumoto, Yuma Ishigami, Masayuki Ebina, Akihiko Muto, Yuho Sato, Sayaka Kumagai, Kyoko Ochiai, Tsutomu Suzuki, and Kazuhiko Igarashi. 2017. “S-Adenosylmethionine Synthesis Is Regulated by Selective N<sup>6</sup>-Adenosine Methylation and mRNA Degradation Involving METTL16 and YTHDC1.” *Cell Reports* 21 (12): 3354–63. <https://doi.org/10.1016/J.CELREP.2017.11.092>.
- Shimba, Shigeki, Joseph A. Bokar, Fritz Rottman, and Ram Reddy. 1995. “Accurate and Efficient N-6-Adenosine Methylation in Spliceosomal U6 Small Nuclear RNA by HeLa Cell Extract in Vitro.” *Nucleic Acids Research* 23 (13): 2421–26. <https://doi.org/10.1093/NAR/23.13.2421>.
- Shimodaira, Hideki, Atsuko Yoshioka-Yamashita, Richard D. Kolodner, and Jean Y.J. Wang. 2003. “Interaction of Mismatch Repair Protein PMS2 and the P53-Related Transcription Factor P73 in Apoptosis Response to Cisplatin.” *Proceedings of the National Academy of Sciences of the United States of America* 100 (5): 2420–25. <https://doi.org/10.1073/PNAS.0438031100/ASSET/E94CF208-9349-4C8F-90F0-4BA28C9FC980/ASSETS/GRAPHIC/PQ0438031005.JPEG>.
- Shirjang, Solmaz, Behzad Mansoori, Samira Asghari, Pascal H.G. Duijf, Ali Mohammadi, Morten Gjerstorff, and Behzad Baradaran. 2019. “MicroRNAs in Cancer Cell Death Pathways: Apoptosis and Necroptosis.” *Free Radical Biology & Medicine* 139 (August):1–15. <https://doi.org/10.1016/J.FREERADBIOMED.2019.05.017>.
- Siddik, Zahid H. 2003. “Cisplatin: Mode of Cytotoxic Action and Molecular Basis of Resistance.” *Oncogene* 22 (47): 7265–79. <https://doi.org/10.1038/sj.onc.1206933>.
- Siegel, Richard M., John K. Frederiksen, David A. Zacharias, Francis Ka Ming Chan, Michele Johnson, David Lynch, Roger Y. Tsien, and Michael J. Lenardo. 2000. “Fas Preassociation Required for Apoptosis Signaling and Dominant Inhibition by

- Pathogenic Mutations.” *Science (New York, N.Y.)* 288 (5475): 2354–57.  
<https://doi.org/10.1126/SCIENCE.288.5475.2354>.
- Sikorski, Vilbert, Simona Selberg, Maciej Lalowski, Mati Karelson, and Esko Kankuri. 2023. “The Structure and Function of YTHDF Epitranscriptomic M<sup>6</sup>A Readers.” *Trends in Pharmacological Sciences* 44 (6): 335–53.  
<https://doi.org/10.1016/J.TIPS.2023.03.004>.
- Slattery, Martha L., Lila E. Mullany, Lori C. Sakoda, Roger K. Wolff, Wade S. Samowitz, and Jennifer S. Herrick. 2018. “Dysregulated Genes and MiRNAs in the Apoptosis Pathway in Colorectal Cancer Patients.” *Apoptosis* 23 (3–4): 237–50.  
<https://doi.org/10.1007/S10495-018-1451-1/TABLES/4>.
- Śledź, Paweł, and Martin Jinek. 2016. “Structural Insights into the Molecular Mechanism of the m(6)A Writer Complex.” *ELife* 5 (September).  
<https://doi.org/10.7554/ELIFE.18434>.
- Slobodin, Boris, Ruiqi Han, Vittorio Calderone, Joachim A.F.Oude Vrielink, Fabricio Loayza-Puch, Ran Elkon, and Reuven Agami. 2017. “Transcription Impacts the Efficiency of mRNA Translation via Co-Transcriptional N<sup>6</sup>-Adenosine Methylation.” *Cell* 169 (2): 326-337.e12.  
<https://doi.org/10.1016/J.CELL.2017.03.031>.
- Smith, Tom, Andreas Heger, and Ian Sudbery. 2017. “UMI-Tools: Modeling Sequencing Errors in Unique Molecular Identifiers to Improve Quantification Accuracy.” *Genome Research* 27 (3): 491–99. <https://doi.org/10.1101/GR.209601.116>.
- Song, Huiwen, Xing Feng, Heng Zhang, Yunmei Luo, Juan Huang, Meihua Lin, Junfei Jin, et al. 2019. “METTL3 and ALKBH5 Oppositely Regulate M<sup>6</sup>A Modification of TFEB mRNA, Which Dictates the Fate of Hypoxia/Reoxygenation-Treated Cardiomyocytes.” *Autophagy* 15 (8): 1419.  
<https://doi.org/10.1080/15548627.2019.1586246>.
- Steensma, David P., Michael Timm, and Thomas E. Witzig. 2003. “Flow Cytometric Methods for Detection and Quantification of Apoptosis.” *Methods in Molecular Medicine* 85:323–32. <https://doi.org/10.1385/1-59259-380-1:323>.
- Stefanouidakis, Dimitrios, Nikhita Kathuria-Prakash, Alexander W. Sun, Melissa Abel, Claire E. Drolen, Camille Ashbaugh, Shiliang Zhang, et al. 2023. “The Potential

- Revolution of Cancer Treatment with CRISPR Technology.” *Cancers* 15 (6).  
<https://doi.org/10.3390/CANCERS15061813>.
- Su, Rui, Lei Dong, Chenying Li, Sigrid Nachtergaele, Mark Wunderlich, Ying Qing, Xiaolan Deng, et al. 2018. “R-2HG Exhibits Anti-Tumor Activity by Targeting FTO/M<sup>6</sup>A /MYC/CEBPA Signaling.” *Cell* 172 (1–2): 90-105.e23.  
<https://doi.org/10.1016/j.cell.2017.11.031>.
- Subramanian, Aravind, Pablo Tamayo, Vamsi K. Mootha, Sayan Mukherjee, Benjamin L. Ebert, Michael A. Gillette, Amanda Paulovich, et al. 2005. “Gene Set Enrichment Analysis: A Knowledge-Based Approach for Interpreting Genome-Wide Expression Profiles.” *Proceedings of the National Academy of Sciences of the United States of America* 102 (43): 15545–50.  
[https://doi.org/10.1073/PNAS.0506580102/SUPPL\\_FILE/06580FIG7.JPG](https://doi.org/10.1073/PNAS.0506580102/SUPPL_FILE/06580FIG7.JPG).
- Sun, Tong, Zhikun Wu, Xiufang Wang, Yilin Wang, Xiaoyun Hu, Wenyan Qin, Senxu Lu, et al. 2020. “LNC942 Promoting METTL14-Mediated M<sup>6</sup>A Methylation in Breast Cancer Cell Proliferation and Progression.” *Oncogene* 39 (31): 5358–72.  
<https://doi.org/10.1038/S41388-020-1338-9>.
- Tanaka, Hirokazu, Itaru Matsumura, Sachiko Ezoe, Yusuke Satoh, Toshiyuki Sakamaki, Chris Albanese, Takashi Machii, Richard G. Pestell, and Yuzuru Kanakura. 2002. “E2F1 and C-Myc Potentiate Apoptosis through Inhibition of NF-KappaB Activity That Facilitates MnSOD-Mediated ROS Elimination.” *Molecular Cell* 9 (5): 1017–29. [https://doi.org/10.1016/S1097-2765\(02\)00522-1](https://doi.org/10.1016/S1097-2765(02)00522-1).
- Thomas, Paul D., Dustin Ebert, Anushya Muruganujan, Tremayne Mushayahama, Laurent Philippe Albou, and Huaiyu Mi. 2022. “PANTHER: Making Genome-Scale Phylogenetics Accessible to All.” *Protein Science* 31 (1): 8–22.  
<https://doi.org/10.1002/PRO.4218>.
- Tran, Nhan Van, Felix G.M. Ernst, Ben R. Hawley, Christiane Zorbas, Nathalie Ulryck, Philipp Hackert, Katherine E. Bohnsack, et al. 2019. “The Human 18S RRNA M<sup>6</sup>A Methyltransferase METTL5 Is Stabilized by TRMT112.” *Nucleic Acids Research* 47 (15): 7719–33. <https://doi.org/10.1093/NAR/GKZ619>.
- Tsukatani, T., H. Suenaga, M. Shiga, and K. Matsumoto. 2014. “A Rapid Microplate Method for the Proliferation Assay of Fungi and the Antifungal Susceptibility Testing

- Using the Colorimetric Microbial Viability Assay.” *Letters in Applied Microbiology* 59 (2): 184–92. <https://doi.org/10.1111/LAM.12264>.
- Tsvetkova, Dobrina, and Stefka Ivanova. 2022. “Application of Approved Cisplatin Derivatives in Combination Therapy against Different Cancer Diseases.” *Molecules* 27 (8). <https://doi.org/10.3390/MOLECULES27082466>.
- Ule, Jernej, Hun Way Hwang, and Robert B. Darnell. 2018. “The Future of Cross-Linking and Immunoprecipitation (CLIP).” *Cold Spring Harbor Perspectives in Biology* 10 (8). <https://doi.org/10.1101/CSHPERSPECT.A032243>.
- Usanova, Svetlana, Andrea Piée-Staffa, Ulrike Sied, Jürgen Thomale, Astrid Schneider, Bernd Kaina, and Beate Köberle. 2010. “Cisplatin Sensitivity of Testis Tumour Cells Is Due to Deficiency in Interstrand-Crosslink Repair and Low ERCC1-XPF Expression.” *Molecular Cancer* 9 (September). <https://doi.org/10.1186/1476-4598-9-248>.
- Uzonyi, Anna, David Dierks, Ronit Nir, Oh Sung Kwon, Ursula Toth, Isabelle Barbosa, Cindy Burel, et al. 2023. “Exclusion of M<sup>6</sup>A from Splice-Site Proximal Regions by the Exon Junction Complex Dictates M<sup>6</sup>A Topologies and mRNA Stability.” *Molecular Cell* 83 (2): 237-251.e7. <https://doi.org/10.1016/j.molcel.2022.12.026>.
- Vaux, David L., Suzanne Cory, and Jerry M. Adams. 1988. “Bcl-2 Gene Promotes Haemopoietic Cell Survival and Cooperates with c-Myc to immortalize Pre-B Cells.” *Nature* 335 (6189): 440–42. <https://doi.org/10.1038/335440a0>.
- Visvanathan, A., V. Patil, A. Arora, A. S. Hegde, A. Arivazhagan, V. Santosh, and K. Somasundaram. 2018. “Essential Role of METTL3-Mediated M<sup>6</sup>A Modification in Glioma Stem-like Cells Maintenance and Radioresistance.” *Oncogene* 37 (4): 522–33. <https://doi.org/10.1038/ONC.2017.351>.
- Volarevic, Vladislav, Bojana Djokovic, Marina Gazdic Jankovic, C. Randall Harrell, Crissy Fellabaum, Valentin Djonov, and Nebojsa Arsenijevic. 2019. “Molecular Mechanisms of Cisplatin-Induced Nephrotoxicity: A Balance on the Knife Edge between Renoprotection and Tumor Toxicity.” *Journal of Biomedical Science* 26 (1): 1–14. <https://doi.org/10.1186/S12929-019-0518-9>.
- Vu, Ly P., Brian F. Pickering, Yuanming Cheng, Sara Zaccara, Diu Nguyen, Gerard Minuesa, Timothy Chou, et al. 2017. “The N<sup>6</sup>-Methyladenosine (M<sup>6</sup>A)-Forming

- Enzyme METTL3 Controls Myeloid Differentiation of Normal Hematopoietic and Leukemia Cells.” *Nature Medicine* 23 (11): 1369–76. <https://doi.org/10.1038/nm.4416>.
- Waddington, C. H. 2012. “The Epigenotype.” *International Journal of Epidemiology* 41 (1): 10–13. <https://doi.org/10.1093/IJE/DYR184>.
- Waissbluth, Sofia, and Sam J. Daniel. 2013. “Cisplatin-Induced Ototoxicity: Transporters Playing a Role in Cisplatin Toxicity.” *Hearing Research* 299 (May):37–45. <https://doi.org/10.1016/J.HEARES.2013.02.002>.
- Wan, Weijun, Xiang Ao, Quan Chen, Yang Yu, Luoquan Ao, Wei Xing, Wei Guo, et al. 2022. “METTL3/IGF2BP3 Axis Inhibits Tumor Immune Surveillance by Upregulating N6-Methyladenosine Modification of PD-L1 mRNA in Breast Cancer.” *Molecular Cancer* 21 (1): 1–16. <https://doi.org/10.1186/S12943-021-01447-Y/FIGURES/6>.
- Wang, Chuhan, Danli ma, Huimin Yu, Zhihong Zhuo, and Zhiying Ye. 2023. “N6-Methyladenosine (M<sup>6</sup>A ) as a Regulator of Carcinogenesis and Drug Resistance by Targeting Epithelial-Mesenchymal Transition and Cancer Stem Cells.” *Heliyon* 9 (3): e14001. <https://doi.org/10.1016/J.HELİYON.2023.E14001>.
- Wang, Chunxin, and Richard J. Youle. 2009. “The Role of Mitochondria in Apoptosis.” *Annual Review of Genetics* 43 (December):95. <https://doi.org/10.1146/ANNUREV-GENET-102108-134850>.
- Wang, Haolan, Ming Guo, Hudie Wei, and Yongheng Chen. 2023. “Structural Basis of the Specificity and Interaction Mechanism of Bmf Binding to Pro-Survival Bcl-2 Family Proteins.” *Computational and Structural Biotechnology Journal* 21 (January):3760–67. <https://doi.org/10.1016/J.CSBJ.2023.07.017>.
- Wang, Hong, Bei Xu, and Jun Shi. 2020. “N6-Methyladenosine METTL3 Promotes the Breast Cancer Progression via Targeting Bcl-2.” *Gene* 722 (January):144076. <https://doi.org/10.1016/J.GENE.2019.144076>.
- Wang, Lude, Xiaoya Zhao, Jianfei Fu, Wenxia Xu, and Jianlie Yuan. 2021. “The Role of Tumour Metabolism in Cisplatin Resistance.” *Frontiers in Molecular Biosciences* 8 (June). <https://doi.org/10.3389/FMOLB.2021.691795>.

- Wang, N., M. S. Hou, Y. Zhan, X. B. Shen, and H. Y. Xue. 2018. "MALAT1 Promotes Cisplatin Resistance in Cervical Cancer by Activating the PI3K/AKT Pathway." *European Review for Medical and Pharmacological Sciences* 22 (22): 7653–59. [https://doi.org/10.26355/EURREV\\_201811\\_16382](https://doi.org/10.26355/EURREV_201811_16382).
- Wang, Ping, Katelyn A. Doxtader, and Yunsun Nam. 2016. "Structural Basis for Cooperative Function of Mettl3 and Mettl14 Methyltransferases." *Molecular Cell* 63 (2): 306–17. <https://doi.org/10.1016/J.MOLCEL.2016.05.041>.
- Wang, Qiang, Wei Geng, Huimin Guo, Zhangding Wang, Kaiyue Xu, Chen Chen, and Shouyu Wang. 2020. "Emerging Role of RNA Methyltransferase METTL3 in Gastrointestinal Cancer." *Journal of Hematology and Oncology* 13 (1): 1–10. <https://doi.org/10.1186/s13045-020-00895-1>.
- Wang, Shan, Xiangde Shi, Hao Li, Pei Pang, Lei Pei, Huiyong Shen, and Youming Lu. 2017. "DAPK1 Signaling Pathways in Stroke: From Mechanisms to Therapies." *Molecular Neurobiology* 54 (6): 4716–22. <https://doi.org/10.1007/S12035-016-0008-Y/FIGURES/4>.
- Wang, Tianyi, Shan Kong, Mei Tao, and Shaoqing Ju. 2020. "The Potential Role of RNA N6-Methyladenosine in Cancer Progression." *Molecular Cancer* 19 (1): 1–18. <https://doi.org/10.1186/S12943-020-01204-7>.
- Wang, Xiang, Jing Feng, Yuan Xue, Zeyuan Guan, Delin Zhang, Zhu Liu, Zhou Gong, et al. 2016. "Structural Basis of N6-Adenosine Methylation by the METTL3–METTL14 Complex." *Nature* 534 (7608): 575–78. <https://doi.org/10.1038/nature18298>.
- Wang, Xiao, Zhike Lu, Adrian Gomez, Gary C. Hon, Yanan Yue, Dali Han, Ye Fu, et al. 2014. "N6-Methyladenosine-Dependent Regulation of Messenger RNA Stability." *Nature* 505 (7481): 117–20. <https://doi.org/10.1038/NATURE12730>.
- Wang, Xinxia, Ruifan Wu, Youhua Liu, Yuanling Zhao, Zhen Bi, Yongxi Yao, Qing Liu, Hailing Shi, Fengqin Wang, and Yizhen Wang. 2020. "M<sup>6</sup>A mRNA Methylation Controls Autophagy and Adipogenesis by Targeting Atg5 and Atg7." *Autophagy* 16 (7): 1221–35. <https://doi.org/10.1080/15548627.2019.1659617>.
- Wanna-udom, Sasithorn, Minoru Terashima, Hanbing Lyu, Akihiko Ishimura, Takahisa Takino, Matomo Sakari, Toshifumi Tsukahara, and Takeshi Suzuki. 2020. "The M<sup>6</sup>A

- Methyltransferase METTL3 Contributes to Transforming Growth Factor-Beta-Induced Epithelial-Mesenchymal Transition of Lung Cancer Cells through the Regulation of JUNB.” *Biochemical and Biophysical Research Communications* 524 (1): 150–55. <https://doi.org/10.1016/J.BBRC.2020.01.042>.
- Warda, Ahmed S, Jens Kretschmer, Philipp Hackert, Christof Lenz, Henning Urlaub, Claudia Höbartner, Katherine E Sloan, and Markus T Bohnsack. 2017. “Human METTL16 Is a N6-Methyladenosine (M<sup>6</sup>A ) Methyltransferase That Targets Pre-mRNAs and Various Non-Coding RNAs.” *EMBO Reports* 18 (11): 2004–14. <https://doi.org/10.15252/EMBR.201744940>.
- Wei, Wenwen, Baosheng Huo, and Xiulan Shi. 2019. “MiR-600 Inhibits Lung Cancer via Downregulating the Expression of METTL3.” *Cancer Management and Research* 11:1177–87. <https://doi.org/10.2147/CMAR.S181058>.
- Wei, Yuanyan, Jianhai Jiang, Dan Liu, Jin Zhou, Xiaoning Chen, Si Zhang, Hongliang Zong, Xiaojing Yun, and Jianxin Gu. 2008. “Cdc34-Mediated Degradation of ATF5 Is Blocked by Cisplatin.” *Journal of Biological Chemistry* 283 (27): 18773–81. <https://doi.org/10.1074/jbc.M707879200>.
- Wen, Jing, Ruitu Lv, Honghui Ma, Hongjie Shen, Chenxi He, Jiahua Wang, Fangfang Jiao, et al. 2018. “Zc3h13 Regulates Nuclear RNA M<sup>6</sup>A Methylation and Mouse Embryonic Stem Cell Self-Renewal.” *Molecular Cell* 69 (6): 1028-1038.e6. <https://doi.org/10.1016/J.MOLCEL.2018.02.015>.
- Weng, Hengyou, Huilin Huang, Huizhe Wu, Xi Qin, Boxuan Simen Zhao, Lei Dong, Hailing Shi, et al. 2018. “METTL14 Inhibits Hematopoietic Stem/Progenitor Differentiation and Promotes Leukemogenesis via mRNA M<sup>6</sup>A Modification.” *Cell Stem Cell* 22 (2): 191-205.e9. <https://doi.org/10.1016/J.STEM.2017.11.016>.
- Wilkinson, Emma, Yan Hong Cui, and Yu Ying He. 2022. “Roles of RNA Modifications in Diverse Cellular Functions.” *Frontiers in Cell and Developmental Biology* 10 (March):444. <https://doi.org/10.3389/FCCELL.2022.828683/BIBTEX>.
- Wu, Baixing, Shichen Su, Deepak P. Patil, Hehua Liu, Jianhua Gan, Samie R. Jaffrey, and Jinbiao Ma. 2018. “Molecular Basis for the Specific and Multivariant Recognitions of RNA Substrates by Human HnRNP A2/B1.” *Nature Communications* 9 (1). <https://doi.org/10.1038/S41467-017-02770-Z>.

- Wu, Qunying, Xing Xie, Yiming Huang, Shanshan Meng, Youcheng Li, Huifeng Wang, and Yanling Hu. 2021. “N6-Methyladenosine RNA Methylation Regulators Contribute to the Progression of Prostate Cancer.” *Journal of Cancer* 12 (3): 682–92. <https://doi.org/10.7150/JCA.46379>.
- Wu, Rong, Ang Li, Baofa Sun, Jian Guang Sun, Jinhua Zhang, Ting Zhang, Yusheng Chen, et al. 2019. “A Novel M<sup>6</sup>A Reader Prrc2a Controls Oligodendroglial Specification and Myelination.” *Cell Research* 29 (1): 23–41. <https://doi.org/10.1038/S41422-018-0113-8>.
- Xiao, Wen, Samir Adhikari, Ujwal Dahal, Yu Sheng Chen, Ya Juan Hao, Bao Fa Sun, Hui Ying Sun, et al. 2016. “Nuclear m(6)A Reader YTHDC1 Regulates MRNA Splicing.” *Molecular Cell* 61 (4): 507–19. <https://doi.org/10.1016/J.MOLCEL.2016.01.012>.
- Xie, Daxing, Crystal Gore, Jian Zhou, Rey Chen Pong, Haifeng Zhang, Luyang Yu, Robert L. Vessella, Wang Min, and Jer Tsong Hsieh. 2009. “DAB2IP Coordinates Both PI3K-Akt and ASK1 Pathways for Cell Survival and Apoptosis.” *Proceedings of the National Academy of Sciences of the United States of America* 106 (47): 19878–83. [https://doi.org/10.1073/PNAS.0908458106/SUPPL\\_FILE/0908458106SI.PDF](https://doi.org/10.1073/PNAS.0908458106/SUPPL_FILE/0908458106SI.PDF).
- Xu, Fei, Jiajia Li, Mengdong Ni, Jingyi Cheng, Haiyun Zhao, Shanshan Wang, Xiang Zhou, and Xiaohua Wu. 2021. “FBW7 Suppresses Ovarian Cancer Development by Targeting the N6-Methyladenosine Binding Protein YTHDF2.” *Molecular Cancer* 20 (1): 1–16. <https://doi.org/10.1186/S12943-021-01340-8/FIGURES/6>.
- Xu, Jingwen, and David A. Gewirtz. 2022. “Is Autophagy Always a Barrier to Cisplatin Therapy?” *Biomolecules* 12 (3). <https://doi.org/10.3390/BIOM12030463>.
- Xu, Youqin, Mu Song, Ziyang Hong, Wancheng Chen, Qianbing Zhang, Jianlong Zhou, Chao Yang, et al. 2023. “The N6-Methyladenosine METTL3 Regulates Tumorigenesis and Glycolysis by Mediating M<sup>6</sup>A Methylation of the Tumor Suppressor LATS1 in Breast Cancer.” *Journal of Experimental and Clinical Cancer Research* 42 (1): 1–15. <https://doi.org/10.1186/S13046-022-02581-1/FIGURES/7>.
- Yan, Jijun, Xiufang Huang, Xiongjie Zhang, Zhijie Chen, Chao Ye, Wencai Xiang, and Zhengbin Huang. 2020. “LncRNA LINC00470 Promotes the Degradation of PTEN MRNA to Facilitate Malignant Behavior in Gastric Cancer Cells.” *Biochemical and*

*Biophysical Research Communications* 521 (4): 887–93.  
<https://doi.org/10.1016/J.BBRC.2019.11.016>.

Yang, Li, Tingyan Shi, Fei Liu, Chunxia Ren, Ziliang Wang, Yingyi Li, Xiaoyu Tu, Gong Yang, and Xi Cheng. 2015. “REV3L, a Promising Target in Regulating the Chemosensitivity of Cervical Cancer Cells.” *PloS One* 10 (3).  
<https://doi.org/10.1371/JOURNAL.PONE.0120334>.

Yang, Yang, Lixia Liu, Yu Tian, Miaomiao Gu, Yanan Wang, Milad Ashrafizadeh, Amir Reza Aref, et al. 2024. “Autophagy-Driven Regulation of Cisplatin Response in Human Cancers: Exploring Molecular and Cell Death Dynamics.” *Cancer Letters* 587 (April):216659. <https://doi.org/10.1016/J.CANLET.2024.216659>.

Yang, Zejia, Lisa M. Schumaker, Merrill J. Egorin, Eleanor G. Zuhowski, Zhongmin Quo, and Kevin J. Cullen. 2006. “Cisplatin Preferentially Binds Mitochondrial DNA and Voltage-Dependent Anion Channel Protein in the Mitochondrial Membrane of Head and Neck Squamous Cell Carcinoma: Possible Role in Apoptosis.” *Clinical Cancer Research : An Official Journal of the American Association for Cancer Research* 12 (19): 5817–25. <https://doi.org/10.1158/1078-0432.CCR-06-1037>.

Yao, Xuemei, Wei Li, Liqi Li, Menghuan Li, Youbo Zhao, De Fang, Xiaohua Zeng, and Zhong Luo. 2022. “YTHDF1 Upregulation Mediates Hypoxia-Dependent Breast Cancer Growth and Metastasis through Regulating PKM2 to Affect Glycolysis.” *Cell Death & Disease* 13 (3): 1–13. <https://doi.org/10.1038/s41419-022-04711-1>.

Yaylak, Bilge, Ipek Erdogan, and Bunyamin Akgul. 2019. “Transcriptomics Analysis of Circular RNAs Differentially Expressed in Apoptotic HeLa Cells.” *Frontiers in Genetics* 10 (MAR): 436737. <https://doi.org/10.3389/FGENE.2019.00176/BIBTEX>.

Yin, Xinming, Shijie Zhao, Mengxue Zhang, Jie Xing, Jiamin Zhou, Wujiang Gao, Lu Chen, et al. 2024. “M<sup>6</sup>A -Modified RIPK4 Facilitates Proliferation and Cisplatin Resistance in Epithelial Ovarian Cancer.” *Gynecologic Oncology* 180 (January):99–110. <https://doi.org/10.1016/j.ygyno.2023.11.034>.

Yoon, Je Hyun, and Myriam Gorospe. 2016. “Cross-Linking Immunoprecipitation and QPCR (CLIP-QPCR) Analysis to Map Interactions Between Long Noncoding RNAs and RNA-Binding Proteins.” *Methods in Molecular Biology (Clifton, N.J.)* 1402 (January):11–17. [https://doi.org/10.1007/978-1-4939-3378-5\\_2](https://doi.org/10.1007/978-1-4939-3378-5_2).

- Yu, Jie, Peiwei Chai, Minyue Xie, Shengfang Ge, Jing Ruan, Xianqun Fan, and Renbing Jia. 2021. "Histone Lactylation Drives Oncogenesis by Facilitating M<sup>6</sup>A Reader Protein YTHDF2 Expression in Ocular Melanoma." *Genome Biology* 22 (1): 1–21. <https://doi.org/10.1186/S13059-021-02308-Z/FIGURES/8>.
- Yu, Wangie, Yunyun Chen, Julien Dubrulle, Fabio Stossi, Vasanta Putluri, Arun Sreekumar, Nagireddy Putluri, Dodge Baluya, Stephen Y. Lai, and Vlad C. Sandulache. 2018. "Cisplatin Generates Oxidative Stress Which Is Accompanied by Rapid Shifts in Central Carbon Metabolism." *Scientific Reports* 8 (1): 1–12. <https://doi.org/10.1038/s41598-018-22640-y>.
- Yuan, Chung Hsiang, Maria Filippova, and Penelope Duerksen-Hughes. 2012. "Modulation of Apoptotic Pathways by Human Papillomaviruses (HPV): Mechanisms and Implications for Therapy." *Viruses* 4 (12): 3831–50. <https://doi.org/10.3390/V4123831>.
- Yuan, Ye, Gege Yan, Mingyu He, Hong Lei, Linqiang Li, Yang Wang, Xiaoqi He, et al. 2021. "ALKBH5 Suppresses Tumor Progression via an M<sup>6</sup>A -Dependent Epigenetic Silencing of Pre-MiR-181b-1/YAP Signaling Axis in Osteosarcoma." *Cell Death & Disease* 12 (1): 1–16. <https://doi.org/10.1038/s41419-020-03315-x>.
- Zaccara, Sara, and Samie R. Jaffrey. 2020. "A Unified Model for the Function of YTHDF Proteins in Regulating M<sup>6</sup>A -Modified mRNA." *Cell* 181 (7): 1582-1595.e18. <https://doi.org/10.1016/J.CELL.2020.05.012>.
- Zamble, Deborah B., Yuji Mikata, Christina H. Eng, Karen E. Sandman, and Stephen J. Lippard. 2002. "Testis-Specific HMG-Domain Protein Alters the Responses of Cells to Cisplatin." *Journal of Inorganic Biochemistry* 91 (3): 451–62. [https://doi.org/10.1016/S0162-0134\(02\)00472-5](https://doi.org/10.1016/S0162-0134(02)00472-5).
- Zeng, Zhan-Cheng, Qi Pan, Yu-Meng Sun, Heng-Jing Huang, Xiao-Tong Chen, Tian-Qi Chen, Bo He, et al. 2023. "METTL3 Protects METTL14 from STUB1 -mediated Degradation to Maintain m<sup>6</sup>A Homeostasis ." *EMBO Reports* 24 (3). <https://doi.org/10.15252/EMBR.202255762>.
- Zhang, Canfeng, Liping Chen, Di Peng, Ao Jiang, Yunru He, Yanru Zeng, Chen Xie, et al. 2020. "METTL3 and N<sup>6</sup>-Methyladenosine Promote Homologous Recombination-

- Mediated Repair of DSBs by Modulating DNA-RNA Hybrid Accumulation.” *Molecular Cell* 79 (3): 425-442.e7. <https://doi.org/10.1016/J.MOLCEL.2020.06.017>.
- Zhang, Feiran, Yunhee Kang, Mengli Wang, Yujing Li, Tianlei Xu, Wei Yang, Hongjun Song, Hao Wu, Qiang Shu, and Peng Jin. 2018. “Fragile X Mental Retardation Protein Modulates the Stability of Its M<sup>6</sup>A -Marked Messenger RNA Targets.” *Human Molecular Genetics* 27 (22): 3936–50. <https://doi.org/10.1093/HMG/DDY292>.
- Zhang, Jixiang, Xiaoli Wang, Vikash Vikash, Qing Ye, Dandan Wu, Yulan Liu, and Weiguo Dong. 2016. “ROS and ROS-Mediated Cellular Signaling.” *Oxidative Medicine and Cellular Longevity* <https://doi.org/10.1155/2016/4350965>.
- Zhang, Kun, Yucheng Zhang, Yunash Maharjan, Febri Gunawan Sugiokto, Jun Wan, and Renfeng Li. 2021. “Caspases Switch off the M<sup>6</sup>A Rna Modification Pathway to Foster the Replication of a Ubiquitous Human Tumor Virus.” *MBio* 12 (4). [https://doi.org/10.1128/MBIO.01706-21/SUPPL\\_FILE/MBIO.01706-21-SF009.TIF](https://doi.org/10.1128/MBIO.01706-21/SUPPL_FILE/MBIO.01706-21-SF009.TIF).
- Zhang, Xiao, Lian Huan Wei, Yuxin Wang, Yu Xiao, Jun Liu, Wei Zhang, Ning Yan, et al. 2019. “Structural Insights into FTO’s Catalytic Mechanism for the Demethylation of Multiple RNA Substrates.” *Proceedings of the National Academy of Sciences of the United States of America* 116 (8): 2919–24. <https://doi.org/10.1073/PNAS.1820574116>.
- Zhao, Weihao, Shang Zhang, Yumin Zhu, Xiaochen Xi, Pengfei Bao, Ziyuan Ma, Thomas H. Kapral, et al. 2022. “POSTAR3: An Updated Platform for Exploring Post-Transcriptional Regulation Coordinated by RNA-Binding Proteins.” *Nucleic Acids Research* 50 (D1): D287. <https://doi.org/10.1093/NAR/GKAB702>.
- Zhao, Yanchun, Yuanfei Shi, Huafei Shen, and Wanzhuo Xie. 2020. “M<sup>6</sup>A -Binding Proteins: The Emerging Crucial Performers in Epigenetics.” *Journal of Hematology and Oncology* 13 (1): 1–14. <https://doi.org/10.1186/s13045-020-00872-8>.
- Zheng, Guanqun, John Arne Dahl, Yamei Niu, Peter Fedorcsak, Chun Min Huang, Charles J. Li, Cathrine B. Vågbo, et al. 2013. “ALKBH5 Is a Mammalian RNA Demethylase That Impacts RNA Metabolism and Mouse Fertility.” *Molecular Cell* 49 (1): 18–29. <https://doi.org/10.1016/J.MOLCEL.2012.10.015>.

- Zhong, Silin, Hongying Li, Zsuzsanna Bodi, James Button, Laurent Vespa, Michel Herzog, and Rupert G. Fray. 2008. "MTA Is an Arabidopsis Messenger RNA Adenosine Methylase and Interacts with a Homolog of a Sex-Specific Splicing Factor." *The Plant Cell* 20 (5): 1278. <https://doi.org/10.1105/TPC.108.058883>.
- Zhou, Huimin, Kai Yin, Yue Zhang, Jie Tian, and Shengjun Wang. 2021. "The RNA M<sup>6</sup>A Writer METTL14 in Cancers: Roles, Structures, and Applications." *Biochimica et Biophysica Acta (BBA) - Reviews on Cancer* 1876 (2): 188609. <https://doi.org/10.1016/J.BBCAN.2021.188609>.
- Zhou, J., Z. Ning, B. Wang, E. J. Yun, T. Zhang, R. C. Pong, L. Fazli, et al. 2015. "DAB2IP Loss Confers the Resistance of Prostate Cancer to Androgen Deprivation Therapy through Activating STAT3 and Inhibiting Apoptosis." *Cell Death & Disease* 6 (10). <https://doi.org/10.1038/CDDIS.2015.289>.
- Zhu, Hongtao, Xiaoling Gan, Xingwei Jiang, Shuai Diao, Huan Wu, and Jianguo Hu. 2019. "ALKBH5 Inhibited Autophagy of Epithelial Ovarian Cancer through MiR-7 and BCL-2." *Journal of Experimental & Clinical Cancer Research: CR* 38 (1). <https://doi.org/10.1186/S13046-019-1159-2>.
- Zhu, Tian Yu, Lian Lian Hong, and Zhi Qiang Ling. 2023. "Oncofetal Protein IGF2BPs in Human Cancer: Functions, Mechanisms and Therapeutic Potential." *Biomarker Research* 2023 11:1 11 (1): 1–15. <https://doi.org/10.1186/S40364-023-00499-0>.
- Zhu, Zhiyuan, Qi Qian, Xia Zhao, Liang Ma, and Ping Chen. 2020. "N<sup>6</sup>-Methyladenosine ALKBH5 Promotes Non-Small Cell Lung Cancer Progress by Regulating TIMP3 Stability." *Gene* 731 (March). <https://doi.org/10.1016/J.GENE.2020.144348>.
- Zoghbi, Huda Y., and Arthur L. Beaudet. 2016. "Epigenetics and Human Disease." *Cold Spring Harbor Perspectives in Biology* 8 (2): 1–28. <https://doi.org/10.1101/CSHPERSPECT.A019497>.
- Zou, Shui, Joel D.W. Toh, Kendra H.Q. Wong, Yong Gui Gao, Wanjin Hong, and Esther C.Y. Woon. 2016. "N<sup>6</sup>-Methyladenosine: A Conformational Marker That Regulates the Substrate Specificity of Human Demethylases FTO and ALKBH5." *Scientific Reports* 2016 6:1 6 (1): 1–12. <https://doi.org/10.1038/srep25677>.

# VITAE

Full Name Ayşe Bengisu GELMEZ

## EDUCATION

01/09/2018 – 01/07/2024 Doctor of Philosophy (Ph.D)  
*İzmir Institute of Technology (İzmir, Türkiye)*

01/02/2015 – 01/07/2018 Master of Science (M.Sc.)  
*İzmir Institute of Technology (İzmir, Türkiye)*

01/09/2007 – 24/06/2013 Bachelor of Science (B.Sc.), *cum laude*  
*Hacettepe University (Ankara, Türkiye)*

## AWARDS & HONORS

07 – 12/2023 The Scientific and Technological Council of Turkey (TUBITAK), Graduate Performance Program Fellowship.

01 – 06/2023 The Scientific and Technological Council of Turkey (TUBITAK), Graduate Performance Program Fellowship.

01/2021 – 07/2024 Abdi İbrahim Foundation Ph.D. Scholarship.

07 – 14/2019 COST, Epitran Training School Fellowship.

24/06/2013 Bachelor's Degree Graduation (*Cum Laude*).

## PUBLICATIONS

Alasar AA, Tüncel Ö, **Gelmez AB**, Sağlam B, Vatansever İE, Akgül B. Genomewide m<sup>6</sup>A Mapping Uncovers Dynamic Changes in the m<sup>6</sup>A Epitranscriptome of Cisplatin-Treated Apoptotic HeLa Cells. *Cells*. 2022 Dec 2;11(23):3905. doi 10.3390/cells11233905. PMID: 36497162; PMCID: PMC9738315.